Precursor Chemistry for Main Group Elements in Semiconducting Materials

Mohammad Azad Malik, Mohammad Afzaal, and Paul O'Brien*

School of Chemistry and Manchester Materials Science Centre, The University of Manchester, Oxford Road, Manchester, M13 9PL, United Kingdom

Received December 17, 2009

Contents

1.	Introduction	4417
2.	Precursor Requirements	4418
3.	Precursors for II−VI Materials	4418
3.1.	Precursors for II−VI Thin Films	4418
3.1.1.	Alternate Chalcogenide Precursors	4419
3.1.2.	Adducts of Metal Alkyls	4419
3.1.3.	Single-Molecule Precursors	4419
3.2.	Precursors for II−VI Nanoparticles	4425
4.	Precursors for III−V Materials	4428
4.1.	Precursors for III−V Thin Films	4428
4.1.1.	Alternative Group V Sources	4428
4.1.2.	III−V Adducts	4429
4.1.3.	III Nitrides	4429
4.1.4.	III Phosphides and Arsenides	4430
4.1.5.	III Antimonides	4431
4.2.	Precursors for III−V Nanoparticles	4431
5.	Precursors for III−VI Materials	4432
5.1.	Precursors for III−VI Thin Films	4432
5.1.1.	Thiolato Complexes	4432
5.1.2.	Thiocarbamato Complexes	4433
5.1.3.	Xanthato and Monothiocarbamato Complexes	4433
5.1.4.	Dichalcogenoimidodiphosphinato Complexes	4433
5.2.	Precursors for III−VI Nanoparticles	4434
6.	Precursors for IV−VI Materials	4434
6.1.	Precursors for IV−VI Thin Films	4434
6.2.	Precursors for IV−VI Nanoparticles	4437
7.	Precursors for V−VI Materials	4437
7.1.	Precursors for V−VI Thin Films	4437
7.2.	Precursors for V−VI Nanoparticles	4440
8.	Conclusions	4441
9.	Acknowledgments	4442
10.	References	4442

1. Introduction

The birth of the modern electronics industry can be traced to the invention of the first transistor by Shockley, Brattain, and Bardeen at Bell Laboratories in 1948. This transistor was based on a semiconducting layer of germanium on quartz, and they received the Nobel Prize in Physics in 1956. The integrated monolithic silicon chip (the integrated circuit, IC) was probably the next major breakthrough, for which Jack Kilby of Texas Instruments was awarded a Nobel Prize in 2000. Indeed, silicon continues to dominate the microelectronics industry.

However, compound semiconductors such as gallium arsenide (GaAs) have some electronic properties which are superior to those of silicon. GaAs has a higher saturated electron velocity and higher electron mobility, allowing transistors made from it to function at frequencies in excess of 25 GHz. Also, GaAs devices generate less noise than do those of silicon devices when operated at high frequencies. They operate at higher power levels than the equivalent silicon devices because they have higher breakdown voltages. Another advantage is a direct band gap, a common advantage of compound semiconducting materials, which leads to more efficient optoeclectronic behavior, especially the emission and absorption of photons.

Compound semiconductors based on combinations of elements from Groups II and VI, III and V, III and VI, and IV and VI have had a significant impact on our everyday lives. Materials such as GaAs, aluminum gallium arsenide (AlGaAs), gallium nitride (GaN), indium phosphide (InP), zinc selenide (ZnSe), cadmium telluride (CdTe), and copper indium gallium selenide CuInGaSe (CIGS) have a wide variety of applications in satellite TV receivers, optical fiber communications, compact disk players, barcode readers, full color advertising displays, and solar cells. These semiconductors are at present generally useful in the form of thin films, but nanoparticles and solids are important with a great future predicted for nanoparticles and perhaps most especially quantum dots. The most common chemistry-based method to thin films is chemical vapor deposition (CVD). Manasevit was the first to grow such thin films (GaAs) in 1968 by the molecular organic (MO) CVD method.[1] These techniques now employ metal−organic compounds of high purity. As the complexity of electronic devices increases, the suit of materials on which diversity is written increases; the demand for elegant precursors decomposing cleanly at lower temperature often to deliver complex phases is ever increasing.

The most important factor which effects the composition and structure of the deposited material is the nature and purity of the precursors. In CVD processes, molecular precursors must shed the ligands that contributed to their volatility in order to produce a film of a solid-state material. Thermal decomposition of a precursor is the key step which produces a thin film, and ideally the ligands associated with the precursor are cleanly lost into the gas phase. However, that is not often the case, and when complex ligands are involved (heteroleptic compounds), more complex fragmentation takes place. A rational development of precursors for a specific application is thus only possible on the basis of some insights into the molecular decomposition pathways. Study on the precursor decomposition mechanism, in principle, needs to be carried out in the gas phase of the molecules directly,

* To whom correspondence should be addressed. Phone: 0161 275 4652. Fax: 0161 275 4616. E-mail: paul.obrien@manchester.ac.uk.

10.1021/cr900406f © 2010 American Chemical Society
Published on Web 05/19/2010

Mohammad Azad Malik completed his Ph.D. degree at the University of London in 1990 and since then has been working with Professor Paul O'Brien initially at Queen Mary University of London (1990−1995), then Imperial College (1995−2000), and currently The University of Manchester (2000 to current). He has been involved in various projects and has a wide range of experience including single-source molecular precursors for II/VI, III/V, III/VI, and IV/VI semiconductors, MOCVD, AACVD, CBD, and the colloidal synthesis of nanoparticles.

Mohammad Afzaal graduated from Aston University, Birmingham, in 2000 and moved to the University of Manchester to carry out his Ph.D. studies with Professor Paul O'Brien, studying growth of semiconductor thin films using single-source precursors. After completing his Ph.D. degree in 2003, he remained with Professor Paul O'Brien and took his current postdoctoral position, studying nanoparticles and thin film deposition for various applications.

Paul O'Brien is Professor of Inorganic Materials Chemistry in the School of Chemistry and the School of Materials at the University of Manchester. He was Head of the School of Chemistry from 2002 to 2009 and Research Dean from 2000 to 2002. He graduated from Liverpool University in 1975, obtained his Ph.D. degree from the University of Wales, Cardiff, in 1978, and was immediately appointed as a lecturer at Chelsea College of Science and Technology, University of London. He moved to Queen Mary and Westfield College in 1984 and was promoted to a chair in 1994. In 1995, he moved to Imperial College and became the Sumitomo/STS Professor of Materials Chemistry (1997−2003). He was Regents appointed Visiting Professor at the Georgia Institute of Technology (1996−1999). He is a Fellow of the Institute of Materials, Minerals, and Mining (FIMMM) and a Chartered Engineer (C. Eng). He received the 2007 Kroll Medal from the IOMMM and the first Peter Day Award for Materials Chemistry from the RSC in 2009. In 2006 he was awarded the first ever honorary D.Sc. degree of the University of Zululand, South Africa.

and subsequently surface reactions of the precursors or relevant fragments have to be investigated. It is interesting to know how a metal complex decomposes by application of thermal energy. Detailed gas-phase/surface studies are very complex and can only be carried out online.

We have, for several years, been developing single-source precursors (SSPs) for thin films and nanocrystals. The use of SSPs can potentially provide several key advantages over other routes. For example, the existence of preformed bonds can lead to a material with fewer defects and/or better stoichiometry. In the case of thin film deposition by CVD, conditions of flow and temperature become simpler. It is also possible to carry out deposition with relatively simple installations. Several of the SSP are also air stable and therefore easier to handle and characterize. Systematic studies comparing the performance of precursors in similar conditions remain scarce. This review will highlight some relevant examples of relationships between precursors and materials deposited and discuss the advances made in the design and preparation of precursors involving main group elements and their use for synthesis of semiconducting materials in the form of thin films and nanoparticles.

2. Precursor Requirements

The most important requirement for a precursor is its purity to prevent contamination of the deposited material and other undesirable side products. Purification techniques and methods during precursor preparation or possible alternative precursor preparation methods are therefore very important. A precursor is also required to decompose at elevated temperatures on the substrate surface to give the desired thin film. For low-pressure (LP) CVD volatility is a requirement. It is desirable for a precursor to be readily volatile at a temperature well below that of its decomposition. However, due to developments in CVD systems, e.g., aerosol-assisted (AA) CVD and liquid-injection (LI) CVD, this is no longer crucial. The precursor is also required to be stable and have a low degree of toxicity for easy use and storage. Ultimatly, precursor must be able to be synthesized in quantities of at least several grams with as few synthetic steps as possible. The synthesis must be adaptable to larger scale production without major problems including cost and environmental impact.

3. Precursors for II−VI Materials

3.1. Precursors for II−VI Thin Films

The growth of II−VI thin films by a chemical method became practical with Manasevit's use of volatile metal alkyls such as dimethylcadmium (Me_2Cd) or dimethylzinc (Me_2Zn) in a combination with H_2S, H_2Se, or Me_2Te delivered in dihydrogen[1] as a carrier gas, effectively inventing and defining the process of MOCVD. Many films were grown including ZnS, ZnSe, CdS, CdSe, and CdTe.[1]

The method involves the delivery of both a metal alkyl and a chalcogenide source in the vapor phase to a mixing chamber and onward to a deposition zone; particulate material can form before the vapors reach the heated substrate, sometimes termed '*prereaction*'. To overcome some of these problems, new precursors were developed to control volatility, reduce toxic hazard, improve the quality of the grown layers, and reduce the temperature required for growth. These precursors include alternate chalcogenide precursors, metal alkyls adducts, and single-source precursors.

3.1.1. Alternate Chalcogenide Precursors

Alkyl chacogenides can be used as alternative chalcogen sources to the hydrides. MeSeH,[2] Et_2Se,[3,4] ^tBuSeH,[5] and $^tBu_2Se$[6] have been used but require higher deposition temperatures due to their thermal stability. Similarly, dialkyltellurides, alkylally1tellurides, and diallyltellurides have been used[7] but cannot be stored longer than a few days due to their lack of stability.[8] A detailed investigation of the decomposition mechanism of tellurium precursors has underlined the importance of homolytic Te−C bond scission and the role of surface-bound alkyl or ally1 radicals during film growth.[9] The formation of radicals in $R_2Te/CdMe_2$ mixtures has been shown to lead to alkyl group scrambling, e.g., $^iPr_2Te$ can be partly converted to thermally more stable (and hence less suitable) derivatives such as Me_2Te_2 and $MeTe^iPr$. The detailed chemistry of alkyl chalcogenide precursors has been described in several reviews.[10−14]

3.1.2. Adducts of Metal Alkyls

Suppression of the homogeneous reaction in the system Me_2Zn/H_2Se/pyridine at pyridine to Zn ratios as low as 0.05: 1[15] suggests that the Lewis base does not directly protect the metal dialkyls but may do so via intermediates such as $[MeM(SH)]_n$. The alkyls of group 12 are weak Lewis acids with Lewis acidity decreasing in the sequence Zn > Cd > Hg. Replacement of alkyl groups with sulfur, which is a more electronegative element, increases the Lewis acidity at the metal and hence its tendency to bind additional ligands or form aggregates of higher nuclearity.

The oligomeric structures of alkylzinc thiolates [RZn(SR′)] such as the $[MeZn(S^tBu)]_5$ pentamer (Figure 1a),[16,17] $[MeZn(S^iPr)]_8$,[18] an octamer, and $[EtZn(SEt)_{10}]$, a decamer,[19] provide a good indication that the species might be initially formed as the gas-phase nucleation products.[20] The reaction of pyridine with pentameric compound $[MeZn(S^tBu)_5]$[17] to give dimeric adducts $[MeZn(S^tBu)(py)]_2$ (Figure 1b) shows how these ligands might effectively block the polymerization of thiolato intermediates. All of the dimers formed by the reaction of pyridine with $[MeZn(S^tBu)_5]$ have similar structures with a four-coordinate zinc, the methyl and amine groups are monodentate, and the thiolates form bridges. The crystallographic structures of several adducts were investigated, and the four-coordinate structure of the dimethylzinc adduct with hexahydrotrimethyltriazine has been reported.[21]

3.1.3. Single-Molecule Precursors

3.1.3.1. Chalcogenolato Complexes. Cadmium or zinc complexes with ligands such as thiolates generally result in the formation of involatile polymeric structures with a tetrahedral metal center.[22−24] However, many such chalcogen-containing complexes have been shown to give II−VI material on thermal decomposition, but their lack of volatility means that they are not generally useful as precursors in MOCVD even at low pressure.

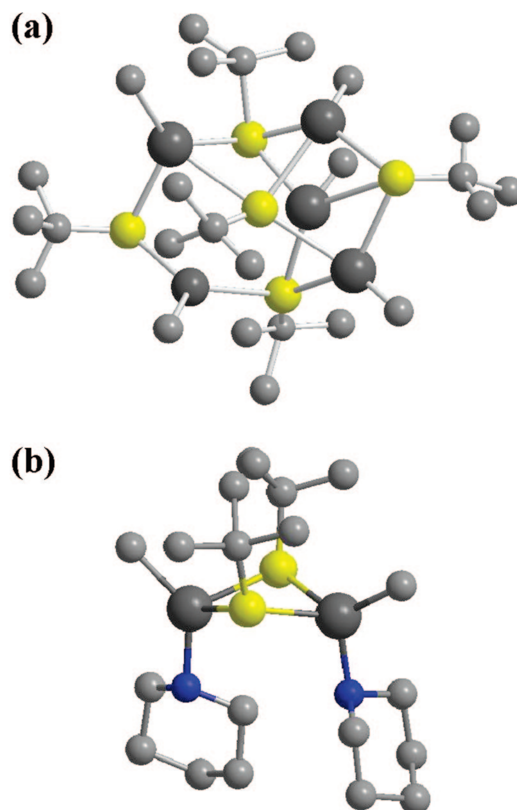

Figure 1. Structures of (a) $[MeZn(S^tBu)]_5$ and (b) $[MeZn(S^tBu)(Py)]_2$.

One approach is to reduce the molecularity of these complexes by forming adducts. Steigerwald and co-worker reported a series of precursors prepared with 1,2-bis(diethylphosphino)ethane (depe), $M(ER)_2$ (M = Zn, Cd, Hg; E = S, Se, Te).[25] Complexes with one or two mole equivalents of the phosphine have been synthesized. The 1:2 species are polymeric and the 1:1 complexes dimers; crystal structures have been reported for the complexes $[Cd_2(SeC_6H_5)_4(depe)]_n$ and $[Hg(SeC_6H_5)_2(depe)]_2$.[25] Thermal decomposition of $[Cd_2(SeC_6H_5)_4(depe)]_n$ in high-boiling-point solvents, such as 4-ethylpyridine, resulted in the deposition of subnanometer clusters of CdSe. Similarly, decomposition of bischalcogenato complexes[26,27] gives rise to metal chalcogenides. Hampden-Smith and co-workers prepared a compound of stoichiometry $[Zn(SEt)Et]_{10}$ by insertion of sulfur into the Zn−C bond of dimethylzinc.[28] Although this decameric thiolate possesses a similar arrangement of zinc and sulfur atoms to that found in wurtzite, pyrolysis of the material at 250 °C led to predominantly cubic ZnS; AACVD does however lead to the hexagonal form.[28]

Another approach used to reduce the molecularity of these complexes involved bulky chalcogenide ligands such as 2,4,6-triisopropylbenzenethiol (tipt). A series of low-coordination metal complexes were prepared with 2,4,6-triisopropylbenzenethiol (tipt) by Dilworth et al.[29] Bochmann et al.[30−33] produced a range of precursors for II−VI materials based on 2,4,6-tri-*tert*-butylphenylchalcogenolate. The general preparation method of one such complex is shown in eqs 1−3.

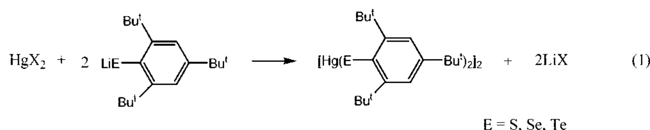

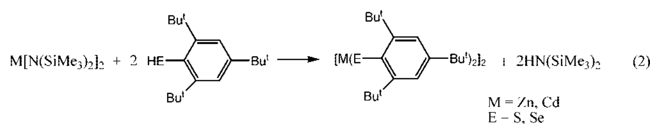

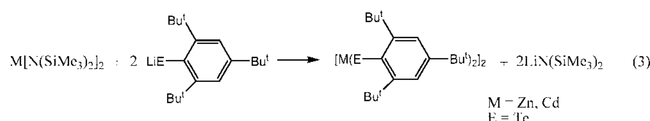

The compounds are dimeric, even in the vapor phase, and can be used in LP-MOCVD for the deposition of II−VI materials.[34,35] For example, $[Cd(SC_6H_2{}^iBu_3\text{-}2,4,6)]_2$ gave polycrystalline CdS thin films at a substrate temperature of 450 °C (10^{-2} Torr). The mercury analogues readily decomposed via a reductive elimination path to form atomic Hg and diary1dichalcogenides, which may indicate that these compounds are more suitable for the photoassisted rather than the thermal MOCVD method.[32] Organometallic chalcogenates[36] with aryl chalcogenates RMSeR′ (R′ = $C_6H_2{}^iPr_3$-2,4,6; M = Zn, R = Me, Et, Pr, ^{i}Pr; M = Cd, R = Me) have also been prepared but have not to date been evaluated for thin film studies.

A series of related precursors are silicon-based systems of stoichiometry $M[ESi(SiMe)_3]_2$ (M = Zn, Cd, Hg; E = S, Se, or Te) as devised by Arnold and co-workers to deposit a range of chalcogenides.[37,38] The most detailed work was reported on the tellurides: thin films of the tellurides have been deposited by LP-MOCVD.[39] The tellurium-containing ligand $HTeSi(SiMe_3)_3$ is termed HSitel, and this reagent is potentially useful in the preparation of metal tellurolates.[40−42] Metal complexes of Site1 are generally prepared as illustrated below, eq 4.

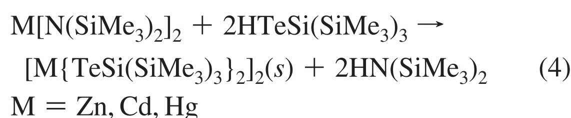

$$\begin{aligned}&M[N(SiMe_3)_2]_2 + 2HTeSi(SiMe_3)_3 \rightarrow \\ &\quad [M\{TeSi(SiMe_3)_3\}_2]_2(s) + 2HN(SiMe_3)_2 \qquad (4)\\ &M = Zn, Cd, Hg\end{aligned}$$

ZnTe was deposited at temperatures between 250 and 350 °C onto quartz, Si, InAs, and GaSb substrates. The cadmium precursor gave hexagonal material with a better stoichiometry than those of ZnTe.

3.1.3.2. Dithio-/Diselenophosphinato Complexes. In early work, Takahashi[43] deposited CdS using dimethylthiophosphinates $[M(S_2PMe_2)_2]$ (M = Cd or Zn) and Evans and Williams reported[44] that highly orientated CdS films could be grown using the diethyldithiophosphinates as precursors.

CdS and ZnS films have been deposited from $[Cd(S_2P^iBu_2)_2]_2$ and $[Zn(S_2P^iBu_2)_2]_2$, respectively, using a homemade cold-wall low-pressure reactor.[45] The cadmium complex has a classic C_i-symmetric two-step ladder (or "chair") structure (Figure 2) of type 23 for the central eight-membered $Cd_2S_4P_2$ ring.[46] This geometry contrasts with the C_2-symmetric "boat" conformation observed for the closely related isopropoxide complex $Cd_2[(i\text{-}C_3H_7O)_2PS_2]_4$.[47] X-ray analysis of the zinc complex shows it to adopt a geometry for the $Zn_2S_8P_4$ core that is virtually identical with that seen in the cadmium and zinc complexes with *O*,*O*-diisopropylphosphordithioate.[47]

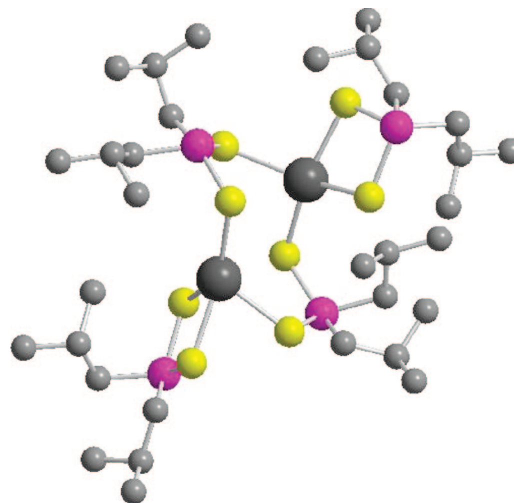

Figure 2. Molecular structure of $[Cd(S_2P^iBu_2)_2]_2$ showing its "chair" conformation.

A series of metal complexes of bis(dialkylselenophosphinyl)selenide $[(R_2PSe_2)Se]$ (R = Ph, ^{i}Pr) with the general formula $[M(R_2PSe_2)_n]$ (M = Zn, Cd, Pb, In, Ga, Cu, Bi, Ni; R = ^{i}Pr, Ph) and $[Mo_2O_2Se_2(Se_2P^iPr_2)_2]$ have been synthesized and used for the growth of metal selenide thin films by CVD.[48,49] The ligands $[(R_2PSe_2)_2Se]$ (R = ^{i}Pr, Ph) were prepared from the reaction of NEt_3 with Ph_2PCl or $^iPr_2PCl$ and $HSiCl_3$ in cold toluene (eqs 5 and 6).

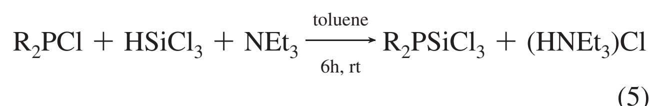

$$R_2PCl + HSiCl_3 + NEt_3 \xrightarrow[\text{6h, rt}]{\text{toluene}} R_2PSiCl_3 + (HNEt_3)Cl \qquad (5)$$

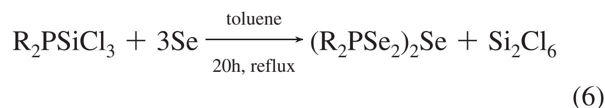

$$R_2PSiCl_3 + 3Se \xrightarrow[\text{20h, reflux}]{\text{toluene}} (R_2PSe_2)_2Se + Si_2Cl_6 \qquad (6)$$

Reaction with different metal salts was then carried out in methanolic solutions and gave the metal complexes as precipitates, which were subsequently recrystallized from dichloromethane or toluene. Indium forms (Figure 3a), as expected, the $[In(^iPr_2PSe_2)_3]$ complex. All three diselenophosphinate ligands are chelating to form four-membered rings (Se−P−Se−In) with In−Se bond distances that range from 2.729(6) to 2.768(6) Å. The geometry at indium is trigonally-distorted octahedral due to the restricted bite angle of the chelating diselenophosphinate ligand.

The structure of $[Ga(^iPr_2PSe_2)_3]$ (Figure 3b) has a four-coordinate gallium center, in contrast to the six-coordinate indium. Until recently,[50] all reports on structurally characterized pairs of analogues In/Ga tris (chelates) with (O, O′) or (S, S′) ligands have been shown to be isostructural.[51,52] The first such four-coordinate structure for a gallium complex was tris(diisobutyldithiophophinato)gallium($[Ga(Ph_2PS_2)_3]$[53] with one chelating and two pendant diisopropyldiselenophosphinate ligands in a distorted tetragonal geometry. The phenyl analogue $[Ga(Ph_2PSe_2)_3]$[48] showed a similar coordination pattern.

3.1.3.3. Bis(dialkydithio/selenocarbamato)metal Species. Dialkyldithio/diselenocarbamato metal complexes with the general formula $[(M(E_2CNR_2)_2]$ (symmetrical) or $[M(E_2CNRR')_2]$ (unsymmetrical) (R, R′ = alkyl, E = S, Se; M = Zn, Cd) are precursors that have been used for the deposition of II−VI thin films. All of these compounds are

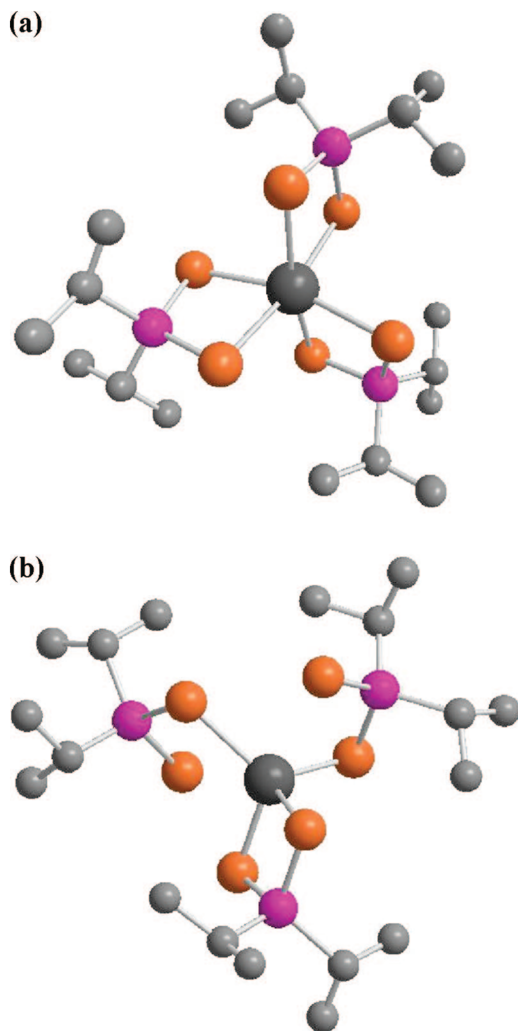

Figure 3. Structures of (a) [In(^{i}Pr$_2$PSe$_2$)$_3$] and (b) [Ga(^{i}Pr$_2$PSe$_2$)$_3$].

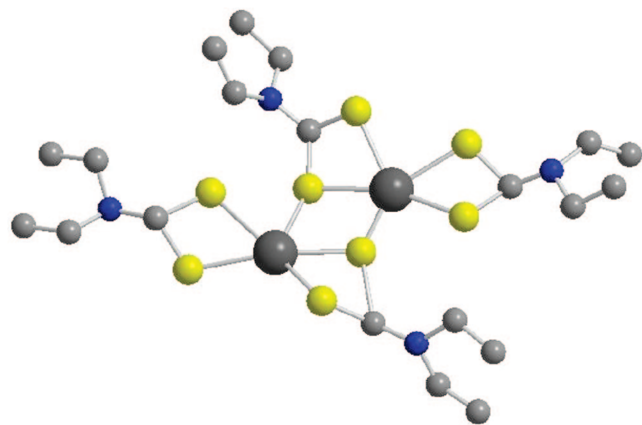

Figure 4. Structure of Cd(S$_2$CNEt$_2$)$_2$.

stable crystalline solids with some volatility. Their solid-state structures have been determined by X-ray crystallography. Most of them, including [Zn(S$_2$CNR$_2$)$_2$] (R = Me, Et, or ^{i}Pr),[54−56] [Cd(S$_2$CNEt$_2$)$_2$] (Figure 4), [Zn(Se$_2$CNEt$_2$)$_2$], [Cd(Se$_2$CNEt$_2$)$_2$], and [Zn(S$_2$CNMeR)$_2$] (R = Et, ^{n}Pr, ^{i}Pr, or ^{n}Bu), have dimeric structures.[57−60] Saunders et al.[61] were the first to use diethyldithiocarbamates [M(S$_2$CNEt$_2$)$_2$] (M = Cd, Zn) for the deposition of ZnS, CdS, and Zn$_x$Cd$_{1-x}$S thin films by the LP-MOCVD method. The same precursors were used to grow heterostructures by organometallic vapor-phase epitaxy (OMVPE).[62,63] Frigo et al. deposited good-quality CdS or Zn$_x$Cd$_{1-x}$S films prepared from an equimolar mixture of the precursors [Zn(S$_2$CNEt$_2$)$_2$] and [Cd(S$_2$CNEt$_2$)$_2$] on (100)-oriented GaAs or InP substrates[64] by LP-MOCVD. The quality of ZnS films deposited from [Zn(S$_2$CNEt$_2$)$_2$] was poor.

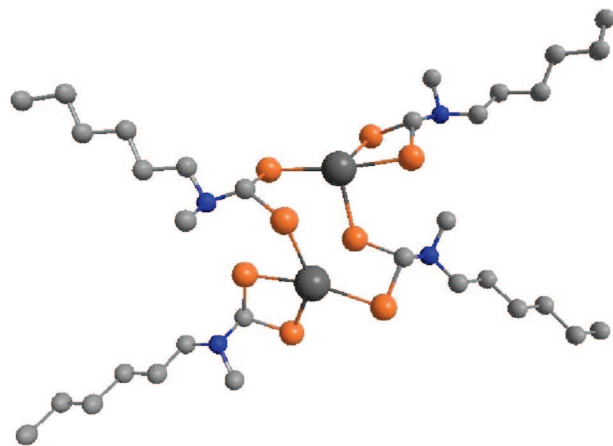

Figure 5. Structure of [Cd(Se$_2$CNMe^{n}Hex)$_2$]$_2$.

Deposition by MOCVD of ZnS usually gives the hexagonal, α-ZnS, wurtzite, but Nomura et al. deposited the cubic, β-ZnS, zinc blende epitaxially on (111)-Si by OMVPE using [Zn(S$_2$CNEt$_2$)$_2$] in a cold-wall horizontal reactor.[65] It was observed that the deposition conducted at low pressure (10^{-2} Torr) produced hexagonal α-ZnS of poor crystallinity and morphology, whereas depositions with introduction of a carrier gas (N$_2$) gave good-quality (111)-oriented β-ZnS. Fainer et al. used [Cd(S$_2$CNEt$_2$)$_2$] with He or H$_2$ as a carrier gas in LP-MOCVD[66] and plasma-enhanced MOCVD (PE-MOCVD)[67] to grow CdS on SiO$_2$, Al$_2$O$_3$ (sapphire), (111)-Si, and (111)-InP.[66]

Bis(dialkyldithio/selenocarbamato)cadmium/zinc compounds have had the advantage of stability for years, but the volatility of the precursors can be a limiting factor. In addition, for selenides the quality of the films was often poor with elemental selenium contamination. However, air-stable unsymmetrical precursors based on [M(S$_2$CNRR′)$_2$] (M = Cd or Zn; RR′ = alkyl groups) decompose cleanly in MOCVD to selenides or sulfides.[68−70] Volatilization experiments shown that the unsymmetrically substituted [Zn(S$_2$CNMeEt)]$_2$, [Zn(S$_2$CNMe^{n}Pr)]$_2$, and [Zn(S$_2$CNMe^{n}Bu)]$_2$ volatilize well above their melting points, whereas [Zn(S$_2$CNEt$_2$)$_2$]$_2$ sublimes as a solid.[60] ZnS film was grown on glass from [Zn(S$_2$CNMe^{n}Bu)]$_2$ by LP-MOCVD at 450 °C in a cold-wall reactor.[60] Deposition studies on [Cd(S$_2$CNEt$_2$)$_2$] and [Cd(S$_2$CNMe^{n}Bu)$_2$] showed that the methyl butyl derivative was more volatile[71] and that the films grown on InP at 500 °C were of polycrystalline CdS.

A series of other unsymmetrical dithio- and diselenocarbamates has also been synthesized and used as SSPs for deposition of thin films. Bis(*n*-hexyl(methyl)dithio/selenocarbamato)cadmium/zinc (Figure 5) proved to be the best of the unsymmetrical derivatives for growth of chalogenides.[72]

Since dithio- and diselenocarbamates and their derivatives have been used widely in the deposition of thin films and nanoparticles, a mechanistic study of their decomposition behavior was carried out by O'Brien et al.[70] Wold[73] studied the decomposition products of [Zn(S$_2$CNEt$_2$)$_2$] using GC-MS, and their reported deposition path shows the clean

Figure 6. Structure of $[Zn(Se_2CNMe^nHex)_2]$.

elimination of ZnS from the precursor (eqs 7 and 8 below). However, the proposed decomposition route is somewhat different from the step-by-step fragmentation observed in the EI-MS of the compound (eq 9). This difference can be attributed to inherent differences between the two techniques.

$$Zn(S_2CNEt_2)_2 \rightarrow ZnS + EtNCS + Et_2NCS_2Et \quad (7)$$

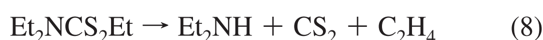

$$Et_2NCS_2Et \rightarrow Et_2NH + CS_2 + C_2H_4 \quad (8)$$

$$Zn(S_2CNEt_2)_2 \xrightarrow{-S_2CNEt_2} Zn(S_2CNEt_2)_2 \xrightarrow{-SCNEt_2} ZnS \quad (9)$$

In contrast, the analogous diethyl-diselenocarbamates have been shown to be poor sources for deposition of ZnSe or CdSe films. Under similar reaction conditions ($10^{-3}-10^{-4}$ Torr, 370−420 °C), the diethyl-diselenocarbamates precursors give films of the metal selenide heavily contaminated with selenium.[59] However, the mixed alkyl diselenocarbamates complex have been used successfully to deposit thin films of CdSe or ZnSe.[74,75]

ZnSe films were deposited from $[Zn(Se_2CNMe^nHex)_2]$, which has two different alkyl substituents at the nitrogen. This complex is monomeric in the solid phase[68] (Figure 6), in contrast to the analogous diethyl-diselenocarbamates and the mixed alkyl-diselenocarbamates complexes, which are both dimers. All of the dithiocarbamates prepared can be used to deposit CdS or ZnS by MOCVD, but the diselenocarbamates show a different pattern of behavior; $[M(Se_2CNEt_2)_2]$ (M = Zn, Cd) deposit films heavily contaminated with selenium, whereas $[M(Se_2CNRR')_2]$ (M = Zn, Cd) and $[EtZnSe_2CNEt_2]_2$ deposit the metal selenide. It was of interest to study the decomposition of the compounds by GC-MS and EI-MS to determine why the latter are successful precursors and also plausible decomposition pathways for comparison with the dithiocarbamato complexes. Plausible schemes for decomposition of the precursor have been proposed (Scheme 1).

Among several limiting factors in the deposition of chalcogenides from these compounds is the volatility of the complexes which can particularly influence the results of the deposition. Some attempts to obtain more volatile dithiocarbamato complexes have been made. The dithiocarbamato complexes derived from trimethylpropylenediamine were synthesized[76,77] by a comproportionation reaction. This complex showed a different structure from the dimers and is a weakly bonded polymer, as shown in Figure 7. The compound is apparently more volatile than the simpler dithiocarbamates and has successfully been used in deposition experiments to deposit CdS thin film on glass or GaAs substrates at 350 °C.[76]

Scheme 1. Decomposition Mechanism of Bis(hexyl(methyl)-diselenocarbamato)zinc

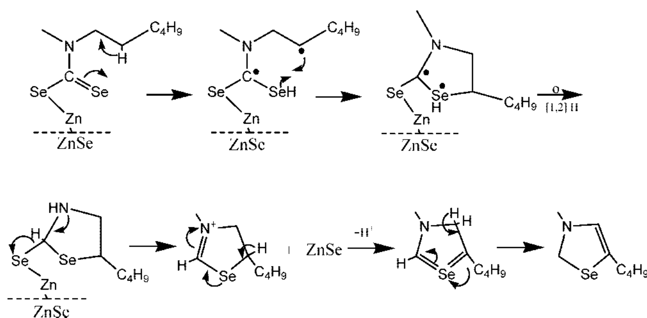

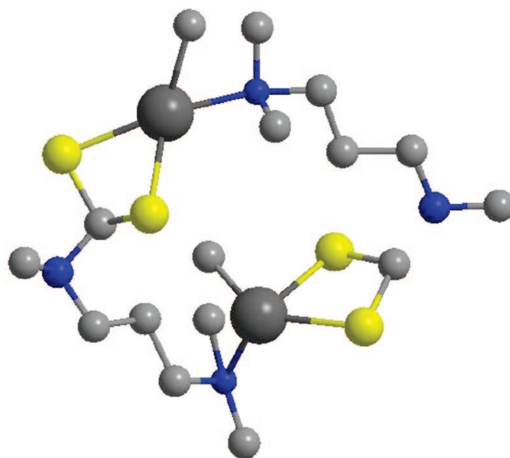

Figure 7. Structure of $[MeCd(MeN(CH_2)_3NMe_2)]_n$.

3.1.3.4. *N*-Alkyldithiocarbamato Complexes. Another related class of compounds *N*-alkyldithiocarbamato $[M(S_2CNHR)_2]$ has potential as precursors. These complexes have received scant attraction[78] because of a perceived lack of stability and expectation of low volatility. Recently, O'Brien et al.[79] synthesized a series of complexes of cadmium or zinc with varying alkyl chain lengths $[M(S_2CNHR)_2]$ (M = Cd, Zn; R = ethyl, ^{n}butyl, ^{n}hexyl, ^{n}dodecyl).

Condensation of the primary amines with carbon disulfide in the presence of metal salts produced $[M(S_2CNHR)_2]$ (M = Cd or Zn) in reasonable purity and with a good yield. Most of these complexes were only sparingly soluble in organic solvents. The zinc complexes were comparatively stable and more soluble. The compound $[Zn(S_2CNHHex)_2]$ was recrystallized from dichloromethane to give good-quality crystals used for X-ray study (Figure 8).[79]

The cadmium complexes decomposed to a cadmium sulfate complex with pyridine and water, which crystallized from pyridine. Stable bis(*N*-alkyldithiocarbamato) cadmium complexes have been prepared by metathesis between lithium *N*-alkyldithiocarbamato salts and cadmium chloride in neutral aqueous solution.[80] The *N*-alkyldithiocarbamato complexes are less stable than their corresponding *N*,*N*-dialkyldithiocarbamato complexes due to the presence of the acidic hydrogen at the nitrogen.

Thermogravimetric analysis (TGA) was conducted to evaluate the decompositional behavior of the *N*-alkyldithiocarbamato complexes of cadmium and zinc.[79] The cadmium compounds decompose in an unresolved two-step mecha-

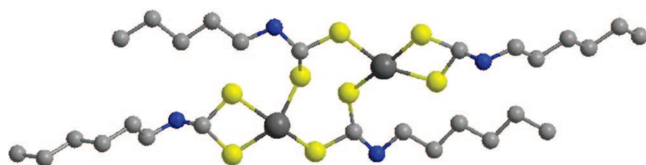

Figure 8. Structure of $[Zn(S_2CNHHex)_2]_2$.

nism. In contrast, the zinc compounds decomposed in a single step. It was surprising to note that the decomposition behavior of the compounds changed as the chain length was increased, indicated by the final residue of compounds. The remaining residues from $[M(S_2CNHR)_2]$ (M = Zn, Cd; R = ^{n}Hex, ^{n}dodecyl) were very close to the values calculated for bulk metal sulfide, whereas shorter substituted alkyl chain compounds such as ethyl or butyl gave a significantly larger residue than expected from the stoichiometric ratio, indicating incomplete decomposition or inclusion of impurities after decomposition of precursor.

3.1.3.5. Mixed Alkyl/Dithio- or Diselenocarbamato Complexes. These compounds were first prepared by Noltes[81] using an insertion reaction[82] (eq 10).

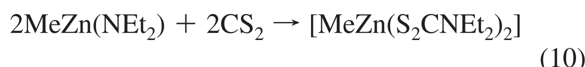

$$2MeZn(NEt_2) + 2CS_2 \rightarrow [MeZn(S_2CNEt_2)_2] \quad (10)$$

Comproportionation (eq 11) can provide a more convenient route to these compounds.[83−85]

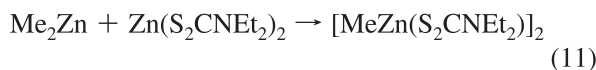

$$Me_2Zn + Zn(S_2CNEt_2)_2 \rightarrow [MeZn(S_2CNEt_2)]_2 \quad (11)$$

The compounds are dimers[82] in the solid state, and the parent dimeric structure has been confirmed for a wide range of compounds where R = Me, Et, ^{t}Bu, or Me_3CCH_2, M = Zn or Cd, E = S or Se, R′ = Me or Et.[86,87] X-ray single-crystal structures of neopentylcadmium and diethyldiselenocarbamate are shown in Figure 9a and 9b.[88]

An interesting application of the comproportionation reaction is the preparation of a mixed species such as methylcadmium/methylzinc diethyldiselenocarbamate, which is useful for the deposition of thin films of the ternary solid solutions of $Cd_{0.5}Zn_{0.5}Se$. Thus, reaction of Me_2Zn with $[Cd(Se_2CNEt_2)_2]$ gave $[Me_2CdZn(Se_2CNEt_2)_2]$ as shown in eq 12.

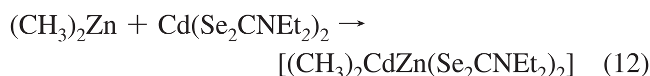

$$(CH_3)_2Zn + Cd(Se_2CNEt_2)_2 \rightarrow [(CH_3)_2CdZn(Se_2CNEt_2)_2] \quad (12)$$

A polycrystalline $Cd_{0.5}Zn_{0.5}Se$ layer with a band gap of 2.1 eV, was deposited on a glass substrate by LP-MOCVD (450 °C, 0.2 Torr). The mixed compound showed similar dimeric molecular units $[RM(Se_2CNEt_2)]_2$ to other alkylmetal dithio- and diselenocarbamates. In the solid-state structures, the cadmium and zinc atoms were modeled as randomly occupying the metal sites.[75] Many of these mixed alkyl diseleno- and dithiocarbamato compounds have been used to deposit thin films of metal chalcogenides by LP-MOCVD (10^{-2}−10^{-3} Torr).

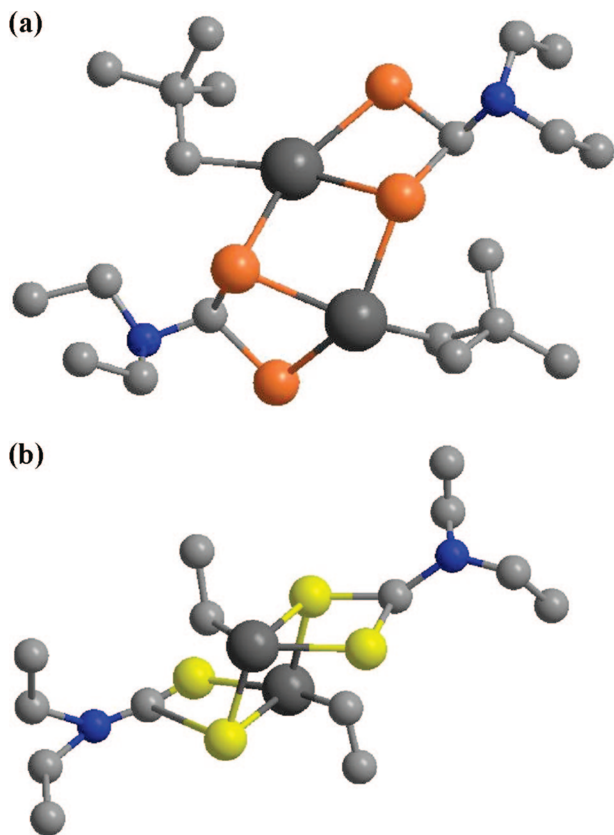

Figure 9. Structures of (a) $[NpCdSe_2CNEt_2]_2$ and (b) $EtZnSe_2CNEt_2]_2$.

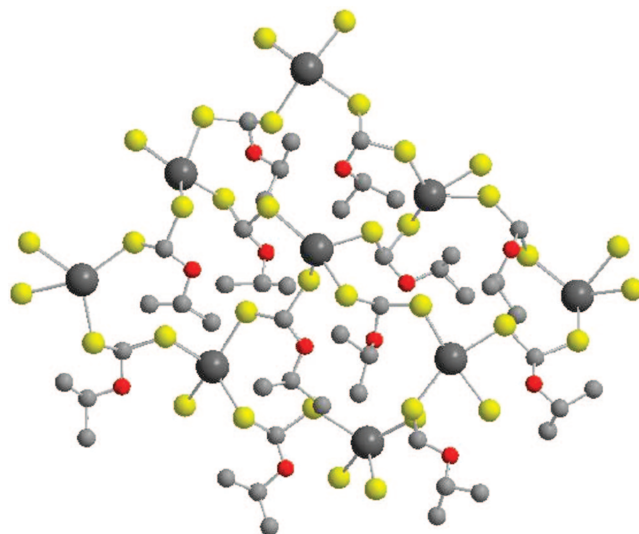

Figure 10. Structure of $[Cd(S_2OCC_3H_7)_2]_n$.

3.1.3.6. Xanthate Complexes. Nanocrystalline ZnS and CdS thin films were deposited onto Si/SiO_2 substrates by CVD at temperatures between 200 and 450 °C from $[M(S_2COC_3H_7)_2]$ (M = Zn, Cd).[94] Thermal decomposition and fragmentation of $[M(S_2COC_3H_7)_2]$ was also investigated by thermal analyses and mass spectrometry.

Barrecal et al. investigated the properties of $[M(S_2COCHR)_2]$ (M = Cd; R = Et or ^{i}Pr) as a potential SSPs for the CVD of CdS thin films.[95] The structure of bis(*O*-isopropyldithiocarbonato)cadmium $[Cd(S_2COPr)_2]$ is shown in Figure 10.[96] Two distinct motifs are known for $[Cd(S_2COR)_2]$, a square-planar geometry with R = CH_2CH_2OMe, and weak Cd−S interactions above and below the square plane[97] and tetratetrahedrally coordinated Cd, i.e., when R = Et[98] and R = Bu.[99] The recently reported structure of $[Cd(S_2COPr)_2]$ also conforms to this motif.[100]

3.1.3.7. Monothiocarbamato Complexes. Bis(diethylmonothiocarbamato)cadmium has some volatility despite its polymeric structure[101] and was used to deposit films of CdS by LP-MOCVD at temperatures between 300 and 400 °C.[102] Compounds with the general formulas $[M(SOCR)_2(tmeda)]$ (tmeda = *N*,*N*,*N*,*N*-tetramethylethylenediamine, R = Me[83] or ^{t}Bu,[120] were used to grow CdS, ZnS, and $Cd_xZn_{1-x}S$ by the AACVD method. $[Zn(SOCCH_3)_2(tmeda)]$ and $[Cd(SOCCH_3)_2(tmeda)]$ are isostructural, monomeric complexes in the solid state with the metal atom in a distorted

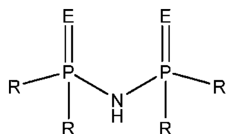

Figure 11. Dichalcogenoimidodiphosphinate anions (E = O, S, Se; R = methyl, isopropyl, butyl, phenyl).

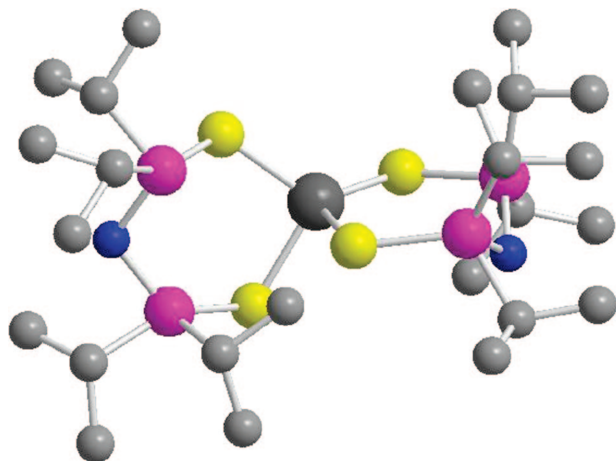

Figure 12. Structure of $Cd[(SeP^iPr_2)_2N]_2$.

tetrahedral coordination environment comprising two nitrogens and two sulfurs.[83]

3.1.3.8. Dichalcogenoimidodiphosphinato Complexes. The dichalcogenoimidodiphosphinate anions (Figure 11) were first synthesized by Schmidpeter et al. in the 1960s.[85]

In 1995, Woollins and co-workers initiated the chemistry of the selenium analogue.[103] Much of the early development of the coordination chemistry of these ligands with both main group[104] and transition metals[104,105] was carried out on the phenyl derivatives. In 2004 it was demonstrated that metal complexes incorporating the more volatile isopropyl ligands are excellent precursors for the production of a variety of binary metal selenides.[106−108]

Imino-diisopropylphosphine selenides are prepared by oxidative insertion of elemental selenium into $NH(P^iPr_2)_2$.[109] The cadmium compound $Cd[(SeP^iPr_2)_2N]_2$ (Figure 12) was first synthesized by Woollins et al.[109] from diisopropylchlorophosphine via a two-step strategy. Improved yields for $Cd[(SeP^iPr_2)_2N]_2$ above those reported can be afforded by utilizing $CdCl_2$/NaOMe conditions rather than $CdCO_3$ (eqs 13−15).

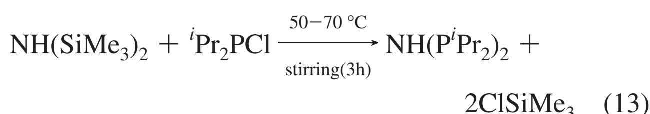

$$NH(SiMe_3)_2 + {}^iPr_2PCl \xrightarrow[\text{stirring(3h)}]{50-70\ °C} NH(P^iPr_2)_2 + 2ClSiMe_3 \quad (13)$$

$$NH(P^iPr_2)_2 \xrightarrow[\text{reflux}]{E=S,\ Se} NH(EP^iPr_2)_2 \quad (14)$$

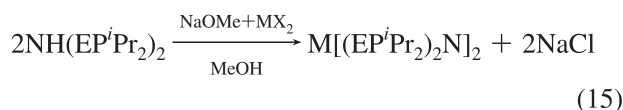

$$2NH(EP^iPr_2)_2 \xrightarrow[\text{MeOH}]{NaOMe+MX_2} M[(EP^iPr_2)_2N]_2 + 2NaCl \quad (15)$$

Imino-bis(dialkylphosphine selenide) complexes have been used in CVD.[110,111] The $[NH(SeP^iPr_2)_2]$ ligand is more thermally stable than bulky selenolate ligands, such as $[SeSi(SiMe_3)_3]^-$, and thermolysis of its complexes produces cleaner products with reduced contamination caused by undesirable ligand degradation reactions.[112,113] $[M[(EP^iPr_2)_2N]_2]$ (M = Cd, Zn; E = S, Se) and $[M[(SePPh_2)_2N]_2]$ (M = Cd, Zn) complexes have been used as precursors for zinc/cadmium selenide films by LP-MOCVD[110,111,114] at temperatures between 400 and 500 °C. The complex $[MeCd[(SeP^iPr_2)_2N]]_2$ was prepared by the comproportionation of Me_2Cd and $[Cd[(SeP^iPr_2)_2N]_2]$ in anhydrous toluene.[115] The structure of the compound (Figure 13)[115] was determined by X-ray crystallography and consists of dimeric molecular units; each diselenoimidodiphosphinate chelates to one cadmium atom and bridges to the next. Each cadmium is four coordinated and bound to three selenium atoms and one carbon.

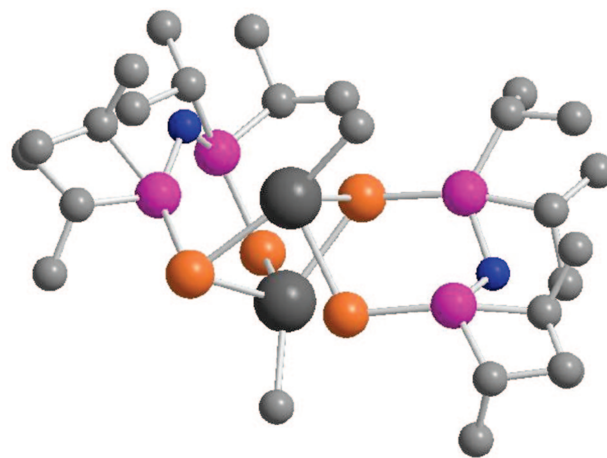

Figure 13. Structure of $[MeCd\{(SeP^iPr_2)_2N\}]_2$.

Scheme 2. Synthetic Scheme for $M[(TeP^iPr_2)_2N]_2$ (M = Cd, Hg)

$$Na[(P^iPr_2)_2N] + 2Te \xrightarrow[\text{TMEDA}]{\text{Hot Toluene}} (tmeda)Na[N(TeP^iPr_2)_2]$$

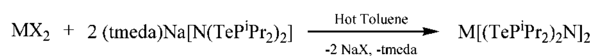

$$MX_2 + 2\,(tmeda)Na[N(TeP^iPr_2)_2] \xrightarrow[\text{-2 NaX, -tmeda}]{\text{Hot Toluene}} M[(TeP^iPr_2)_2N]_2$$

M = Cd(1), X = I; M = Hg(2), X= Cl, tmeda = tetramethylethylenediamine

AACVD of CdTe has been carried out using $[Cd[(TeP^iPr_2)_2N]_2]$ at substrate temperatures between 375 and 475 °C.[116] Synthesis of the Te analogue of $[Cd[(SeP^iPr_2)_2N]_2]$ could not be achieved by direct reaction of $NH(P^iPr_2)_2$ with tellurium. An alternative approach involved metalation of $NH(PR)_2$ with NaH prior to reaction with tellurium, which facilitates the preparation of $[Na[N(TePR_2)_2]]$ (R = Ph, ^iPr).[117,118] This reagent was then used in metathetical reactions with metal halides to generate homoleptic complexes of the type $[M[(TeP^iPr_2)_2N]_2]$ (M = Cd, Hg) (Scheme 2).[118] Although crystalline samples of these metal complexes can be handled in air for short periods, extended exposure to moisture results in decomposition, especially for powdered samples.

The AACVD of $[Hg[(TeP^iPr_2)_2N]_2]$ resulted in deposition of hexagonal tellurium,[119] which may be due to reductive elimination of mercury at higher temperatures. Previously, mercury chalcogenide compounds have been shown to produce R_2E_2 (E = S, Se, Te) and Hg under CVD conditions rather than HgE.[119−121] It is known that the anionic ligand $[(TeP^iPr_2)_2N]_2$ is readily oxidized to the ditelluride $[(TeP^iPr_2N^iPr_2PTe_2)_2]$.[121]

3.1.3.9. Dimorpholinodithioacetylacetonato Complexes. The ligand dimorpholinodithioacetylacetonate (msacmsac) was prepared by the reaction of morpholine with sulfur and allyl propyl ether at 110 °C for several hours.[122] Susequent

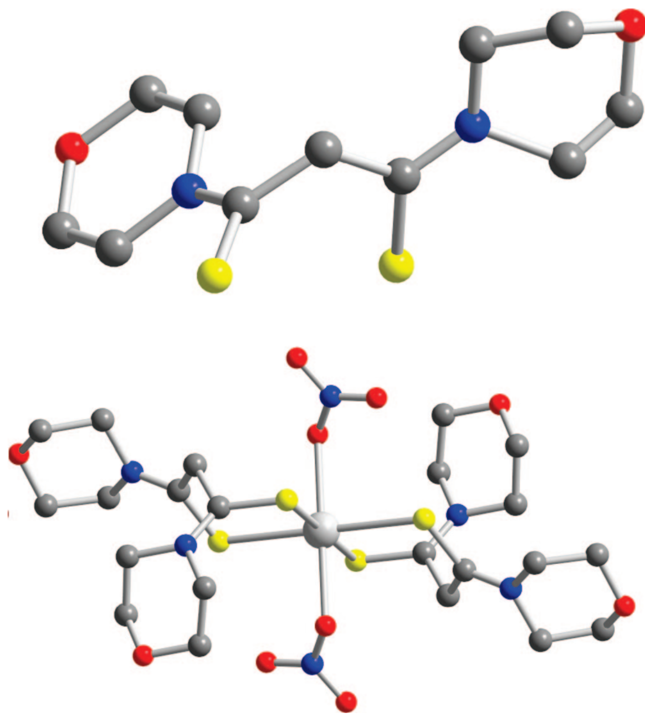

Figure 14. Structure of ligand msacmsac and cadmium complex [Cd(msacmsac)$(NO_3)_2$].

reaction of the ligand with cadmium nitrate resulted in the corresponding complex. The structure of the complex is shown in Figure 14. CdS thin films comprising of nanorods were obtained by the AACVD method.

3.1.3.10. Thiobiurets and Dithioburets. Thiobiurets and dithioburets have only recently been explored for the synthesis of metal complexes and deposition of materials including Co, Ni, Fe, Zn, Cd, In, and Cu.[123] Thioburet, dithiobiurets, and their related compounds have attracted condiderable attention due to their physiological and potential chemotherapeutic properties[124] and possible technical applications in the field of plastics and resins.[125] Armstrong et al. described the synthsis of the Zn complex of 1,1,5,5-tetraethyl-2-thiobiuret.[126]

The reaction of *N*,*N'*-dialkylcarbamyl chloride, sodium thiocyanate, and dialkylamine produced 1,1,5,5-tetraalky-l-2-thiobiuret ligand in high yield. Addition of a methanolic solution of metal acetate to this reaction gave the corresponding metal complexes. The same method was followed to prepare dithiobiuret complexes starting with *N*,*N'*-dialkylthiocarbamylchloride (Scheme 3).

The structure of zinc complex $[Zn(S_2N_3C_{10}H_{20})_2]$[127] (Figure 15) shows that it has a distorted tetrahedral geometry with ligand bite angles of 102.55(2)° and 103.41(2)°, somewhat smaller than the perfect tetrahedral angle.

All of these complexes have been used as SSP to deposit thin films of metal chalcogenides by AACVD.[127]

Scheme 3. Synthesis of Thiobiurets or Dithiobiurets Ligand and Their Metal Complexes

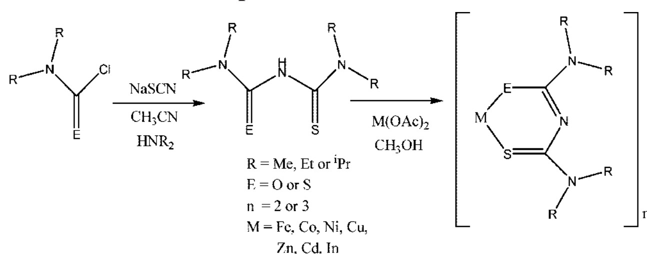

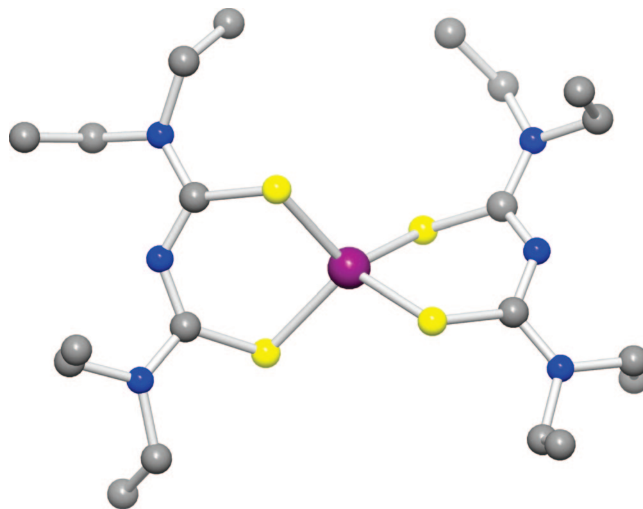

Figure 15. Structure of Zn{N$(SCNEt_2)_2$}$_2$. Alkyl groups are removed for clarity.

3.1.3.11. Thiosemicarbazide Complexes. These complexes are easily prepared by reaction of thiosemicarbazide with metal salts in hot water. The complexes are air and moisture stable and suitable as SSPs for metal sulfide thin films or nanoparticles. We reported the use of the thiosemicarbazide complex of cadmium to prepare tri-*n*-octylphosphine oxide (TOPO) capped CdS nanorods without the help of shape-directing agent.[128] Hexagonal nanoparticles of PbS have also been deposited from lead thiosemicarbazide complex by thermolysis in TOPO at 240 °C.[129] A cadmium complex of selenosemicarbazide was also synthesized and used to grow CdSe.[130]

3.2. Precursors for II–VI Nanoparticles

Steigerwald and co-workers used a high-boiling solvent to thermolyze $M(ER)_2$ (M = Zn, Cd, Hg; E = S, Se, Te; R = alkyl or aryl).[25] These complexes can be converted to the corresponding materials in their solid state by pyrolysis.[26,27] However, due to their polymeric nature, it is difficult to isolate these complexes in pure form.[131] Pyrolysis of these complexes in 4-ethylpyridine gave nanoparticles of ZnS, ZnSe, CdS, CdSe, CdTe, and HgTe, whereas the same process in the solid phase gave the corresponding bulk materials. Murray et al.[132] produced high-quality monodisperesed nanoparticles of CdSe, CdS, and CdTe by thermolyses of organometallic precursors in a high-boiling coordinating solvent. Slow growth and annealing in the coordinating solvent results in a uniform surface and regular core structure. The method involved the preparation of TOPSe or TOPTe stock solution by addition of Se or Te to TOP.[25] In one method, two separate solutions were prepared. Solution A contained dimethylcadmium in TOP, and solution B consisted of 1 M TOPSe solution. Both solutions were then mixed and injected into TOPO at 250 °C. In the second method the phosphine chalcogenide precursors were replaced by $(TMS)_2S$, $(TMS)_2Se$, and $(BDMS)_2S$, and growth was carried out at temperatures of 290–320 °C. This reaction produced TOPO-capped nanocrystallites of CdSe. The size of the particles is principally controlled mainly by the temperature of the reaction, with larger particles being obtained at higher temperatures. This TOPO method has advantages over previous synthetic methods, including producing monodispersity ($\sigma \approx 5\%$) and the ability to produce hundreds of milligrams of materials in a single

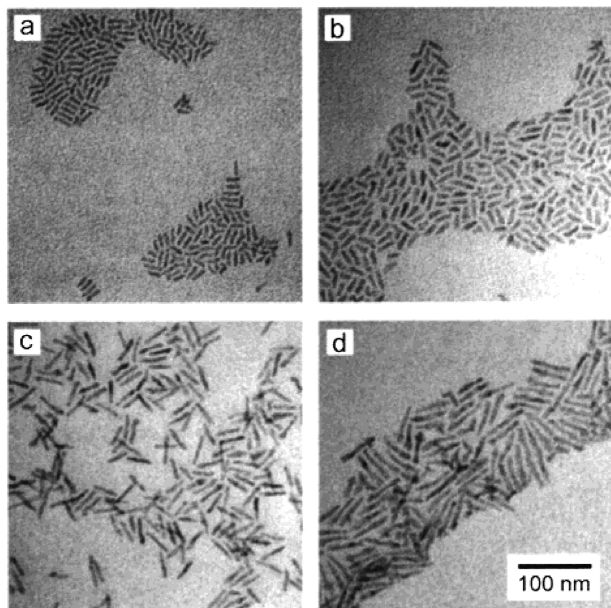

Figure 16. Transmission electron micrographs (TEMs) of the short (5.0−18 nm) CdSe core nanorods (a) and the same cores with a CdS/ZnS shell (b). TEMs of the long (4.5−36 nm) CdSe core nanorods (c) and the same cores with a CdS/ZnS shell (d).

experiment. In a series of subsequent papers interesting rod and tetrapodal structures have been grown especially in the CdSe system (Figure 16).[133] The method was readily adapted to the production of core−shell structures[134,135] and materials with high quantum efficiencies.

Numerous complexes of chalcogen-containing ligands have been studied as precursors for deposition of group II/VI compound semiconductor materials. Dithiocarbamato complexes $[M(S_2CNR_2)_2]$ (M = Zn or Cd, R = Alkyl) have been widely used to deposit ZnS or CdS thin films by MOCVD (see section 3.1.3.3), Figure 4. The dithiocarbamate ligand is a 3-electron donor ligand which has the ability to stabilize metal centers in a variety of oxidation states.[136] The complexes have a wide range of applications in the rubber industry,[137] analysis,[138] and the petrochemical industry.[139] Dithiocarbamato complexes are air stable with reasonable volatility and give clean deposition with little carbon incorporation.[60] We used $[Cd(E_2CNEt_2)]$ (E = S, Se)) (Figure 4) to synthesize CdS and CdSe nanoparticles.[140] The complexes were dissolved and refluxed in 4-ethylpyridine to produce nanomaterials. 4-Ethylpyridine is a high-boiling (168 °C,) coordinating solvent, and dilute solutions of bis(dithio- or diselenocarbamato)cadmium in it remain optically clear for days. In an extension of the TOPO method devised by Murray et al.[132,141−143] TOPO-capped CdSe and CdS nanoparticles were prepared using mixed alkyl compounds $[MeCdE_2CNEt_2]_2$ (E = S, Se).[144] These particles were also used as starting materials to prepare composite using other organic ligands such as 2,2-bipyrimidine. Using single molecular precursors clearly avoids the use of dimethylcadmium at high temperatures. The other advantage is that a variety of high-quality nanoparticles can be produced by the design of precursors. These considerations were important in the preparation of micrometric inorganic colloids[145−147] and in biomineralization[148] processes where the morphological properties were dependent on the chemical nature of the precursor. $[Cd(Se_2CNEt_2)_2]$ gave elemental selenium as the major product with some hexagonal CdSe nanoparticles, whereas $[Cd(S_2CNEt_2)_2]$ produced CdS nanoparticles.[140] Other mixed alkyl compounds of cadmium such as $[NpCd(E_2CNEt_2)]_2$ (E = S, Se) (Figure 9a) give good-quality nanoparticles of CdSe or CdS. The optical properties of CdS nanoparticles obtained from using $[Cd(S_2CNEt_2)_2]$ show a red shift as compared to those particles obtained from $[RCd(E_2CNEt_2)]_2$, indicating the larger size of particles under similar reaction conditions.[144] TOPO-capped, close to monodispersed nanoparticles of ZnSe and ZnS have been prepared by a single-source route using $[EtCd(E_2CNEt_2)]_2$[149] and $[EtZn(E_2CNEt_2)]_2$[150] as precursors. Several methods have been employed to prepare ZnSe nanoparticles including nucleation and growth from a supersaturated glass solution,[151] from nonaqueous solution,[152] and by a sol−gel process.[153]

Although high-quality nanoparticles had been synthesized using SSPs of mixed alkyl derivatives, these compounds are air sensitive and cannot be stored for long times. $[Cd(S_2CNEt_2)_2]$ has the advantage of stability for years, but the yield and quality of nanoparticles was not good. $[M(ECNMe^nHex)_2]$ (M = Cd, Zn; E = S, Se) (Figure 5 and 6) proved to be the best unsymmetrical derivatives for growth of chalogenide materials.[72] Good-quality monodispered nanoparticles of II−VI materials were synthesized in a "one-pot" synthesis in TOPO[154] using $[M(E_2CNMe^nHex)_2]$. CdSe has been extensively studied and is an attractive material because its band gap can be tuned across the visible region by varying the size of the material in the range 400−800 nm. TOPO-capped nanoparticles of CdSe were synthesized using this complex.[155−157] In a similar approach, $[Bi(S_2CNMe^nOctadecyl)_3]$ was synthesized[154] and used for the preparation of self-capped Bi_2S_3 nanoparticles. The bismuth complex was pyrolyzed in a silica vessel heated (150−300 °C) in a furnace under vacuum. The residue was dissolved in pyridine, and the nonsoluble impurities were separated by centrifugation. The resultant particles showed different colors depending on the temperature of preparation. Self-capped CdS quantum dots were prepared using the same method from $[Cd(S_2CNMe^nOctadecyl)_3]$.[155] IR and NMR spectroscopies were used to establish the nature of the capping agent. The CdS nanoparticles prepared at 150−250 °C were cubic, whereas the nanoparticles prepared at 300 °C were hexagonal.

A decomposition mechanism for dithio- and selenocarbamates has been studied by O'Brien et al.[70] and Wold et al.[73] which shows the clean elimination of ZnS from the $[Zn(S_2CNEt_2)_2]$. In contrast, the analogous diethyldiselenocarbamates have been shown to be poor sources for the deposition of ZnSe or CdSe films. Under similar reaction conditions, the diethyl precursors give selenium-contaminated films.[59] However, the mixed alkyldiselenocarbamato complexes give complex thin films of CdSe or ZnSe.[156,157]

Highly monodispersed CdSe/CdS core/shell nanoparticles have been prepared by thermolysis in TOPO using $[Cd(Se_2CN(Me)^nHex)_2]$ (250 °C for 30 min) or $[Cd(S_2CNMe^nHex)_2]$ (250 °C for 30 min) in a "one-pot" synthesis.[158,159] $[Cd(Se_2CNMe^nHex)_2]$ dissolved in TOP was injected into hot TOPO and grown for 30 min. Then a solution of $[Cd(S_2CNMe^nHex)_2]$ in TOP was injected into the deep red reaction mixture to give luminescent CdSe/CdS nanoparticles. It was first shown by O'Brien et al.[160] that nanodispersed materials could be prepared in TOPO using cadmium salts in a modification of the original route by Murray et al.[132] Peng et al.[161] further developed this method to synthesize CdTe, CdSe, and CdS nanocrystals using CdO, TOPO, and hexylphosphonic acid (HPA) or tetradecylphos-

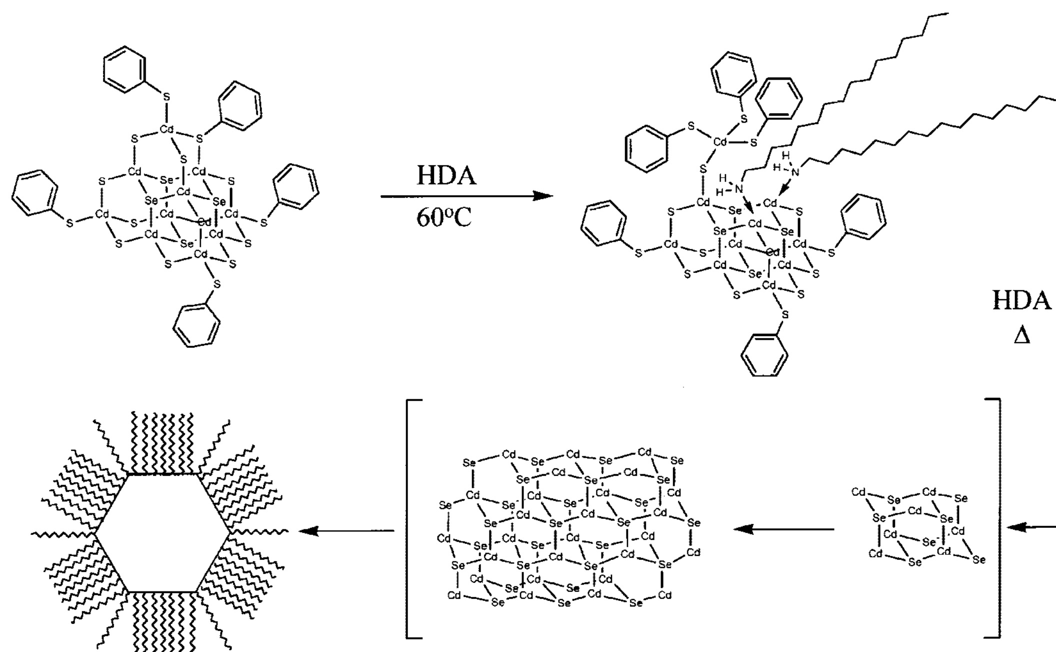

Figure 17. Proposed reaction mechanism for formation of CdSe nanocrystals from cluster precursors. The thiol and amine ligands for the clusters and nanomaterials have been minimized for clarity.

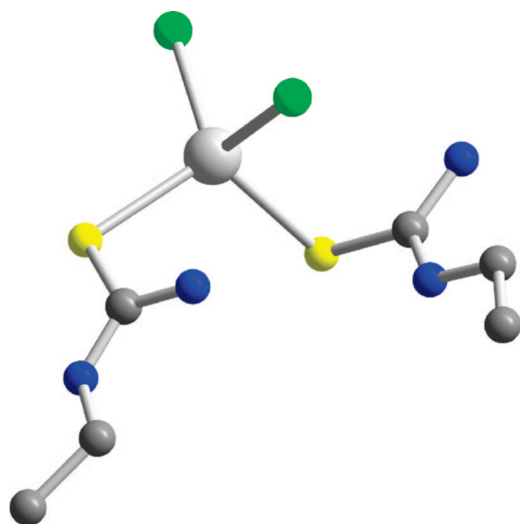

Figure 18. Molecular structure of $CdCl_2(CS(NH_2)NHCH_2CH_3)_2$.

phonic acid (TDPA) at 300 °C. Addition of tellurium, selenium, and sulfur stock solutions yielded the corresponding nanoparticles.

Air-stable inorganic molecular clusters such as $[M_{10}E_4(EPh)_{16}]^{4+}$ (where M = Cd or Zn; E = S, Se) and $[M_8E(EPh)_{16}]^{2-}$ have been prepared[162,163] and used for highly monodispersed nanoparticles (Figure 17).[164] One-step size-controlled synthesis of QDs was also carried out by the thermolysis of $Cd[(SeP^iPr_2)_2N]_2$.[107] The sizes of QDs derived from $Cd[(SeP^iPr_2)_2N]_2$ can be varied quite accurately by changing the reaction time. The dots luminesce in the visible region of the electromagnetic spectrum, and the emission wavelength varies over a wide range (up to 650 nm) depending on the particle size.

The cadmium complexes of thiourea and *N*-alkylthioureas (with alkyl groups methyl or ethyl) have been used as precursors for the preparation of TOPO-capped CdS nanoparticles (Figure 18). The precursors are air stable, easy to prepare, and inexpensive. These compounds decompose cleanly to give good-quality crystalline materials.[167] Polycrystalline ZnSe nanoparticles were synthesized from Me_2Zn:NEt_3 and H_2Se gas diluted in H_2[165] using a vapor-phase technique[166] in a counter flow jet reactor (CJR). This method provides a direct vapor-phase route for nanoparticles preparation.

Doped semiconductor nanocrystals have the potential to become mainstream emissive materials. Mn- and Cu-doped ZnSe dots can cover an emission window similar to that of CdSe nanocrystals. In the doped dots cadmium is replaced by less toxic zinc, and these dots can overcome some intrinsic disadvantages of undoped quantum dot emitters, that is, strong self-quenching caused by their small ensemble Stokes shift (energy difference between absorption spectrum and emission band)[168,169] and sensitivity to thermal, chemical, and photochemical disturbances.[170−172] These properties of undoped dots may make them less than ideal for potential applications LEDs,[173] lasers,[174] solid-state lighting,[175] beads-based barcoding,[176] and others requiring significant power and/or high density of nanocrystals. Mn-doped ZnS or CdS nanoparticles were synthesized by using $[Zn(S_2CNEt_2)_2]$ or $[Cd(S_2CNMe^nHex)_2]$ with $MnCl_2$ for ZnS:Mn and CdS:Mn particles.[177] The doping of manganese into II/VI semiconductor nanoparticles potentially gives a new class of materials.[178] Mn-doped ZnS and CdS quantum dots both have orange luminescence attributed to the spin forbidden $^4T_1-^6A_1$ electronic transition of the manganese in a tetrahedral site.[178−184] These properties are due to the strong exchange coupling between the localized moments of the paramagnetic dopant and the band electrons of the semiconductor. Most reports on Mn-doped ZnS and CdS nanoparticles use a colloidal route based on the simultaneous precipitation of both CdS (or ZnS) and MnS.[178−183] $Cd_{1-x}Mn_xS$ has also been synthesized by a coprecipitation reaction in reverse micelles.[183] Bawendi and co-workers[184] synthesized TOPO-capped Mn-doped CdSe using two different manganese precursors. They found that almost all of the manganese resides near the surface in the doped sample obtained by using manganese salts, whereas by use of an organometallic

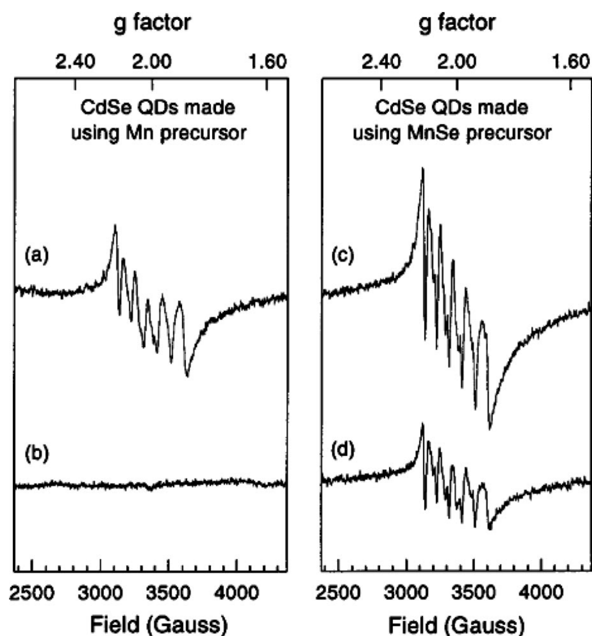

Figure 19. Low-temperature (5 K) EPR spectra of 40 Å diameter CdSe quantum dots prepared using (a and b) a Mn only precursor and (c and d) the $[Mn_2(\mu\text{-}SeMe)_2(CO)_8]$ precursor. Before purification (a and c), both samples display the 6-line pattern characteristic of Mn. After pyridine cap exchange (b and d), only the sample prepared with the MnSe precursor shows any Mn signal. The hyperfine splitting in spectrum d is 83×10^{-4} cm^{-1}.

complex $[Mn_2(\mu\text{-}SeMe)_2(CO)_8]$ manganese was incorporated in the lattice (Figure 19). Mn-doped ZnSe dots with quantum yields of 50% were also prepared from manganese stearate, TBPSe, and zinc undecylenate in octadecylamine at 240−280 °C.[185]

Cadmium diisopropyldiselenophosphinate $[Cd(^iPr_2PSe_2)_2]$ was used as a SSP in a microfluidic reactor (microcapillary tube) to deposit CdSe nanoparticles.[186] The precursor dissolved in TOP and oleylamine was injected into a reactor composed of fused silica microcapillary at 200 °C under a flow rate of 50 μL/min (residence time = 8.5 s). In order to obtain highly luminescent nanoparticles the resulting CdSe nanoparticles were mixed with $[Cd(S_2CNMe^nHex)_2]$ and reinjected into the capillary layer to obtain CdSe/CdS core−shell nanoparticles. The quantum yield increased from 12% for CdSe to 33% for CdSe/CdS. This technique has opened an easy and convenient path to mass produce high-quality semiconductor nanoparticles.

4. Precursors for III−V Materials

4.1. Precursors for III−V Thin Films

The metal−organic precursors originally employed included the volatile Group III trialkyls, trimethylgallium (Me_3Ga), trimethylaluminium (Me_3Al), and trimethylindium (Me_3In), in combination with the Group V hydride gases arsine (AsH_3) and phosphine (PH_3). The films grown from these sources showed very low carbon contamination. This observation is attributed to the large quantity of active atomic hydrogen released by the pyrolysis of AsH_3 or PH_3, which causes the clean removal of carbon-containing fragments from the growth surface.[187] A proposed reaction[187b] for the growth of GaAs from Me_3Ga and AsH_3 is given in Scheme 4.

Scheme 4. Proposed Mechanism for the Growth of GaAs from Me_3Ga and AsH_3

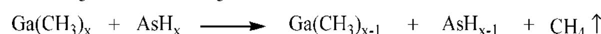

$$Ga(CH_3)_x + AsH_x \longrightarrow Ga(CH_3)_{x-1} + AsH_{x-1} + CH_4\uparrow$$

Most of the methyl radicals react with AsH species to form methane, which is easily removed from the surface as stable gas. However, a small proportion became more strongly adsorbed and subsequently decomposes, leaving carbon incorporated into the films in an electrically active form (i.e., as a p-dopant). On the basis of infrared data under UHV conditions, it has been proposed[187b] that carbon incorporation proceeds via dehydrogenation of adsorbed methyl radicals to give strongly bound carbene-like species ($=CH_2$). Further dehydrogenation of these species leads to carbon incorporation in the GaAs layers.

The concentration of carbon incorporated in GaAs grown from Me_3Ga/AsH_3 is extremely low (ca. 0.001 atomic ppm), and the layers are high purity.[188] Similarly, high-purity InP, essentially free from carbon impurities, can readily be grown from Me_3In and PH_3. There is little reason to look for alternative precursors as far as the purity of the films is concerned. However, the toxicity of these gases has stimulated research into safer liquid replacements for Group V hydride gases, and similar reasons have prompted chemists to investigate SSPs for III−V materials.

4.1.1. Alternative Group V Sources

AsH_3 and PH_3 are extremely toxic gases and stored in high-pressure cylinders, and their use needs to be carefully managed. Substantial work has been carried out[189] to develop safer liquid alternatives which disperse more slowly in the atmosphere in the case of accidental release. Trialkylarsine compounds, such as trimethylarsine (Me_3As) and triethylarsine (Et_3As), give heavily carbon-contaminated GaAs layers due to the absence of active AsH species necessary for carbon removal. Therefore, arsenic precursors which contain one or more hydrogen atoms such as the ethylarsines (Et_2AsH, $EtAsH_2$) or *tert*-butylarsine ($^tBuAsH_2$) are better. The most successful liquid arsenic source is $^tBuAsH_2$ with a convenient vapor pressure which pyrolyzes at a lower temperature than AsH_3 (50% pyrolyzed at 425 °C compared with 575 °C for AsH_3). The more efficient pyrolysis of $^tBuAsH_2$ relative to AsH_3 allows the growth of GaAs at lower V/III ratios, and the increased concentration of active AsH species on the substrate reduces carbon contamination.[187] Pyrolysis of $^tBuAsH_2$ may proceed by homolytic fission of the As−C bond to give $[C_4H_9\bullet]$ and $[AsH_2\bullet]$. Subsequent radical disproportionation, recombination, and exchange reactions produce fragments such as C_4H_8, C_4H_{10}, and C_8H_{18}.[190] In an alternative mechanism,[191] two competing decomposition pathways were identified. The dominant route was proposed to be an intramolecular hydrogen transfer in $^tBuAsH_2$, leading to elimination of C_4H_{10} and formation of [AsH] species. However, at substrate temperatures >350 °C this route is accompanied by a minor decomposition route involving β-hydride elimination of C_4H_8 and formation of AsH_3.

In addition to safety considerations, there are good technological reasons for seeking a replacement for PH_3. The high thermal stability of PH_3 (only 50% decomposed at 700 °C) in the presence of less thermally stable AsH_3 leads to problems of composition control in the growth of quaternary alloys such as InGaAsP. The trialkylphosphines (e.g., Me_3P, Et_3P) are not useful, as they are more thermally stable than

PH_3 and would in any case lead to increased carbon contamination.

The most successful alternative phosphorus source is, to date, *tert*-butylphosphine ($^tBuPH_2$),[169] which is a liquid with a convenient vapor pressure (184.9 mbar at 10 °C) suitable for a wide range of MOVPE applications. The intrinsic toxicity of $^tBuPH_2$ is lower than that of PH_3 and pyrolyzes at a significantly lower temperature (50% pyrolyzed at 450 °C), probably by homolytic phosphorus carbon bond fission. The reduced thermal stability of $^tBuPH_2$ relative to PH_3 allows the growth of InP at lower V−III ratios and leads to substantial improvements in the uniformity of the InGaAsP deposited. In addition to these advantages, $^tBuPH_2$ has more favorable gas-phase chemistry than other RPH_2 precursors, which can prereact with Me_3In, even at room temperature, to liberate methane and deposit a white solid (probably an $(MeInPR)_n$ polymer). In contrast, $^tBuPH_2$ undergoes little or no homogeneous reaction, and this effect may be due to the large steric hindrance of the bulky *tert*-butyl group, inhibiting formation of gas-phase intermediates such as $[Me_3InPH_2{}^tBu]$, likely precursors to the polymeric $(MeInPR)_n$ deposit.[187]

4.1.2. III−V Adducts

Several reviews have been published on the adduct-related complexes for III−V material deposition.[192−194] Benz et al. used III−V adducts as substitutes for highly reactive group III trialkyls,[195] and Moss and Evans used adducts as precursors but synthesized them from the components directly in the reactor in order to avoid side reactions.[196] Constant et al. proposed the use of Lewis acid−base adducts of general formula $R_2GaCl\cdot ER'_3$ (E = As, P; R and R′ = Me, Et) to overcome the problem of the high reactivity and toxicity of conventional dual sources.[197] Films of GaP[198,199] and InP[199] have been grown from the corresponding $[Et_2M-PEt_2]_3$ complexes (M = Ga, In), two cyclic trimeric molecules with covalent metal−phosphorus bonds.[200] Epitaxial growth of GaAs has been achieved using $R_2GaCl\cdot AsEt_3$ (R = Me, Et).[201] On the same kinds of substrate, MOVPE of GaAs from $(C_6F_5)Me_2Ga\cdot AsEt_3$ and $(Et_2GaCl\cdot AsEt_2)_2CH_2$ was attempted. The former gave epilayers on (111)-GaAs in the 600−700 °C temperature range, while with the latter epitaxial growth was observed on both types of substrate in the lower temperature range 500−625 °C.[202] These precursors belong to two series of compounds of general formula $(C_6F_5)_{3-x}Me_xGa\cdot AsEt_3$ (x = 0 or 2) and $(ClR_2Ga\cdot AsEt_2)_2CH_2$ (R = Me, Et),[203] whose thermal decompositions have been systematically investigated by in-situ mass spectrometric analysis of the vapor in a cold-wall CVD reactor, with He and H_2 as carrier gases.[204,205] In these studies, the role of the relative stabilities of the central M−E bond with respect to the peripheral M−ligand and E−ligand bonds was investigated through two different approaches.[192,206] The first approach involves the use of rather fragile Lewis acid−base dative bonds, whose strength can be tuned by means of the more or less electron-donating nature of alkyl groups and varied admixture of halogen (Cl) or pseudohalogen groups (C_6F_5). There are several drawbacks to this approach, such as loss in volatility and surface mobility. The second approach uses complexes with covalent M−E bonds as developed by Cowley and Jones.[207]

Scheme 5. Proposed Mechanism for the Growth of AlN from Me_3AlNH_3

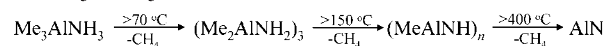

$$Me_3AlNH_3 \xrightarrow[-CH_4]{>70\,°C} (Me_2AlNH_2)_3 \xrightarrow[-CH_4]{>150\,°C} (MeAlNH)_n \xrightarrow[-CH_4]{>400\,°C} AlN$$

4.1.3. III Nitrides

The precursors for metal nitride thin films need to be as nitrogen rich as possible in order to deliver as much active nitrogen to the surface as possible to engender stoichiometric growth. A number of alkylaluminum compounds including $[Al(NR_2)_3]_2$, $[HAl(NR_2)_2]_2$ (R = Me, Et),[208]$(Et_2AlN_3)_3$,[209] $(Me_2AlNH_2)_3$,[210] and $(Me_2AlN^iPr_2)_2$[211] have been used for deposition of AlN films by CVD methods. NH_3 has also been used as a nitrogen source, but the high thermal stability of ammonia necessitates the use of high substrate temperature (>900 °C). This property leads to the loss of nitrogen in the deposited AlN thin films. The films also retain a large amount of residual carbon, which has a direct consequence on the thermal conductivity and electrical resistivity of the films.[212−214] In order to deposit stoichiometric AlN films, trimethylaluminum–ammonia adduct, Me_3AlNH_3, has been used.[215] However, films are contaminated by carbon and oxygen. In contrast to the trimeric amide $(Me_2AlNH_2)_3$, the Me_3AlNH_3 species is monomeric and can be expected to have a higher volatility and more appropriate vapor pressure for MOCVD applications. Pyrolysis studies have indicated that Me_3AlNH_3 decomposes with the evolution of methane to form alkylaluminum amides or imides which contain a strong (Al−N) bond, and the following reaction sequence (Scheme 5) was proposed.[216]

To deposit carbon-free AlN films at even lower temperature (200−250 °C), $Al_2(NMe_2)_6$ has been used in CVD experiments. Other types of compounds used for AlN films include hydrazidoalane dimers, $[R_2Al\text{-}\mu\text{-}N(H)NMe_2]_2$ (R = Me, Et).[217] All of the above-mentioned compounds require the use of NH_3 and Me_3Al. A new type of air-stable precursor, $AlCl_3{:}^tBuNH_2$, a 1:1 adduct of aluminum trichloride ($AlCl_3$) and *tert*-butyl amine ($^tBuNH_2$), has been used in MOCVD experiments.[218] The resulting AlN films have not only low carbon contamination but also a good N/Al atomic ratio. However, Cl contamination from $AlCl_3$ is another concern.

The decreasing bond strength of M−N in the series Al−N > Ga−N > In−N means the related gallium and, in particular, indium species are too unstable and dissociate in the hot zone, resulting in nonstoichiometric, poor-quality films. The amide $[Ga(NMe_2)_3]_2$ only yielded GaN films in the presence of ammonia at substrate temperatures as low as 200 °C.[219] The films are amorphous, but this result indicates that the activation energy of deposition may be lowered significantly when amide precursors are used. In particular, organometallic and inorganic azide compounds, e.g., $[R_2Ga(N_3)]_3$ (R = Me, Et),[220,221] $[(\mu\text{-}NMe_2)Ga(N_3)(NMe_2)]_2$,[222] and $[HClGaN_3]_4$,[223] have been shown to be useful precursors for nitride layers. The azide unit appears to be a very good choice to introduce the nitrogen component. A major drawback of azide derivatives is their potential for exothermic decomposition. Nitrogen-rich compounds such as (H_2GaN_3)[224,225] and $(N_3)_3Ga(R)$ (R = Me, Et)[226] may even detonate under certain conditions. Hydrolysis of the $M-N_3$ bond can take place to produce explosive hydrazoic acid, which represents a major challenge in view of the technical use of azide-type compounds. In order to overcome some of the technical difficulties, the intramolecularly Lewis base-stabilized compound $[(N_3)_2Ga(CH_2)_3NMe_2]$ has been synthesized.[227] Transparent

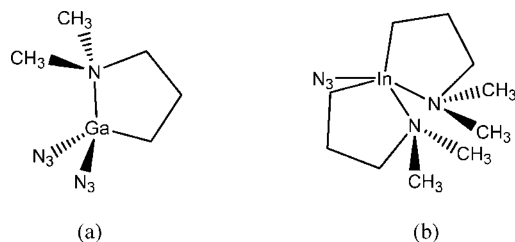

Figure 20. Molecular structures of (a) $[(N_3)_2Ga(CH_2)_3NMe_2]$ and (b) $(N_3)In[(CH_2)_3NMe_2]_2$.

GaN films have been grown from the compound in a cold-wall reactor with or without the use of ammonia. Films deposited without using ammonia contained a small amount of carbon, while the presence of ammonia prevented the incorporation of carbon into the films. In order to obtain information on the decomposition pathway of $[(N_3)_2Ga(CH_2)_3NMe_2]$, (Figure 20a) composition of the gas phase in the boundary layer above the substrate was monitored[228] and species such as $HGaN_6$, GaN_6, $HGaN_2$, and GaN_2 were detected. The data gave clear evidence for the production of nitrogen-rich species in the boundary layer.

Kim et al. synthesized a Lewis acid−base adduct $[Et_2Ga(N_3).MeHNNH_2]$ of (H_2GaN_3) and deposited epitaxial *h*-GaN films on Si(111) substrate by MOCVD.[229] It has been demonstrated that the precursor undergoes protonation of the ethyl ligands by methylhydrazine, and this occurs via loss of the stable N_2, C_2H_6, and MeNNH, yielding good-quality GaN films with little contamination. Other electron-donor ligands such as hydrazine[230] and methylamine[231] have also been employed to increase the volatility and stability of compounds followed by their subsequent use in MOCVD experiments for GaN films (eqs 16 and 17).

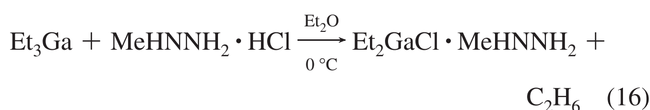

$$Et_3Ga + MeHNNH_2 \cdot HCl \xrightarrow[0\ ^\circ C]{Et_2O} Et_2GaCl \cdot MeHNNH_2 + C_2H_6 \quad (16)$$

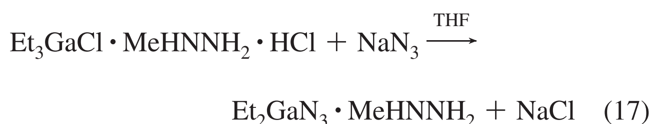

$$Et_3GaCl \cdot MeHNNH_2 \cdot HCl + NaN_3 \xrightarrow{THF} Et_2GaN_3 \cdot MeHNNH_2 + NaCl \quad (17)$$

Among the Group III nitrides, growth of InN is most difficult to achieve because of its low decomposition temperature, and hence, a low growth temperature is essential for InN films.[232] Deposition of InN can be achieved at 300−400 °C with $[(N_3)In[(CH_2)_3NMe_2]_2$ (Figure 20b).[233] Due to the intermolecular Lewis base adduct stabilization, the compound is not pyrophoric or explosive and even air stable (melting point 340 K). At higher temperatures, the gas phase is dominated by In atoms. The In−N bond energy of indium azides or indium amides as well as the dissociation energy of the diatomic species InN is significantly larger than for In−C or weak donor−acceptor adducts. Therefore, conventional indium precursors preferentially produce indium atoms at the usual growth temperatures. Dimeric dimethylindium azide, $[Me_2In(\mu\text{-}N_3)]_2$, prepared from reaction of Me_3In with NH_3 has been used in LP-MOCVD experiments to yield hexagonal InN films on Si(111) substrates in the temperature range 350−450 °C.[234]

Boron nitride (BN) has also received considerable interest due to its technological applications and excellent material properties: high hardness, chemical inertness, and dielectric behavior. A number of physical and chemical techniques have been used to deposit cubic BN;[235] however, there remains a problem in controlling the boron and nitrogen ratio. To control the composition, Boo et al. synthesized a number of compounds, namely, borane−triethylamine, tris(*sec*-butyl)borane,[236] and isopropyl amine and *tert*-butylamine complexes of trietylborane. In the latter case, polycrystalline, crack-free hexagonal BN films have been deposited on Si(100) substrates at 850 °C, and importantly, films retain the desired B:N ratio (1:1).[237] A wide band gap (5.8 eV) is also calculated from the optical transmittance data, and carbon contamination in the films lowers the transmittance. The use of tris(dimethylamino)borane in the presence of ammonia and hydrogen gases has also been demonstrated in CVD to deposit hexagonal BN films and retain correct stoichiometry.[238]

4.1.4. III Phosphides and Arsenides

The chemistry involving a covalent M−E bond was pioneered by Beachly[239,240] and extensively studied by Cowley and Jones,[241−243] Maury,[244,245] and Wells.[246−248] These compounds were prepared to investigate their potential as precursors for the CVD of III/V semiconducting materials. Many of the complexes prepared were used to grow thin films of materials such as GaAs.[249] The structures for these complexes are shown in Figure 21.

Cowley and Jones focused on the design and synthesis of organometallics that feature σ-bonding between Group III and group V elements.[207] Their work on GaAs was reviewed in 1994 as an illustration of the concept of a SSP.[193] They successively tested three tetranuclear precursors: $[Me_2Ga(\mu\text{-}As^tBu_2)]_2$,[207,241,250−252] $[Et_2Ga(\mu\text{-}As^tBu_2)]_2$,[193] and $[Ga(As^tBu_2)_3]$.[252] Both $[Me_2Ga(\mu\text{-}As^tBu_2)]_2$ and $[Et_2Ga(\mu\text{-}As^tBu_2)]_2$ have a (M_2E_2) ring in their solid-state structures.

Preparation of these dimeric precursors[243] involved reaction of di-*tert*-butylarsine and trimethylgallium or triethylindium. This method involves preparation of Grignard, its reaction with arsenic trichloride to obtain $^tBu_2AsCl$, which is then hydrogenated by $LiAlH_4$ to give di-*tert*-butylarsine.[253] A slightly modified method was reported by O'Brien et al.,[254,255] where instead of reacting trimethylgallium and di-*tert*-butylarsine at 57 °C for 4 days as reported by Cowley et al.[243] the reactants were dissolved in diethyl ether and

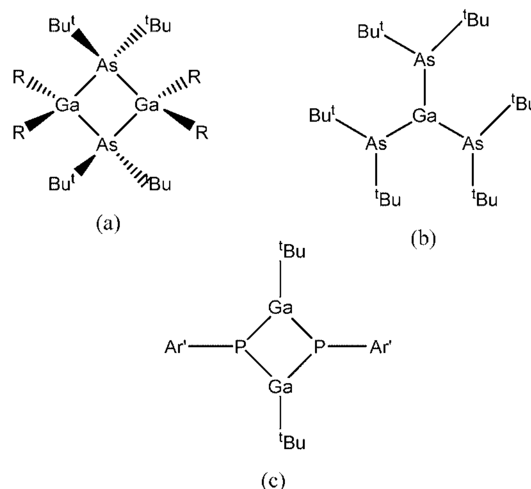

Figure 21. Structure of single-source precursors for III−V materials.

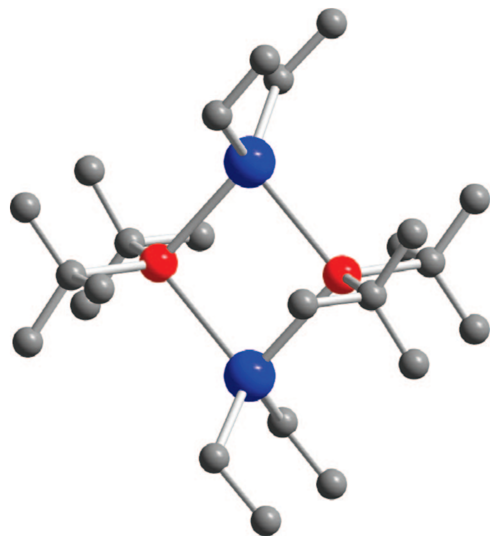

Figure 22. Structures of [^{t}Bu$_2$AsGaMe$_2$]$_2$.

refluxed at 40 °C for 3 days. X-ray single-crystal structures of [^{t}Bu$_2$AsGaMe$_2$]$_2$[254] and [^{t}Bu$_2$AsInEt$_2$]$_2$[255] are shown in Figure 22.

[Me$_2$Ga(μ-As^{t}Bu$_2$)]$_2$ was used to deposit GaAs thin films by LP-CVD at a precursor delivery temperature of 145 °C and deposition temperature of 450−700 °C using H_2 or He as the carrier gas. The films deposited were arsenic deficient.[250] Substitution of ethyl groups for methyl is known to lower carbon contamination. Epitaxial films were obtained from [Et$_2$Ga(μ-As^{t}Bu$_2$)]$_2$ over the temperature range 400−500 °C but showed low Hall mobilities due to the presence of Ga islands caused by highly reactive ethylgallium species.[193] The use of Ga(As^{t}Bu$_2$)$_3$, which contains an excess of arsenic and no gallium−carbon bonds, produced films with carbon levels about two orders of magnitude lower than from the methyl derivative ([Me$_2$Ga(μ-As^{t}Bu$_2$)]$_2$). The excess of arsenic in the precursors gave rise to n-type films, while they were p-type with [Me$_2$Ga(μ-As^{t}Bu$_2$)]$_2$ or [Et$_2$Ga(μ-As^{t}Bu$_2$)]$_2$).[252] Pyrolysis[251,256] and temperature-programmed desorption[252] studies suggest two modes of decomposition for these precursors: As−C bond hydrogenesis to form ^{t}Bu radicals and β-H elimination from ^{t}BuAs moieties followed by $CH_3 \cdots H$ coupling at Ga to form isobutene and methane.

Trimeric hexanuclear complexes such as [Me$_2$Ga(μ-AsMe$_2$)]$_3$ and [Me$_2$Ga(μ-As^{i}Pr$_2$)]$_3$ failed to give GaAs films because of the facile loss of tetraalkyldiarsine, as shown by pyrolysis studies.[256,257] [^{n}Bu$_2$Ga(μ-As^{t}Bu$_2$)]$_2$ has been used to grow epitaxial GaAs either by ultrahigh vacuum MOCVD[258] or by spray pyrolysis.[259] Films of InP have been prepared by Cowley et al.[207,241] and Bradley and coworkers,[260] independently, from the same tetranuclear molecule, [Me$_2$In−P^{t}Bu$_2$]$_2$. Cowley et al.[207,241] carried out the deposition studies at temperatures between 450 and 700 °C in a cold-wall reactor with H_2 or He as the carrier gas. Bradley et al.[260] used an MBE reactor and found that stoichiometric growth was only possible at 480 °C with a simultaneous flux of dissociated phosphine. Indium-rich films were obtained at lower temperature.

4.1.5. III Antimonides

Cowley et al. deposited GaSb and InSb films on Si(100) wafers at 450 °C from six-membered heterocycles of the type [Me$_2$MSb^{t}Bu$_2$]$_3$ (M = Ga, In) in a horizontal hot-wall MOCVD reactor under high-vacuum conditions (10^{-3} mbar).[261] AlSb films on Si(100) and polycrystalline Al_2O_3 substrates have been reported in a cold-wall MOCVD reactor between 300 and 550 °C using [Et$_2$AlSb(SiMe$_3$)$_2$]$_2$ or [^{i}Bu$_2$AlSb(SiMe$_3$)$_2$]$_2$.[262] A large amount of Si contamination has been observed, which is likely to originate from a fragmentation reaction of the SiMe$_3$. Schulz and his group reported alkyl-substituted heterocycles of the type [R$_2$MSbR′$_2$]$_x$ (M = Ga, In; x = 2, 3) by a novel reaction pathway termed a distibine cleavage reaction. Distibines Sb$_2$R$_4$ (R = Me, Et, ^{i}Pr, ^{n}Pr) were found to react with trialkylgallanes and indanes MR′$_3$ (M = Ga, In) with formation of the corresponding Lewis acid−base adduct [R′$_3$M]$_x$[Sb$_2$R$_4$], which then consequently undergoes a Sb−Sb bond cleavage reaction with formation of the four- or six-membered heterocycle [R$_2$MSbR′$_2$]$_x$.[263−265] Crystalline GaSb films were deposited from [^{t}BuGaSbEt$_2$] in a cold-wall MOCVD reactor without the need for any carrier gas, and the best results were obtained at substrate temperatures between 400 and 500 °C (Figure 23).[266]

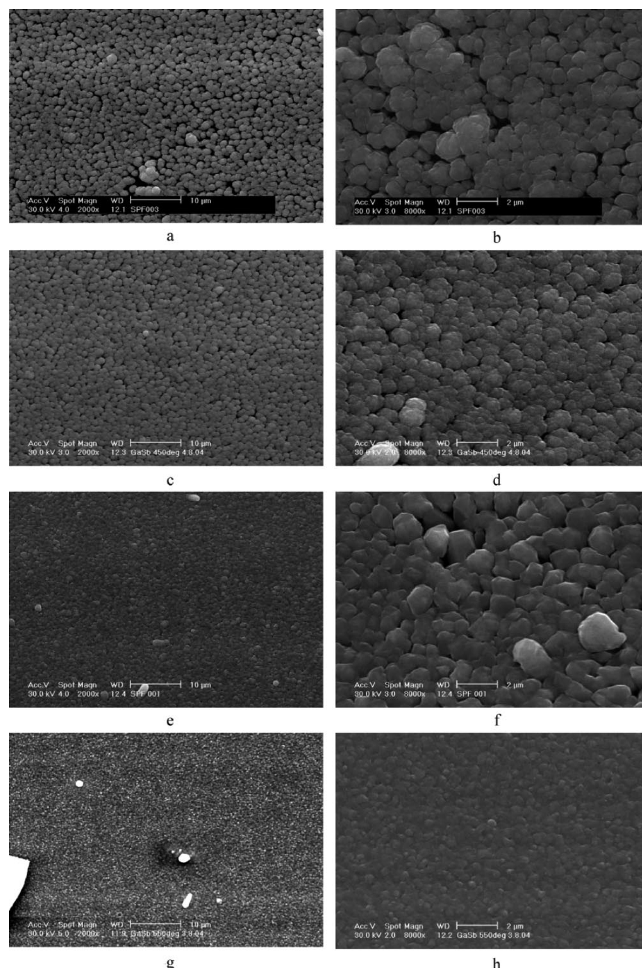

Figure 23. SEM images displaying the surface morphology of GaSb films grown from [^{t}Bu$_2$GaSbEt$_2$]$_2$ at 400 (a and b), 450 (c and d), 500 (e and f), and 550 °C (g and h).

4.2. Precursors for III−V Nanoparticles

Colloidal methods have been used for the preparation of AlN, GaN, and InN nanoparticles. GaN nanocrystals have been prepared by thermal decomposition of compounds including polymeric gallium imide, {Ga(NH)$_{3/2}$}$_n$, and gallium azides, [Et$_2$GaN$_3$]$_3$, (N$_3$)$_2$Ga[(CH$_2$)$_3$NMe$_2$], or (Et$_3$N)Ga(N$_3$)$_3$.[267−269] The amount of azide precursors used affects the size of the

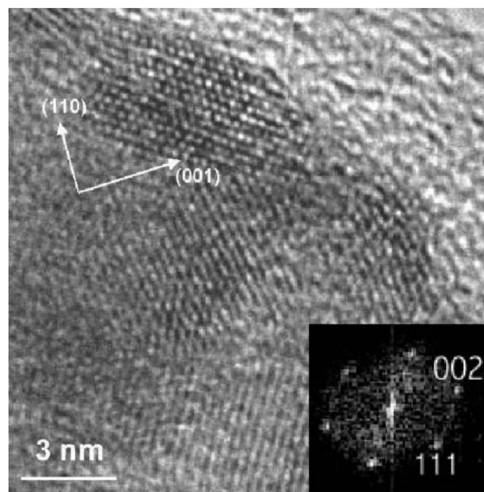

Figure 24. HR-TEM image of InN nanoparticles. The principal zone axes of the cubic unit cell are indicated for the top particle. (Inset) Fourier transform electron diffraction pattern of the particle in the top of the image.

particles, which are usually 20−200 nm agglomerates with nanocrystalline domains of ∼4 nm. The use of poly(imidogallane) precursor for production of GaN requires difficult and hazardous manipulation of pure ammonia.[267] The complex has poor solubility, which is detrimental to particle size control. At high temperature in coordinating solvent only a small percentage of nanosized material is obtained. Pyrolysis of this compound gave GaN.[270] The new method not only significantly improved the yield of colloidal GaN nanocrystals but also eliminated the need for ammonia. This effect is probably due to the good solubility of the dimeric compound and the ability of the coordinating ligands to cap the particle surfaces as soon as GaN nuclei are formed. The pyrolysis reaction appears to involve transamination by hexadecylamine (HDA). In the absence of HDA in the reaction mixture, no GaN is produced.[270] Adducts of metal chlorides and urea such as $[M(H_2NCONH_2)_6]Cl_3$ (M = Al, Ga) and $In(H_2NCONH_2)_3Cl_3$ have been used to form wurtzic (hexagonal) nanocrystals of AlN, GaN, and InN by refluxing the precursors in *n*-trioctylamine.[271] GaN nanocrystals with 2−3 nm in diameter exhibited two emissions bands centered at ca. 380 and 340 nm. In the case of indium precursor, a small proportion of indium oxide is also grown. Similar to $(N_3)_2Ga[(CH_2)_3NMe_2]$, the indium analogue decomposes in TOPO to yield cubic InN nanoparticles in the 2−10 nm size range (Figure 24).[272] Fractionated particles with an average diameter of 4.5 nm exhibited luminescence at 690 nm (1.82 eV), consistent with the band gap of the bulk material being near 0.7 eV. These are the first InN particles in which near band-gap emission was observed.

Solvothermal synthesis of wurtzite InN nanocrystals from $InBr_3$ and NaN_3 is reported in superheated toluene and refluxing in hexadecane at 280 °C.[273] InN from hexadecane and lower temperature toluene reactions produced less crystalline nanoparticles with a zinc blende (cubic) component. Mixed indium and gallium azide precursors in toluene produced mixed metal nitrides, $Ga_{1-x}In_xN$, where x is 0.5 and 0.75. Both InN and Ga−In−N systems showed red- and green-filtered visible fluorescence emission. A mixture of cubic and hexagonal (InGa)N particles has also been reported by ammonolysis of the precursor ammonium hexafluoroindategallate $[(NH_4)_3In_{1-x}Ga_xF_6]$.[274] The ratio of cubic to hexagonal material is ∼9:1. The material exhibited photoluminescence in the visible region around 735 nm (1.69 eV) at room temperature.

InP and GaP nanocrystals were synthesized from diorganophosphides $[M(P^tBu_2)_3]$ (M = Ga, In).[275,276] Thermolysis in dry alkylpyridine results in formation of capped nanoparticles which exhibited distinct optical quantum size effects. The decomposition mechanism of precursors involved a complicated mix of reductive and β-hydrogen elimination, resulting in metal phosphide and metallic impurities. Wells et al. reported GaP nanoparticulates by thermolysis of $[X_2GaP(SiMe_3)_2]_2$ (X = Br, I) or $(Cl_3Ga_2P)_n$, both decomposing at relatively low temperatures under vacuum to yield crystalline monodispersed GaP.[277] Thermolysis of $[H_2GaE(SiMe_3)_2]_3$ (E = P, As) at 450 °C in xylene also gave nanoparticles of GaP or GaAs approximately 5 nm in diameter.[278] HDA-capped InAs and GaAs nanoparticles can be efficiently synthesized from dimeric compounds $[^tBu_2AsInEt_2]_2$ and $[^tBu_2AsGaMe_2]_2$, respectively.[279,280] In both cases, nanoparticles show a considerable blue shift in their optical spectra as compared to parent bulk materials.

5. Precursors for III−VI Materials

5.1. Precursors for III−VI Thin Films

The Group III and VI elements form compounds with several stoichiometries and in a number of phases: M_2E_3 (M = Ga, In; E = S, Se, Te), a zinc-blende type (M = Ga) and a defect spinel (M = In) and ME (with the same layered structure as in M_2E_3).[281] The III−VI materials are alternatives to those in the II−VI series, especially in photovoltaic applications. However, their polytypism and the variety of stoichiometries accessible are a problem as compared to the II−VI materials, and the availability of some of the elements, notably indium, is somewhat limited.

5.1.1. Thiolato Complexes

Preparation of III−VI thin films started with the use of a single-source system[282,283] unlike the II−VI or III−V materials for which growth of the films was initially carried out using two sources. Indium and gallium thiolato complexes are typically involatile polymeric aggregates similar to those formed by Group 12 thiolates.[284] Nomura et al. successfully prepared dimeric volatile alkylindium alkyl thiolates by introducing steric bulk at both the alkyl and the thiolate.[285] These compounds are typically liquids at room temperature and can be distilled under reduced pressure ($>10^{-3}$ Torr). Deposition of the two different types of indium sulfide was controlled by the number of thiolate ligands bound to the indium atom; dialkylindium monothiolates give InS, and monoalkylindium dithiolates produce β-In_2S_3 at 300 °C under static pyrolysis conditions. Nomura's group used $^nBu_2In(S^iPr)$ as a source for indium sulfide deposition, and highly orientated films of β-In_2S_3 with a strongly preferred (103) growth direction were deposited on Si(111) or quartz substrates at temperatures in the range 300−400 °C.[286] Orthorhombic InS films could be deposited at lower temperatures using $Bu_2In(SPr)$ as a source, but the presence of trace amounts of oxygen in the carrier gas caused partial oxidation of the InS layers, leading to highly conductive films of indium oxide doped with sulfur at 275 °C.[287]

Barron and co-workers deposited a novel metastable cubic GaS phase from the $[^tBuGaS]_4$ cube at temperatures in the region of 400 °C; in this case it is tempting to draw a

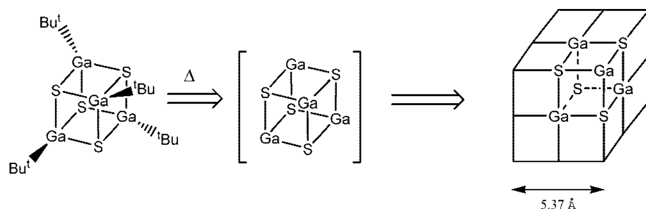

Figure 25. Cubic structure of [^{t}BuGaS]$_4$.

correlation between the cubic phase observed and the cubane structure of the precursor as shown in Figure 25.[288,289] Another interpretation of this observation is that the films deposited are extremely sulfur deficient as deposition also led to an amorphous gallium containing ca. 20% sulfur and that the phase deposited is driven by the ratio of pnictide to metal delivered to the substrate.

In related work the dimeric indium thiolate [^{t}BuIn(μ-S^{t}Bu)]$_2$was used to deposit a polycrystalline, tetragonal high-pressure form of β-In_2S_3.[288,289] The authors believe that the cubic GaS films might be useful as a passivation layer on GaAs wafers. The gallium sulfide cubane can be prepared by reaction of Ga^{t}Bu$_3$ with H_2S followed by static pyrolysis at 45 °C.[289] Gysling et al. deposited thin films of a novel cubic InSe (300−250 °C) and the known hexagonal In_2Se_3 (470−530 °C) on GaAs(100) by a modified MOCVD method using a sonicated spray evaporator from $Me_2InSePh$ and $In(SePh)_3$ as precursors. The structures of the precursors are unknown, and the spray MOCVD process was developed to deal with the relatively low volatility of the precursors.[290]

5.1.2. Thiocarbamato Complexes

Films of indium sulfide have been grown from dimethyl-, diethyl-, or dineopentyl-indium diethyldithiocarbamates ([$R_2InS_2CNEt_2$] with R = Me, Et, or Np), which are air-sensitive compounds.[291,292] The films were grown on (100)-GaAs substrates using a cold-wall, low-pressure reactor. The methyl complex deposits orthorhombic InS and monoclinic In_6S_7 phases between 425 and 400 °C, whereas growth at 325 °C results in cubic β-In_2S_3. In contrast, the ethyl compound deposits monophasic, crystalline β-In_2S_3 over the range 350−400 °C. These results show the role played by the change of alkyl groups. They suggest that the amount of carbon incorporation, which relates to the β-H elimination process, may well influence the film's composition. Experiments with related gallium precursors were less conclusive.

Tris complexes of indium [In(E_2CNMeR)$_3$] have been used in experiments where E = S with R = ^{n}butyl or ^{n}hexyl and E = Se with R = ^{n}hexyl.[292] In_2S_3 films were grown from [In(S_2CNMe^{n}Bu)$_3$] or [In(S_2CNMe^{n}Hex)$_3$] at 450−500 °C onto glass, GaAs, or InP by LP-MOCVD.[293] Cubic α-In_2Se_3 was the predominant phase, sometimes mixed with some hexagonal β-In_2Se_3 phase when the n-butyl derivative was used. Deposition of predominately α-In_2Se_3 regardless of growth conditions shows a clean gas-phase decomposition process. In_2S_3 nanorods with an average diameter of 20 nm and 400−500 nm length were prepared for the first time on glass substrates from a single-source precursor, [Et_2InS_2CNMe^{n}Bu], by AACVD at 375 °C without either template or catalyst.[294]

5.1.3. Xanthato and Monothiocarbamato Complexes

[In(S_2CO^{i}Pr)$_3$] is a volatile complex from which thin films of cubic α-In_2S_3 could be grown at temperatures as low as

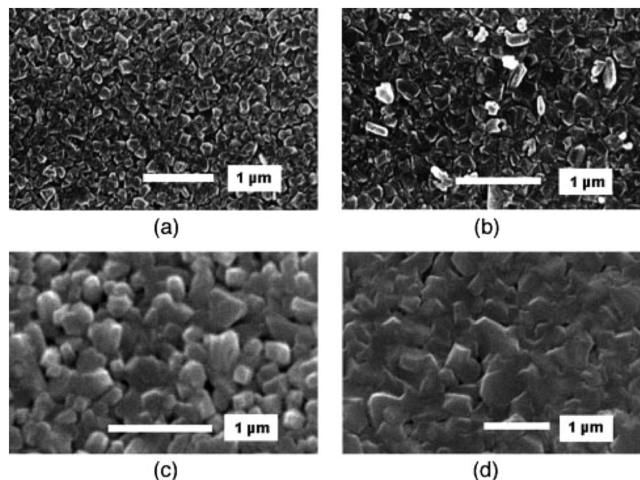

Figure 26. SEM images of β-In_2S_3 films deposited from [In(SOC-N^{i}Pr$_2$)$_3$] at (a) 300, (b) 350, (c) 400, and (d) 450 °C on glass substrates (note, amorphous at 300 °C).

210 °C. Films deposited on glass were (111)-orientated.[295] These results are interesting with regard to the deposition of the related ternary $CuInS_2$ and $CuInSe_2$ using complexes of the type [M[E_2CNMeR]$_n$], where R = ^{n}Bu and ^{n}Hex, M = Cu (n = 2) and In (n = 3).[296] Thin films of In_2S_3 have been produced from [In(SOCNEt$_2$)$_3$][297] and [In(SOCN^i-Pr$_2$)$_3$][298] on glass substrates by LP-MOCVD. [In(SOCN^{i}Pr$_2$)$_3$] proved to be both more volatile and more efficient for film delivery than [In(SOCNEt$_2$)$_3$]. The former led to the tetragonal β-phase at temperatures as low as 350 °C and the latter to the cubic β-phase at 400 °C and above (Figure 26). Hampden-Smith and co-workers used the facile elimination of thioacetic anhydride from polyether adducts of group 2 metal thioacetates to deposit high-purity, stoichiometric metal sulfides[299] and applied it to adducts of gallium and indium thioacetates.[300] Two gallium complexes, MeGa(SCOMe)$_2$-(dmp) and Ga(SCOMe)$_3$(dmp) (dmp = 3,5-dimethylpyridine), and an indium complex, [Hdmp]$^+$[In(SCOCH$_3$)$_4$]$^-$ [301] have been used by the AACVD method to prepare thin films of the metal sesquisulfides. The respective proposed decomposition pathways for the gallium and indium complexes are shown in eqs 18−20.

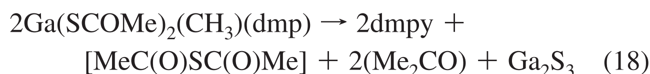

$$2Ga(SCOMe)_2(CH_3)(dmp) \rightarrow 2dmpy + [MeC(O)SC(O)Me] + 2(Me_2CO) + Ga_2S_3 \quad (18)$$

$$2Ga(SCOMe)_2(dmp) \rightarrow 2dmpy + 3[MeC(O)SC(O)Me] + Ga_2S_3 \quad (19)$$

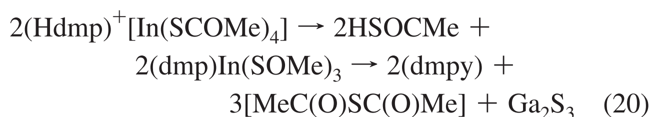

$$2(Hdmp)^+[In(SCOMe)_4] \rightarrow 2HSOCMe + 2(dmp)In(SOMe)_3 \rightarrow 2(dmpy) + 3[MeC(O)SC(O)Me] + Ga_2S_3 \quad (20)$$

5.1.4. Dichalcogenoimidodiphosphinato Complexes

The compounds [M(μ-Te)N(^{i}Pr$_2$PTe)$_2$]$_3$ (M = In, Ga) have been employed to deposit M_2E_3 films onto glass and Si(100) substrates at deposition temperatures between 325 and 475 °C.[302] The indium precursor gave cubic In_2Te_3 exclusively, whereas the gallium complex generated a mixture of cubic Ga_2Te_3, monoclinic GaTe, and hexagonal Te. Mass spectrometric studies indicate that fragmentation of the indium precursor to give In_2Te_3 is accompanied by formation of [In[N(^{i}Pr$_2$PTe)$_2$]$_2$]$^+$ and [N(^{i}Pr$_2$PTe)$_2$]$^-{}_2$. These complexes are

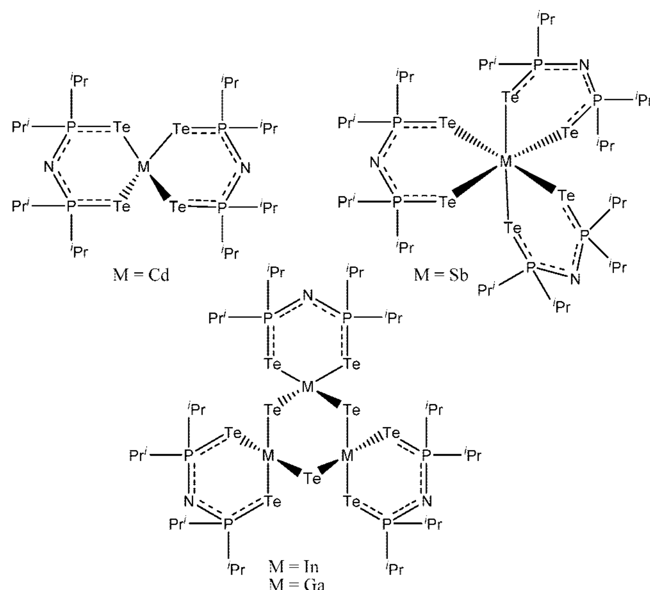

Figure 27. Molecular structures of $Cd[(SeP^{i}Pr_2)_2N]_2$, $Sb[(TeP^{i}Pr_2)_2N]_3$, and $[M(\mu\text{-}Te)[N(^{i}Pr_2PTe)_2]]_3$ (M = In, Ga).

Scheme 6. General Synthesis of Tellurium Derivatives

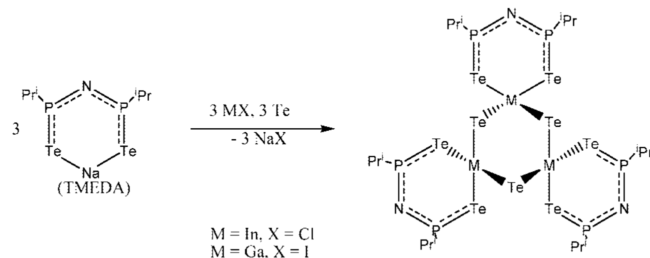

structurally different from the earlier homoleptic Cd precursors of the $[N(^{i}Pr_2PTe)_2]_2$, which contain a central preformed M_3Te_3 (M = In, Ga) ring, with each tetrahedral metal center further coordinated by a $[N(^{i}Pr_2PTe)_2]_2$ ligand (Figure 27).[303] The general method of synthesis is shown in Scheme 6.

The TGA of these complexes showed them to decompose in a single step between 300 and 375 °C for indium complex and 280 and 360 °C for gallium complex. Both precursors afford a significantly large residue (59% for indium complex, 58% for gallium complex), indicating incomplete decomposition or the presence of impurities after decomposition of precursor. The structures of most common ligands used for the preparation of different metal complexes are given Figure 28.

5.2. Precursors for III−VI Nanoparticles

Dimitirjevic and Kamat prepared colloids of In_2Se_3 stabilized with either poly(vinyl alcohol) (PVA) or sodium metaphosphate (SMP).[304] They reported particles with diameters of approximately 2−3 (SMP stabilized) and 30 nm (PVA stabilized) with absorption maxima at 375 and 250 nm (SMP stabilized) and an onset of absorption at approximately 550 nm (PVA stabilized). The same authors reported the synthesis of In_2S_3 colloids in acetonitrile, with particle diameters ranging between 100 and 200 nm.[305] Barron et al.[306] reported the preparation of nanoparticles of GaSe and InSe by MOCVD using the cubane precursors $[(^{t}Bu)GaSe]_4$ and $[(EtMe_2C)InSe]_4$. The GaSe particles had a mean diameter of 42 nm with a standard deviation of 13 nm, whereas the spherical InSe particles were 88 nm in

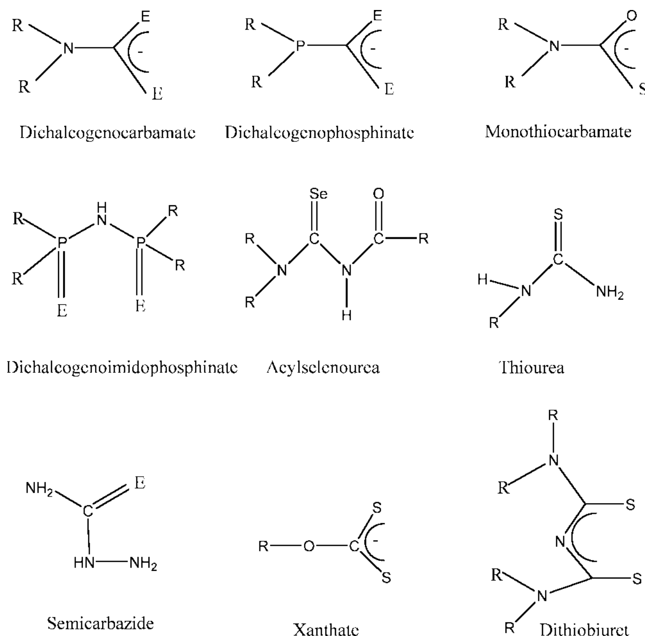

Figure 28. Some common ligands used for metal complexation.

diameter with a standard deviation of 30 nm. The particle size was determined by TEM, and no optical data was reported. O'Brien et al.[307] reported the synthesis of InS and InSe nanoparticles capped with TOPO and nanoparticles of InSe capped with 4-ethylpyridine (Figure 29) from $[In(E_2CNEt_2)_3]$ (E = S, Se).

GaSe nanoparticles (2−6 nm) were prepared from Me_3Ga and TOPSe in a high-boiling solution of TOP and TOPO.[308] GaSe has a hexagonal layered structure[309] consisting of Se−Ga−Ga−Se sheets which are only weakly attracted by van der Waals interactions. GaSe can be either β, γ, or ε phase depending upon the arrangement of layers. GaSe nanoparticles (88 nm) were also synthesized from $(RGaSe)_4$ cubanes by the MOCVD method.[310] TEM images showed nanowire-type structures.

Dutta et al. reported the preparation of In_2S_3 nanoparticles from SSPs such as indium xanthates.[311] The same authors previously used methylindium thiolate complexes but produced indium sulfide nanoparticles of poor quality.[312] Recently, they used polymeric indium and gallium precursors synthesized by reaction of trimethyl gallium/indium ether adduct ($Me_3Ga/InOEt_2$) with 1,2-ethanedithiol ($HSCH_2CH_2SH$) in 1:1 stoichiometry. Ga_2S_3 and In_2S_3 nanoparticles were prepared by pyrolysis of these precursors $[MeM(SCH_2CH_2S)]_n$ (M = In, Ga) in a tube furnace between 300 and 500 °C.[313]

6. Precursors for IV−VI Materials

6.1. Precursors for IV−VI Thin Films

Tin and lead chalcogenates are narrow band-gap semiconductor materials and have attracted considerable interest recently due to their many potential applications. Cubic PbS has been deposited from several lead dithiocarbamato complexes. PbS films have been deposited from $[Pb(S_2CNEt_2)_2]$ in the temperature range 425−500 °C with a source temperature of 210 °C and in the temperature range 230−300 °C by remote plasma-enhanced MOCVD.[314] Due to its volatility, $[Pb(S_2CN^{n}Bu_2)_2]$ was used from among

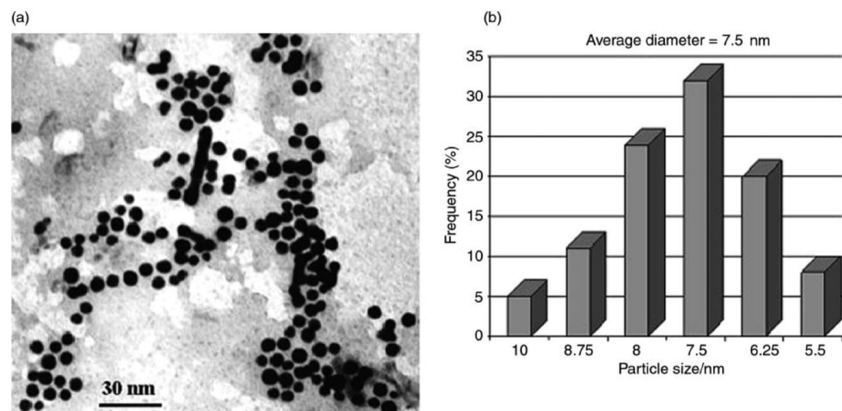

Figure 29. 4-Ethylpyridine-capped InSe nanoparticles from $[In(Se_2CNEt_2)_3]$: (a) TEM micrograph and (b) size distribution histogram.

Scheme 7. Synthetic Scheme for $Pb[(TeP^iPr_2)_2N]_2$

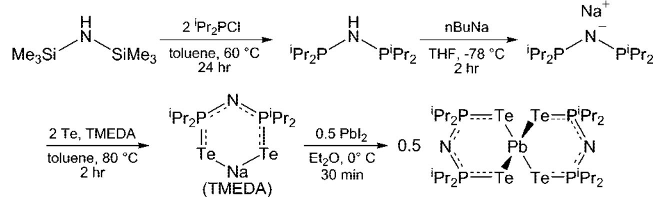

several dithiocarbamato complexes to deposit PbS films onto glass and Si(100) in the temperature range 400−600 °C.[315] Asymmetric derivatives of lead dithiocarbamates $[Pb(S_2CNRR')_2]$ (R = Me, Et; R′ = ^{i}Pr, ^{n}Bu) also proved to be useful in LP-MOCVD and AACVD experiments to deposit cubic PbS films.[316] A degree of control over the morphology of the deposited material can be exerted by a judicious choice of growth technique, precursor, and substrate/precursor temperatures. Dichalcogenoimidodiphosphinato complexes (Scheme 7) of $[Pb[(EP^iPr_2)_2N]_2]$ (E = S, Se, Te) proved to be useful SSPs for lead chalcogenide thin films (Figure 30).[316,317] All compounds are air stable except $[Pb[(TeP^iPr_2)_2N]_2]$, which is highly unstable. Deposition experiments conducted at 475 °C produced pure PbTe films. Deposition at lower growth temperatures lead to formation of both PbTe and Te phases.

Deposition of PbSe thin films from diselenophosphinato and imidodiselenodiphosphinato lead complexes[316] always results in significant contamination with phosphorus. In order to overcome this problem, we synthesized (4-nitro-*N*,*N*-diisobutyl-*N*-benzoylselenoureato)Pb(II) and *N*,*N*-diethyl-*N*-benzoylselenoureato)Pb(II) complexes to be used as SSPs for deposition of PbSe thin films.[318]

Dahmen and co-workers tested bis[bis(trimethylsilyl)methyl]tin chalcogenides, $[Sn\{CH(SiMe_3)_2\}_2(\mu\text{-}E)]_2$ (E = Se, Te), for the MOCVD of SnSe and SnTe thin films.[319,320] They are dimers in solution as well as in the solid state. The compounds are air stable and volatile.[321] MOCVD experiments indicated that both compounds show strong selectivity in the decomposition reaction toward the metallic substrates, thus demonstrating the need for a seeding metallic layer to initiate growth. In the case of nonmetallic substrates, no film deposition was obtained under all experimental conditions.

A number of metal alkoxide precursors have been synthesized and utilized for deposition by CVD production of SnO_x thin films: $[Sn(OCH(CF_3)_2)_4(HNMe_2)_2]$[322] and $Sn(OCMe_3)_4$.[323324] The fluorinated species yield halide-doped films, which are of interest in high-conductivity applications but may be problematic for other applications. The $OCMe_3$ species proved to be useful for production of SnO_2 films without the use of an oxidant. Boyle et al. prepared a family of oxo-alkoxyl precursors which include $[Sn(\mu\text{-}ONep)_2]_\infty$ (ONep = OCH_2CMe_3) and its hydrolysis products $[Sn_5(\mu_3\text{-}O)_2(\mu\text{-}ONep)_6]$ and $[Sn_6(\mu\text{-}O)_4(\mu\text{-}ONep)_4]$ for MOCVD applications.[325,326] All compounds possess relatively low melting points (>190 °C) and volatility for direct vaporization. At low temperatures the oxides are favored, but at higher temperature metallic tin spheres are generated. The in-situ-generated metal droplets act as a catalyst for the growth of SnO_2 wires and ribbons as opposed to uniform thin films.

Tin oxide (SnO_2) films composed of different grain sizes and morphologies particles are obtained by the CVD of $[Sn(O^tBu)_4]$ in the temperature range 500−700 °C.[327] The sensitivity of SnO_2 surfaces toward CO gas significantly depends on the microstructure and specific surface area. The better sensing performance of films deposited at higher temperature (700 °C) is due to the porous structure which increases the amount of oxygen-dangling bonds in the microstructure and overall specific surface area responsible for the improved gas sensitivity.[328] A new volatile precursor $[SnCl_4\{OC(H)OC_2H_5\}_2]$ provides high growth rates (up to 100 Å s^{-1} at 560 °C) in APCVD reactor.[329] Fluorine-doped tin oxide (SnO_2:F) films were deposited from 2,2,2,-trifluoroethyl trifluoroacetate as a fluoride source. Resistivities as low as 5.9×10^{-4} Ω cm and mobilities as high as 27.3 cm^2

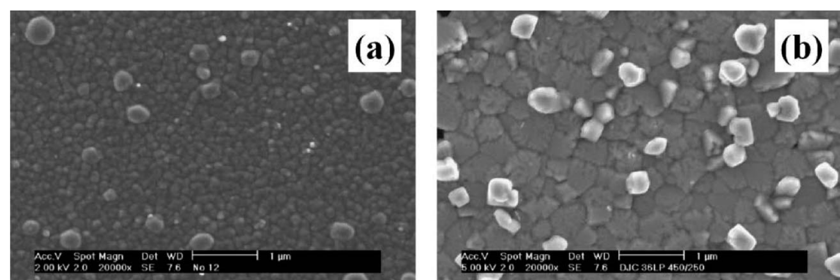

Figure 30. SEM micrographs of PbSe deposited from $Pb[(SeP^iPr_2)_2N]_2$ by LP-MOCVD at (T_{prec}/T_{subs}) (a) 250/425 and (b) 250/450 °C.

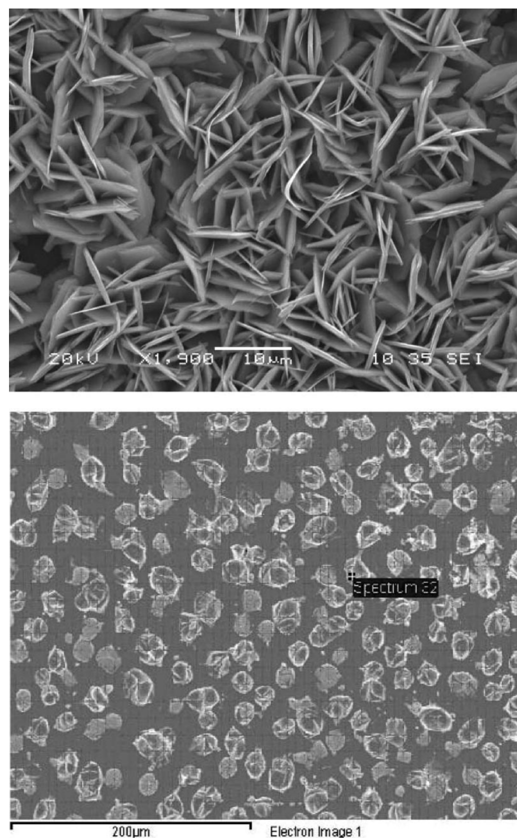

Figure 31. SEM images of SnS_2 (top) and SnS (bottom) deposited from $[SnCl_4\{o\text{-}C_6H_4(CH_2SMe)_2\}]$ at 650 °C.

V^{-1} s^{-1} are routinely observed. No significant variation in growth rate and film thickness is observed for the SnO_2 compared to the SnO_2:F films. Molloy and co-workers developed several organotin fluorocarboxylate compounds for APCVD of fluorine-doped SnO_2 films.[330] $Et_3SnO_2CC_2F_5$, in particular, gives high-quality films with fast deposition rates despite adopting a polymeric, carboxylate-bridged structure. Films grown from $Me_2Sn(O_2CCF_3)_2$ contained high levels of fluorine dopant but exhibited diminished physical properties. The gas-phase structure of $Me_3SnO_2CC_2F_5$ indicated that accessible conformations do not allow contact between tin and fluorine, and therefore, direct transfer is unlikely to be part of the mechanism for fluorine incorporation into SnO_2 films. A mechanism that involved the loss of CO_2 to generate R_3SnR' in situ is much likely.

Deposition of tin sulfide (SnS) films from precursors such as $[Sn(SCH_2CF_3)_4]$ or $[Sn(SPh)_4]$ requires hydrogen sulfide (H_2S) as an additional sulfur source.[331,332] These precursors on their own do not result in SnS. This was attributed to facile disulfide (RS−SR) elimination, which is due to the presence of noncovalently bonded S···S interactions and *cis*-annular interactions in the molecules like $[M(SR)_4]$, where M is a Group IV element.[333] Thermogravimetric analysis and mass spectrometry data showed that $[Sn(SR)_4]$ results in RS−SR in the gas phase, supporting formation of disulfide during the CVD process.[333] However, in the presence of minimal flow of H_2S it was possible to deposit SnS films. It is predicted that the sulfur in tin sulfide may be from H_2S gas and not from the thiolate precursors.[334] Even unsymmetric tin dithiocarbamates[334] and tin complexes containing chelating ligands[333] possessing a direct Sn−S bond may or may not form SnS in the absence of H_2S gas. It was established that chelating thiolate ligands could hinder disulfide elimination.[333] Thus, Parkin et al. reported the use of chelating dithiolato ligand complex $[Sn(SCH_2CH_2S)_2]$ for tin sulfide coatings on glass using AACVD.[333] Recently, we have shown simple tin thiosemicarbazone complexes for the SnS films on glass by AACVD.[335] In such compounds, disulfide elimination is hindered due to the absence of any RS ligand and also the absence of more than one S-containing ligand of any sort. Both molecules contain only

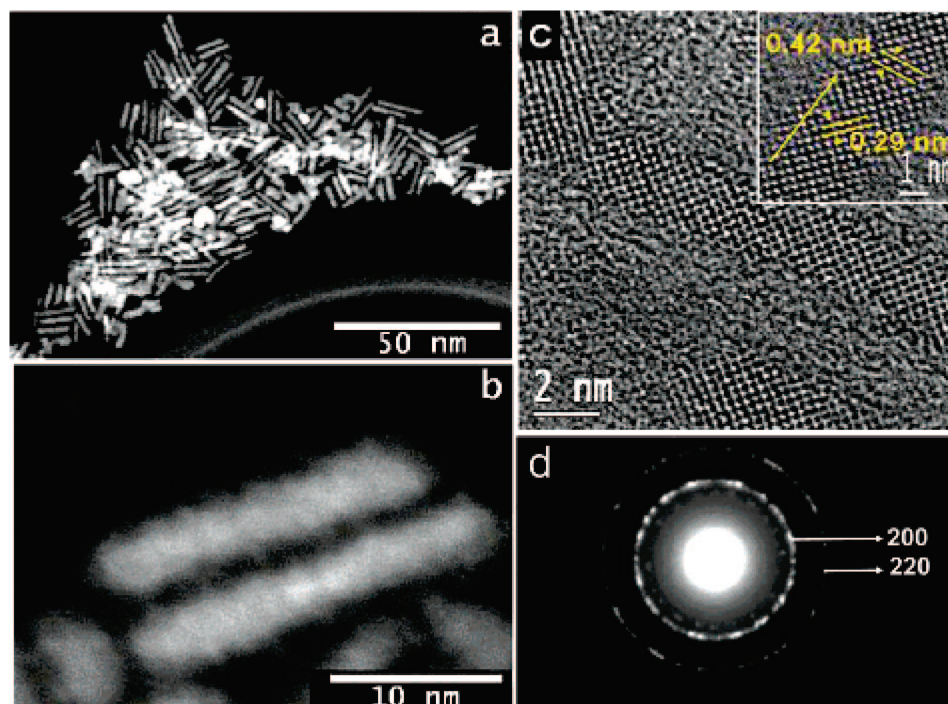

Figure 32. (a and b) Dark field TEM images of ultranarrow PbS rods. (c) HRTEM image of ultranarrow PbS rods showing a diameter of 1.7 nm with well-resolved lattice planes. (Inset) HRTEM showing the interplanar distances of the lattice planes; the arrow indicates the growth direction. (d) SAED pattern from the ultranarrow rods.

one thio ligand, and hence no S···S interaction is possible, i.e., disulfide elimination is not feasible and SnS films are deposited without H_2S gas. New complexes derived from $SnCl_4$ with the *o*-xylyl dichalcogenoethers *o*-$C_6H_4(CH_2EMe)_2$ (E = S, Se) and Et_2Se have been reported.[336] LPCVD of complex $[SnCl_4\{o\text{-}C_6H_4(CH_2SMe)_2\}]$ leads to deposition of hexagonal SnS_2 at lower temperature and orthorhombic SnS at high temperatures (Figure 31), while $[SnCl_4\{o\text{-}C_6H_4(CH_2SeMe)_2\}]$ deposits poor-quality $SnSe_2$ films at 600 °C. The Et_2Se derivative $[SnCl_4(Et_2Se)_2]$ leads to uniform deposition of $SnSe_2$ with growth perpendicular to the substrate.[336] Depositions of SnS and SnS_2 are rare examples of metal sulfide deposition from C−S bond fission within a thioether complex.

Reports on the deposition of germanium chacogenides are extremely rare. Only recently, germanium telluride thin films were reported from a single-source route.[337] Insertion reaction between a germylene and dialkyl telluride leads to a stable alkyl tellurolato compound which has been used to deposit GeTe films in MOCVD studies.

6.2. Precursors for IV−VI Nanoparticles

One of the earliest reports of the deposition of PbS involved the use of the diethyldithiocarbamate to produce well-defined cubes.[338,339] It was subsequently shown that shape control was possible with changes in the reaction conditions.[340] Many precursors have been used to deposit PbS or PbSe.[338−345] Decomposition of lead hexadecylxanthate in trioctylamine has been reported to yield ultranarrow rods with a diameter of ∼1.7 nm and lengths of 12−15 nm (Figure 32).[345] Strong quantum confinement is observed in the absorption and photoluminescence spectra. The absorption band is strongly blue shifted and has a sharp excitonic band at 278 nm and a shoulder at 365 nm.

These bands are of excitonic origin corresponding to the 1Pe to 1Ph, 1Se to 1Ph, and 1Se to 1Sh transitions.[346−348] The PL spectra show strong and sharp band-edge emission at 410 and 434 nm along with a shoulder at 465 nm and a weak band at 500 nm. Recently, Alivisatos and co-workers reported the conversion of Cu_2S rods to PbS simply by cation-exchange reactions.[349] This reaction proved to be much more favorable than converting CdS rods to PbS. This effect is possibly due to fact that the soft base, tri-*n*-butylphosphine, binds strongly to the Cu^+ cation as compared to Cd^{2+} or Pb^{2+} and provides more control.

Vittal et al. synthesized PbS particles by employing a Lewis-base-catalyzed approach to decompose metal alkyl xanthates by using alkyl amines as a solvent to promote decomposition as well as capping ligand for the particles formed.[343] Spherical PbS nanoparticles of diameter 5−10 nm were obtained when long-chain alkylamines were used. When ethylenediamine was used instead, PbS dendrites were isolated from the same precursor at room temperature. Uniform six- and four-armed dendrites were observed, with regular branches of ∼20 nm in diameter growing in a parallel order. These kinds of precursors were stable for periods of months, easy to synthesize, and decomposed with high yields. Cheon and co-workers provided some insight into factors underlying the ripening observed with the PbS nanoparticles from a single-source precursor.[342] By varying the ratio injection temperature, the shape of the resulting particles evolved from rods to multipods to cubes.

Single-source precursors have been used by a hydrothermal process to grow a range of PbS nanocrystals.[350] More

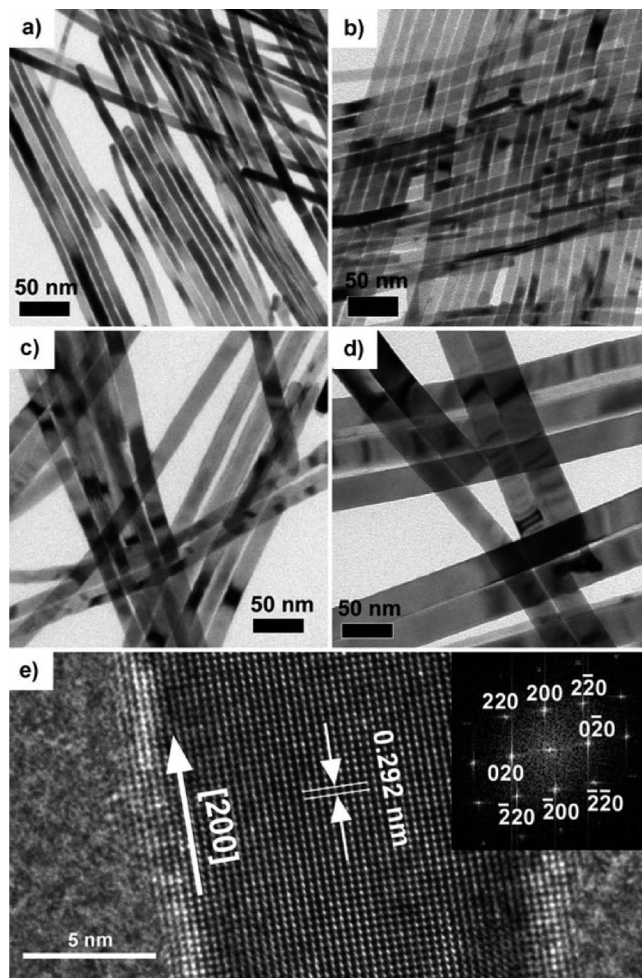

Figure 33. Representative TEM images of PbS nanowires of various diameters (*d*): *d* = (a) 8.7 ± 2.4 (±28%), (b) 11.2 ± 2.3 (±21%), (c) 16.1 ± 2.9 (±18%), and (d) 31.2 ± 3.9 nm (±13%). (e) Lattice-resolved HRTEM image of a 15 nm diameter PbS nanowire. (Inset) Indexed fast-Fourier-transform (FFT) pattern of the image, indicating that the nanowire grows along the 200 direction.

recently, Bi nanoparticles have been used to catalyze solution−liquid−soild (SLS) growth of PbS nanowires from $[Pb(S_2CNEt_2)_2]$ (Figure 33).[351] The minimum controlled nanowire diameters that can be typically achieved from Bi catalysts is ca. 5 nm, because the small Bi nanoparticles (*d* < 5 nm) required to produce smaller nanowire diameters are very unstable with respect to agglomeration.

The use of tin dithiocarbamate $[Sn(S_2CNEt_2)_2]$ in oleylamine has been reported to yield SnS nanocrystals, and reaction conditions do not require the use of hazardous materials such as the use of phosphines and volatile organometallic compounds.[352] The crystalline SnS nanocrystals display strong optical absorption in the visible and NIR spectral regions.

7. Precursors for V−VI Materials

7.1. Precursors for V−VI Thin Films

Only a handful of reports exist concerning the deposition of Group V−VI thin films using a single molecular precursor approach. Thin films of antimony oxide have been deposited by atmospheric-pressure (AP) MOCVD in the temperature range 400−600 °C using the antimony alkoxides tris(*n*-

butoxyantimony) with [Sb(O^{n}Bu)$_3$] and trisethoxyantimony [Sb(OEt)$_3$] as precursors.[353,354] Both precursors have been used to deposit the senarmontite form of Sb_2O_3 with a preferred orientation along the (111) direction, and addition of oxygen gas to the precursor stream leads to formation of the mixed valence oxide, Sb_6O_{13}. Subsequent work has made use of tris(*N,N*-dimethylcarbamato)antimony [Sb(O$_2$CNMe$_2$)$_3$] in LP-MOCVD to deposit the senarmonite form of Sb_2O_3.[355] In another article, the same group described the influence of carefully controlled process parameters on the deposition of

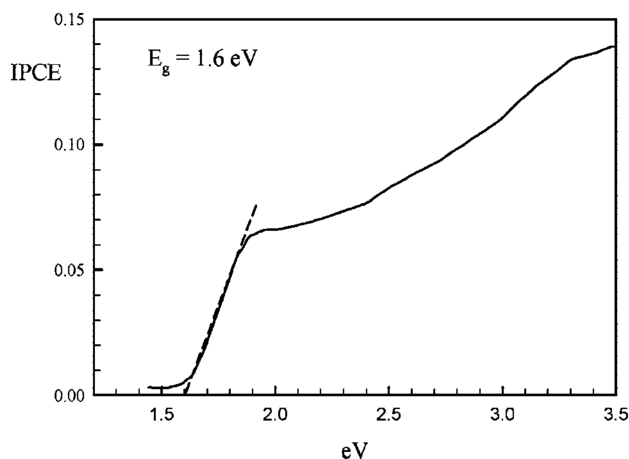

Figure 34. Photocurrent spectra of Sb_2S_3 film deposited on fluorine-doped tin oxide (FTO) in 0.1 M Na_2SO_3(aq), measured at +0.2 V vs Ag|AgCl. Dashed line indicates extrapolation of band edge.

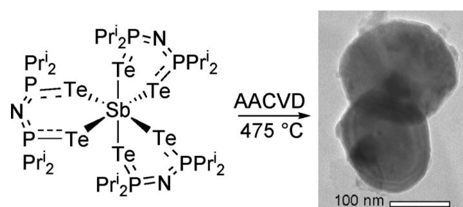

Figure 35. AACVD of SbTe from Cd[(TeP^{i}Pr$_2$)$_2$N]$_3$.

SbO$_x$.[356] A range of antimony(III) and antimony(III/V) oxides can be produced from the precursors antimony(III) ethoxide, butoxide, neopentoxide, and carbamate. At low temperatures, single-phase senarmontite is produced in a hot-wall reactor at atmospheric pressure, and variation of growth parameters, such as growth temperature and choice of precursor, allows control of the films microstructure and texture. Deposition in a cold wall under low pressure leads to formation of granular rather than continuous senarmontite films. Addition of oxygen to the precursor or use of the carbamate precursor allows formation of the higher oxidation state phase.

A series of unsymmetrical antimony dithiocarbamates [Sb(S$_2$CNMeR)$_3$] (R = ^{n}Bu, ^{n}Hex, Bz) has been used in AACVD to deposit Sb_2S_3 films; the film purity was dependent on substrate temperature.[357] Despite their relatively low melting points, none of the compounds proved to be a viable precursor for LPCVD. Transport of the precursors, even at relatively elevated temperatures (90 °C < T < 300 °C), leads to poor substrate coverage and extensive decomposition of the precursor. It is plausible that the dimeric nature of these compounds is responsible for the lack of volatility. Films grown by AACVD at temperatures in excess of ca. 300 °C become susceptible to oxidation, and deposition of oxides and mixed oxide/sulfides becomes more prevalent. The origin of oxygen within the film is uncertain as it is due to traces of oxygen either in the N_2 carrier gas and/or from the solvent. Sb_2S_3 seems especially susceptible to oxidation, even at modest temperatures in CVD; LPCVD as a deposition technique would appear to be more attractive than AACVD in this case. Other monomeric compounds such as antimony thiolates Sb(SR)$_3$ (R = ^{t}Bu, CH$_2$CF$_3$) have been investigated for deposition of antimony sulfide thin films by LPCVD.[358] In both cases, only orthorhombic Sb_2S_3 are deposited at temperatures of 300 and 450 °C. The morphologies of the films show a strong dependence on both precursor and substrate. The film deposited from the *tert*-butyl derivative on conducting glass has a measured band gap of 1.6 eV and is photoactive (Figure 34).

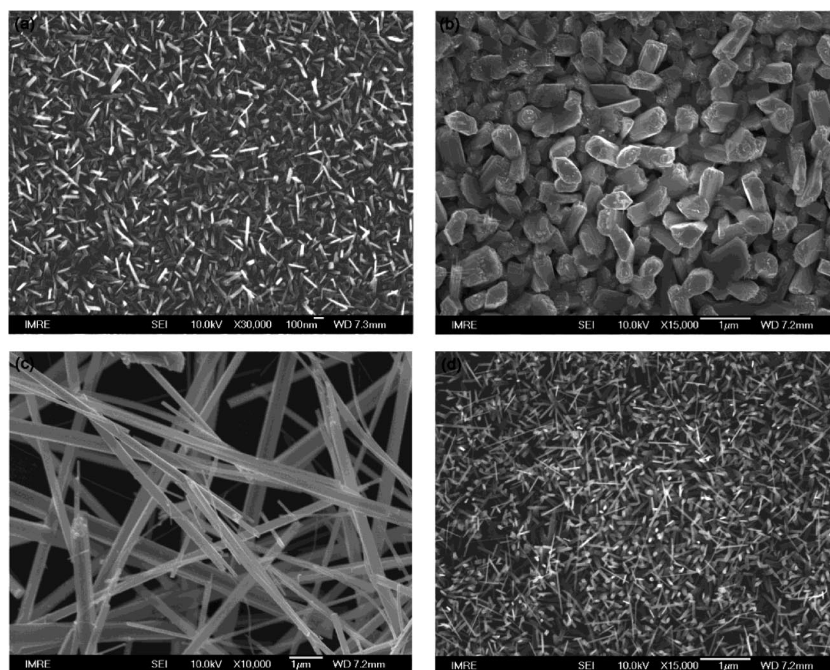

Figure 36. Bi_2S_3 nanorods obtained using [Bi(S$_2$COEt)$_3$] as the single-source precursor: (a) TEM image, (b) electron diffraction pattern, and (c) and (d) HTREM images.

The same group also reported phase pure Sb_2S_3 films from antimony xanthates $[Sb(S_2COR)_3]$ (R = Me, ethyl, ^{i}Pr) in AACVD studies.[359] These precursors lacked sufficient volatility for either AP- or LP-CVD. The advantages of xanthate precursors are rationalized in terms of a facile, low-temperature Chugaev rearrangement. In contrast, dithiocarbamates do not undergo Chugaev elimination since formation of the weaker C═N bond in RNCS (analogous to formation of OCS) works against this. Application of the AACVD technique to the homoleptic antimony(III) complex $[Sb[(TeP^iPr_2)_2N)_2]_3]$ (Figure 35) in the temperature range 375−475 °C produces hexagonal-shaped nanoplates of pure rhombohedral Sb_2Te_3 (Figure 35).[360]

Few examples exist for the deposition of bismuth oxide (Bi_2O_3) films involving single-source precursors. One example is the use of $Bi(tmhd)_3$ (tmhd = 2,2,6,6-tetramethyl-3,5-heptanedione) via its direct liquid injection (DLI) MOCVD, which leads to deposition of Bi_2O_3 films.[361] The Bi_2O_3 film at 300 °C was amorphous and could be converted to crystalline monoclinic α-Bi_2O_3 phase by annealing at temperatures >550 °C. If the annealing temperature is increased to 750 °C, α-Bi_2O_3 phase could be converted to cubic bismuth silicate ($Bi_4Si_3O_{12}$) due to reaction with Si substrate. The effective dielectric constant and leakage current for the amorphous film is 32 and 3.15×10^{-7} A/cm^2 at 3 V, respectively. For the film annealed at 550 °C, a low current of 7.63×10^{-6} A/cm^2 at 3 V was obtained.

Condorelli et al. investigated three different precursors, two less common aryl compounds, namely, *o*- and *p*-tritoluene and the often used $Bi(tmhd)_3$ in the MOCVD studies.[362] All precursors lead to either cubic or tetragonal Bi_2O_3 films at 450 °C. In-situ Fourier-transform infrared (FTIR) measurements during the MOCVD of $Bi(tmhd)_3$ indicate breakage of β-diketonate and formation of ketone, CO, and CO_2. The dissociation mechanism of $Bi(p\text{-tol})_3$ is somewhat different from that of the ortho derivative. MOCVD of $Bi(o\text{-tol})_3$ involves breakage of aromatic rings. For $Bi(p\text{-tol})_3$, it mainly involves the aromatic ring−methyl dissociation.

There are several reports on the use of SSPs for growth of bismuth sulfide (Bi_2S_3) films by CVD. An example of a single-source route is carried out by Monteiro et al. on the deposition of thin films of Bi_2S_3 from bismuth dithiocarbamates, $[Bi(S_2CNRR')_3]$ (R = Et, Me, R′ = hexyl) by LP-MOCVD at 400−450 °C.[363] The resulting films are found to be composed of nanofibers of orthorhombic Bi_2S_3 with direct band gaps of 1.29 eV. In another study, bismuth dithiocarbamtes and related bismuth xanthate species were used in CVD studies to deposit Bi_2S_3 films in the form of the nanorods that vary only in length.[364] TEM analysis (Figure 36) of a single nanorod from $[Bi(S_2COEt_2)_3]$ shows a lattice spacing of 0.4 nm in the (001) direction which agrees with the *c* axis of the orthorhombic structure of Bi_2S_3. Therefore, the *c* axis is parallel to the long axis of the rod. In another HRTEM image, the lattice spacing between two planes is 0.56 nm, which is one-half of the lattice constant along the (100) direction. Formation of the rods is ascribed to two reasons. First, the stronger covalent bond between the planes perpendicular to the *c* axis facilitates a higher growth rate along the *c* axis. Weak van der Waals bonding between the planes perpendicular to the *a* axis limit growth of the rods in the horizontal direction and facilitates their cleavage.

Scheme 8. Ligand Used for Preparation of $M[(EPR_2)_2N]_3$

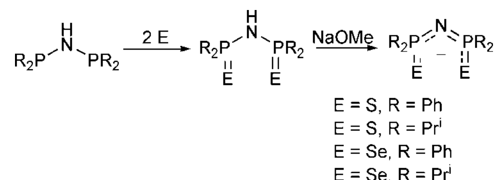

Bismuth chalcogenide films have been reported from CVD studies of air-stable complexes of $Bi[(EPR_2)_2N]_3$ (E = S, Se; R = Ph, ^{i}Pr).[365] The compounds were prepared using the methodology developed by Woollins et al. (Scheme 8).[366] These neutral ligands are readily deprotonated to the monoanions by treatment with bases such as sodium methoxide. Subsequent metathetical reactions with metal halides produce homoleptic complexes in good yields.

Crystalline thin films of rhombohedral Bi_2Se_3 (from $Bi[(SeP^iPr_2)_2N]_3$), hexagonal BiSe (from $Bi[(SePPh_2)_2N]_3$,

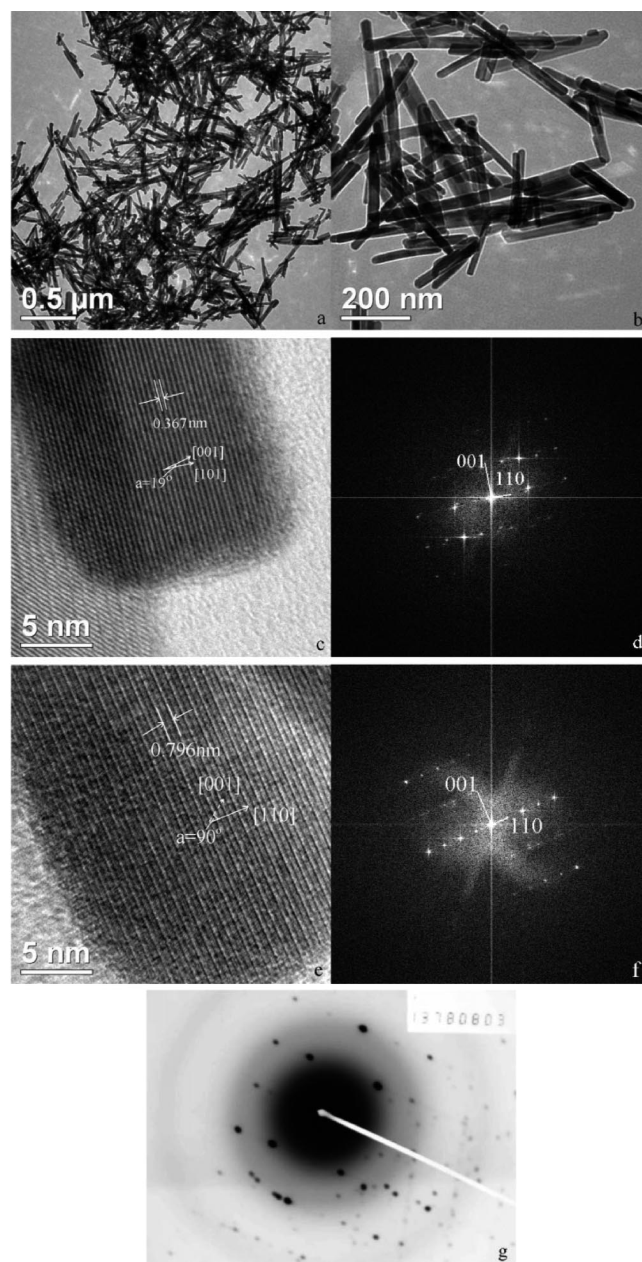

Figure 37. (a and b) TEM images of Bi_2S_3 nanorods. (c and e) HRTEM images and (d and f) corresponding FFTs of two Bi_2S_3 nanorods. (g) ED pattern of a typical Bi_2S_3 nanorod.

and orthorhombic Bi_2S_3 (from $Bi[(SPR_2)_2N]_3$) have been deposited on glass substrates.[365] The suggested reason for deposition of monophasic Bi_2Se_3 and BiSe from isopropyl- and phenyl-substituted precursors, respectively, is highly speculative. It may be that the difference in the electron-donating character of the alkyl group on the P atoms affects the relative bond strengths within the structures and hence the decomposition profiles of the parent molecules. This affect could potentially have a significant impact on the relative amounts of bismuth and selenium reaching, or being retained at, the surface. Thin films composed of hexagonal Bi_2Se_3 nanoplates have also been deposited from MOCVD of bismuth diselenophosphato complex, $[Bi(Se_2P\{O^iPr)_2\}_3]$, on modified and unmodified Si substrates.[367] The deposited Bi_2Se_3 nanoplates have a superior thermoelectric property over bulk Bi_2Se_3.

7.2. Precursors for V−VI Nanoparticles

Several morphologies such as nanorods, nanocrystals, and nanotapes of Bi_2S_3 are obtained from solvent thermolysis of bismuth trisxanthates or bismuth dithiocarbamates in ethylene glycol.[364] The morphology of the Bi_2S_3 crystals depended on the solvent used, the thermolysis temperature, and the

Table 1. Precursors Used for CVD of Thin Films[a]

precursor	material	technique	substrate/growth temp (°C)	ref
$[Cd(SC_6H_2{}^tBu_3)_2]$	CdS	LP-MOCVD	GaAs(111)/460	35
$Zn[TeSi(SiMe_3)_3]_2$	ZnTe	LP-MOCVD	Si, InAs, GaAs/250−350	39
$[Cd(S_2PMe_2)_2]$	CdS	LP-MOCVD	copper-, silver-, gold-coated glass/<500	43
$[Cd(S_2PEt_2)_2]$	CdS	LP-MOCVD	glass, InP(111)/400	44
$[M(S_2P^iBu_2)_2]_2$ (M = Cd, Zn)	CdS, ZnS	LP-MOCVD	glass/400−450	45
$[M(S_2CNEt_2)_2]$ (M = Cd, Zn)	CdS, ZnS	LP-MOCVD	glass, InP(100), GaAs(100)/350−400	64
$[Cd(S_2CNEt_2)_2]/[Zn(S_2CNEt_2)_2]$	$Zn_xCd_{1-x}S$	LP-MOCVD	glass, InP(100), GaAs(100)/400−420	64
$[Zn(Se_2PMe{}^nHex)_2]_2$	ZnSe	LP-MOCVD	glass/400−450	68
$[Cd(S_2CNMe{}^nBu)_2]_2$	CdS	LP-MOCVD	glass/450−500	71
$[Me_2CdZn(Se_2CNEt_2)_2]$	$Cd_{0.5}Zn_{0.5}Se$	LP-MOCVD	glass/450	75
$[M(SOCMe)_2(tmeda)]$ (M = Cd, Zn)	CdS, ZnS, $Cd_{1-x}Zn_xS$	AACVD	Si(100)/100−250	83
$[Cd(SOCNEt_2)_2]$	CdS	LP-MOCVD	glass, GaAs(100)/350−450	102
$[M\{(EPR_2)_2N\}_2]$ (M = Cd, Zn; E = S, Se; R = Ph, ^iPr)	CdS, CdSe, ZnS, ZnSe	LP-MOCVD	glass/400−525	110, 114
$[MeCd\{(SeP^iPr_2)_2N\}]_2$	CdSe	LP-MOCVD	glass/425−450	115
$Cd[(TeP^iPr_2)_2N]_2$	CdTe	AACVD	glass/375−475	116
$[Cd(msacmsac)_2(NO_3)_2]$	CdS	AACVD	glass/450−500	122
$[Me_2Ga(\mu\text{-}As^tBu_2)]_2$	GaAs	LP-MOCVD	GaAs(100), GaAs(111), α-Al_2O_3 (0001)/525	250
$[{}^nBu_2Ga(\mu\text{-}As^tBu_2)]_2$	GaAs	spray MOCVD	GaAs(100)/520−540	259
$[Me_2In{-}P^tBu_2]_2$	InP	modified MBE	InP(100)/480	260
$[Me_2MSb({}^tBu)_2]_3$ (M = Ga, In)	GaSb, InSb	LP-MOCVD	Si(100)/450	261
$[R_2AlSb(SiMe_3)_2]_2$ (R = Et, ^iBu)	AlSb	HV-CVD	Si(100), Al_2O_3/325−550	262
$[{}^tBuGaSbEt_2]$	GaSb	HV-CVD	Si(100)/350−550	266
$^nBuIn(S^iPr)$	In_2S_3	MOCVD	250−400	287
$[{}^tBuIn(\mu\text{-}S^tBu)]_2$	InS	AP-MOCVD	Si(100), KBr/300−400	289
$Me_2In(SePh)$	InSe	spray MOCVD	GaAs(100)/408−477	290
$In(SePh)_3$	In_2Se_3	spray MOCVD	GaAs(100)/473−530	290
$[Me_2InS_2CNEt_2]$	InS, In_6S_7, In_2S_3	LP-MOCVD	GaAs(100)/350−425	291
$[In(S_2CNMeR)_3]$ (R = ^nBu, ^nHex)	In_2S_3	LP-MOCVD	glass, GaAs(100), InP(111)/450−500	293
$[In(S_2CO^iPr)_3]$	In_2S_3			295
$Ga(SCOMe)_3(dmp)$	Ga_2S_3	AACVD	275−310	301b
$[In(\mu\text{-}Te)[N({}^iPr_2PTe)_2]]_3$	In_2Te_3	AACVD	glass, Si(100)/325−475	302
$[Pb(S_2CNRR')_2]$ (R = Me, Et; R′ = ^iPr, ^nBu)	PbS	AACVD, LP-MOCVD	glass/400−450	316
$[Pb(EP^iPr_2)_2N]_2]$ (E = Se, Te)	PbSe, PbTe	AACVD, LP-MOCVD	glass/375−475	316, 317
$[Sn\{CH(\mu\text{-}SiMe_3)_2\}_2(-E)_2$	SnSe, SnTe	LP-MOCVD	Cu/Si, 300, 400	319, 320
$[Sn(OCH(CF_3)_2)_4(NHMe_2)_2]$	SnO_x	LP-MOCVD	glass, Si, quartz, 200−450	322
$Sn(O^tBu)_4$	SnO_2	LP-MOCVD	quartz/500−700	327
$[SnCl_4\{OC(H)OC_2H_5\}_2]$	SnO_2	AP-CVD	glass/360−560	329
$[Sn(SCH_2CH_2S)_2]$	SnS	AACVD	glass/400−500	333
$[SnCl_4\{o\text{-}C_6H_4(CH_2SMe)_2\}]$	SnS, SnS_2	LP-CVD	Si/600−650	336
$[SnCl_4(Et_2Se)_2]$	$SnSe_2$	LP-CVD	Si/500−550	336
$Sb(OR)_3$ (R = Et, ^nBu)	Sb_2O_3	AP-CVD	Si(111)/400−600	353, 354
$[Sb(O_2CNMe_2)_3]$	Sb_2O_3	LP-CVD	glass/380	355
$[Sb(S_2CNMeR)_3]$ (R = Bu, Hex, Bz)	Sb_2S_3	LP-MOCVD and AACVD	glass/<300 and ≥395, respectively	357
$Sb(SR)_3$ (R = ^tBu, CH_2CF_3)	Sb_2S_3	LP-MOCVD	glass, Si/300−450	358
$[Sb(S_2COR)_3]$ (R = Me, Ethyl, ^iPr)	Sb_2S_3	AACVD	glass, Si/200−240	359
$Sb[N(P^iPr_2Te)_2]_3$	Sb_2Te_3	AACVD	glass/325−475	360
$Bi(tmhd)_3$	Bi_2O_3	DLI-MOCVD	Si/225−425	361
$[Bi(S_2CNRR')_3]$ (R,R′ = ethyl, R = methyl, R′ = hexyl)	Bi_2S_3	LP-MOCVD	glass/400−450	363
$[Bi(S_2COEt_2)_3]$	Bi_2S_3	LP-MOCVD	Si(100)/400	364
$Bi\{(EPR_2)_2N\}_3]$ (E = S, Se; R = Ph, ^iPr)	BiSe, Bi_2Se_3,	AACVD, LP-MOCVD	glass/350−475	365
$[Bi(Se_2P\{O^iPr)_2\}_3]$	Bi_2Se_3	LP-MOCVD	Si/350, 450	367

[a] TMEDA = *N*,*N*,*N*,*N*-tetramethylethylenediamine; msacmsac = dimorpholinodithioacetylacetonate; dmp = 3,5-dimethylpyridine; tmhd = 2,2,6,6-tetramethyl-3,5-hepatnedione; MBE = molecular beam epitaxy; DLI = direct liquid injection.

nature of the precursor. The bismuth xanthates exhibited a lower decomposition temperature (<150 °C) than the dithiocarbamate analogues (>200 °C). Precursors adopting the polymeric structures in solution decompose at a higher temperature than those with dimeric structures. The outcome is that polymeric $[Bi(S_2CO^iPr)_3]$ give long Bi_2S_3 nanofibers, whereas dimeric $[Bi(S_2COR)_3]$ (R = alkyl) produce nanocrystals. Bi_2S_3 has the tendency to form nanorods relatively easily due to the inherent Bi−S chain-type structure. It is known that Bi_2S_3 crystallizes with a lamellar structure with linked Bi_2S_3 units forming infinite chains, which, in turn, are connected via van der Waals interactions.[368] Formation of Bi_2S_3 nanorods originates from the preferential directional growth of Bi_2S_3 crystallites along its *c* axis. Nanorods of Bi_2S_3 and Sb_2S_3 are also reported from hydrothermal decomposition of $[M(S_2CNEt_2)_3]$ (M = Bi, Sb).[369] Water exerts an influence on formation of M_2S_3 nanocrystals. A proton and hydroxide anion from H_2O may promote cleavage of one of the C−S bonds and S−M coordination bonds in the precursors to form M_2S_3. Adducts of $Bi(S_2CO^sbutyl)_3$ with pyridine and 1,10-phenanthroline have also been hydrothermally treated to deposit rods with diameters in the range of 20−35 nm and lengths up to several hundreds of nanometers (Figure 37).[370] When PVP is used instead of neutral ligands, highly uniform Bi_2S_3 nanorods with an average diameter of 20 nm are produced. The optical band edge of Bi_2S_3 nanorods from 1,10-phenanthroline derivative is blue shifted with a band gap of ∼1.67 eV. High-quality M_2S_3 nanorods are also reported by solvothermal treatment of metal dithiophosphates $[M(S_2P^nOctyl_2)_3]$ in the presence of oleylamine.[371]

The conditions such as reaction time, temperature, and concentration of precursors all play an important role in determining the size and aspect ratio of the product. Vittal and co-workers reported various morphologies of Bi_2S_3 nanomaterials including nanorods, nanoleaves, nanoflowers, and dandelion-like structures through colloidal solution of $[Bi(SCOPh)_3]$.[372] In the presence of both dodecanethiol and TOPO, Bi_2S_3 nanorods with an average diameter of 21.3 nm and a length of 300 nm are reported. When the surfactant is changed to dodecanethiol and oleylamine, Bi_2S_3 nanorods with grooves are deposited. The oleylamine might have played a key role in making grooves on the surface of Bi_2S_3 nanorods due to its corrosive nature. Previously amines have also been used solely for etching purposes.[373] In the presence of polyvinylpyrrolidone and ethylene glycol, dandelion-shaped Bi_2S_3 nanostructures are obtained. It is possible for PVP to adsorb onto the surface of Bi_2S_3 branches through nitrogen and oxygen atoms in the pyrrolidone groups and prompt formation of dandelion-like structures from individual Bi_2S_3 wires due to its cross-linking ability.[374] Production of Sb_2Se_3 nanowires from $[Sb\{Se_2P(O^iPr)_2\}_3]$ under solvothermal conditions has been reported.[375] In a later study the authors studied the electrical and optical properties of a single Sb_2Se_3 nanorod with an average size of 70 nm in diameter and a length of ∼1−2 μm.[376]

8. Conclusions

This overview shows the contribution of main group element chemistry in evolving the available and potentially useful compound semiconductors as summarized in Tables 1 and 2. Chemists have played a major role in the design and development of precursors and methods for depositing semiconductor materials. The single-source approach is a chemist's answer to the problems posed by the use of separate sources. This review summarizes the use of different families of main group metal complexes that have been used for the preparation of potentially functional materials as thin films or nanoparticles. Several research groups have successfully designed and/or prepared such complexes. Most of the single-source molecules have low volatilities, but volatilities can be enhanced by various chemical modifications. Liquid delivery methods (aerosol, spray, injection) have been increasingly used during the past decade which do not require a volatile precursor. In addition, the most common method used for preparation of nanoparticles involves thermolysis of the precursor in a high-boiling solvent which

Table 2. Precursors Used for the Growth of Nanocrystals[a]

precursor	material	capping ligand	growth temp (°C)	morphology	ref
$[Cd(NH_2CSNHNH_2)_2Cl_2]$	CdS	TOPO	280	nanorods	128
$[Cd(E_2CNEt_2)_2]$ (E = S, Se)	CdS, CdSe	pyridine, 4-ethylpyridine	167	nanocrystals	140
$[MeCdSe_2CNEt_2]_2$	CdSe	TOPO	250	nanocrystals	144
$[Cd(E_2CNMe^nHex)_2]$ (E = S, Se)	CdSe/CdS	TOPO	250	nanocrystals	158
$\{Ga(NH)_{3/2}\}_n$	GaN	trioctylamine	360	nanocrystals	267
$[M(H_2NCONH_2)_6]Cl_3$ (M = Al, Ga)	AlN, GaN	trioctylamine	360	nanocrystals	271
$[(NH_4)_3In_{1-x}Ga_xF_6]$	InGaN		ammonolysis (500)	nanocrystals	274
$M(P^tBu_2)_3$ (M = Ga, In)	InP, GaP	4-ethylpyridine	167	nanocrystals	275, 276
$[X_2GaP(SiMe_3)_2]_2$ (X = Be, I)	GaP		pyrolysis (300)	nanocrystals	277
$[H_2GaE(SiMe_3)_2]_3$ (E = P, As)	GaP, GaAs		pyrolysis (450 and 600)	nanocrystals	278
$[^tBu_2AsInEt_2]_2$	InAs	HDA	280	nanocrystals	279
$[^tBu_2AsGaMes_2]_2$	GaAs	HDA	120	nanocrystals	280
$[(^tBu)GaSe]_4$	GaSe	APCVD	KBr, Si(100)/325−335	nanocrystals	306
$[(EtMe_2C)InSe]_4$	InSe	APCVD	KBr, Si(100)/290	nanocrystals	306
$[In(E_2CNEt_2)_3]$ (E = S, Se)	InS, InSe	4-ethylpyridine, TOPO	250, 167	nanocrystals	307
$[Pb(S_2CNEt_2)_2]$	PbS	TOPO	250	nanocrystals	338
$[Pb(SCOC_6H_5)_2]$	PbS	alkylamines	room temperature	nanocrystals	343
$[Sn(S_2CNEt_2)_2]$	SnS	oleylamine	170	nanocrystals	352
$[M(S_2CNEt_2)_3]$ (M = Bi, Sb)	Sb_2S_3, Bi_2S_3	water, chlorodform, acetonitrile	115−170	nanocrystals	369
$[Bi(S_2COC_4H_9)_3(L)_2]$ (L = pyridine, 1,10-phenanthroline)	Bi_2S_3	PVP	130−180	nanorods	370
$[Bi(SCOPh)_3]$	Bi_2S_3	TOPO, DT, PVP, EG, cysteine, ethylenediamine	150	nanorods	372
$[Sb\{Se_2P(O^iPr)_2\}_3]$	Sb_2Se_3	methanol	100, 150	nanowires, nanorods	375

[a] PVP = poly(vinyl pyrrolidone), DT = dodecanethiol, EG = ethylene glycol.

again has nothing to do with the volatility of the precursor. Thus, the important factors to consider for the design of precursors are purity, stability, toxicity, ease of synthesis, and cost involved for synthesis.

Given the potential importance of these chalcogenides, in applications as diverse as hybrid solar cells, sensors, etc., we anticipate further commercial exploitation of such processes in future years. We envisage that chemists will continue their interests with important objectives led by our need for sustainable process and energy sources, a need to minimize environmental impact, and a need for cost-effective processes for materials based on common (cheaper) elements. These objectives will be mirrored by technological needs such as low-temperature processing (deposition on plastics) and higher and more reproducible optical and electronic properties. The area remains one that is ripe for further development and discovery.

9. Acknowledgments

The authors would thank EPSRC, UK for financial assistance. P.O.B. wrote this review while a visiting fellow at Magdalen College, Oxford. He would like to thank the College for the Fellowship and the President and Fellows for being gracious hosts.

10. References

(1) Manasevit, H. M. *J. Cryst. Growth* **1981**, *55*, 1.
(2) Hirata, S. Y.; Fujita, S.; Isenuera, M. *J. Cryst. Growth* **1990**, *104*, 521.
(3) (a) Giapis, K. P.; Jensen, K. F. *J. Cryst. Growth* **1990**, *101*, 11–1. (b) Giapis, K. P.; Lu, D. C.; Fotiadis, D. I.; Jensen, K. F. *J. Cryst. Growth* **1990**, *104*, 629.
(4) Foster, D. F.; Patterson, I. J.; James, L. D.; Cole-Hamilton, D. J.; Annitage, D. N.; Yates, H. M.; Wright, A. C.; Williams, J. O. *Adv. Mater. Opt. Electron.* **1994**, *3*, 163.
(5) Nishimura, K.; Nagao, Y.; Sakai, K. *J. Cryst. Growth* **1993**, *134*, 293.
(6) (a) Kuhn, W.; Naumov, A.; Stanzl, H.; Bauer, S.; Wolf, K.; Wagner, H. P.; Gebhardt, W.; Pohl, U. W.; Krost, A.; Richter, W.; Dumichen, U.; Thiele, K. H. *J. Cryst. Growth* **1992**, *123*, 605. (b) Sato, G.; Numai, T.; Hoshiyama, M.; Suernune, I.; Machida, H.; Shimoyama, N. *J. Cryst. Growth* **1995**, *150*, 734.
(7) Hails, J. E.; Irvine, S. J. C.; Mullin, J. B.; Shenai-Khatkhate, D. V.; Cole-Hamilton, D. J. *Mater. Res. Soc. Symp. Proc.* **1989**, *131*, 75.
(8) Hails, J. E.; Irvine, S. J. C.; Mullin, J. B. *Mater. Res. Soc. Symp. Proc.* **1990**, *162*, 343.
(9) (a) Bell, W.; Stevenson, J.; Cole-Hamilton, D. J.; Hails, J. E. *Polyhedron* **1994**, *13*, 1253. (b) Stevenson, J.; Bell, W.; Ferry, J.; Cole-Hamilton, D. J.; Hails, I. E. *J. Organomet. Chem.* **1993**, *449*, 141. (c) Hails, J. E.; Cole-Hamilton, D. J.; Bell, W. *J. Cryst. Growth* **1994**, *145*, 596.
(10) Stringfellow, G. B. *Organometallic Vapour Phase Epitaxy: Theory and Practice*; Academic Press: New York, 1989.
(11) Cole-Hamilton, D. J. *Chem. Br.* **1990**, 852.
(12) Mullin, J. B.; Irvine, S. J. C. *Prog. Cryst. Growth Charact.* **1994**, *29*, 217.
(13) (a) Smith, L. M.; Thompson, J. *Chemtronics* **1989**, *4*, 60. (b) Mullin, J. B.; Cole-Hamilton, D. J.; Irvine, S. J. C.; Hails, J. E.; Giess, J.; Gough, J. S. *J. Cryst. Growth* **1990**, *101*, 1.
(14) (a) O'Brien, P. In *Inorganic Materials*; Bruce, D. W., O'Hare, D., Eds.; Wiley: Chichester, U.K., 1992; p 491. (b) O'Brien, P. *Chemtronics* **1991**, *5*, 61. (c) Jones, A. C.; Wright, P. J.; Cockayne, B. *Chemtronics* **1988**, *3*, 35.
(15) Wright, P. J.; Cockayne, B.; Parbrook, P. J.; Oliver, E. P.; Jones, A. C. *J. Cryst. Growth* **1991**, *108*, 525.
(16) Coates, G. E.; Ridley, D. *J. Chem. Soc.* **1965**, 1870. (a) Adamson, G. W. *Acta Crystallogr., Sect. B* **1982**, *38*, 462.
(17) Malik, M. A.; Motevaili, M.; Walsh, J. R.; O'Brien, P.; Jones, A. C. *J. Mater. Chem.* **1995**, *5*, 731.
(18) Adamson, G. W.; Shearer, H. M. M. *J. Chem. Soc., Chem. Commun.* **1969**, 897.
(19) Zeng, D. H.; Hampden-Smith, M. J.; Duesler, E. N. *Inorg. Chem.* **1994**, *33*, 5376.
(20) Bochmann, M. *Chem. Vap. Deposition* **1996**, *2*, 85.
(21) Hursthouse, M. B.; Motevalli, M.; O'Brien, P.; Walsh, J. R.; Jones, A. C. *Organometallics* **1991**, *10*, 3196.
(22) Dance, I. G. *Polyhedron* **1986**, *5*, 1037.
(23) Hursthouse, M. B.; Khan, O. F. Z.; Mazid, M.; Motevalli, M.; O'Brien, P. *Polyhedron.* **1990**, *9*, 541.
(24) Khan, O. F. Z.; O'Brien, P. *Polyhedron.* **1991**, *10*, 325.
(25) (a) Brennan, J. G.; Segrist, T.; Carroll, P. J.; Stuczynski, S. M.; Reynders, P.; Brus, L. E.; Steigerwald, M. L. *J. Am. Chem. Soc.* **1989**, *111*, 4141. (b) Chem. Mater. 1990, *2*, 403.
(26) Osakada, K.; Yamamoto, T. *J. Chem. Soc., Chem. Commun.* **1987**, 117.
(27) Steigerwald, M. L.; Sprinkle, C. R. *J. Am. Chem. Soc.* **1987**, *109*, 7200.
(28) Zeng, D.; Hampden-Smith, M. J.; Densler, E. N. *lnorg. Chem.* **1994**, *33*, 5376.
(29) Blower, P. J.; Dilworth, J. R.; Hutchinson, J. P.; Zubieta, J. A. *J. Chem. Soc., Dalton Trans.* **1985**, 1533.
(30) Bochmann, M.; Webb, K.; Harman, M.; Hursthouse, M. B. *Angew. Chem., Int. Ed. Engl.* **1990**, *29*, 638.
(31) Bochmann, M.; Webb, K. J.; Hursthouse, M. B.; Mazid, M. *J. Chem. Soc., Dalton Trans.* **1991**, 2317.
(32) Bochmann, M.; Webb, K. J. *J. Chem. Soc., Dalton Trans.* **1991**, 2325.
(33) Bochmann, M.; Bwembya, G. C.; Grinter, R.; Powell, A. K.; Webb, K. J.; Hursthouse, M. B.; Abdel Malik, K. M.; Mazid, M. A. *Inorg. Chem.* **1994**, *33*, 2290.
(34) Bochmann, M.; Webb, K. J. *Mater. Res. Soc. Symp. Proc.* **1991**, *204*, 149. *Chem. Abstr.* **1992**, *116*, 3 3194h.
(35) Bochmann, M.; Webb, K. J.; Hails, J.-E.; Wolverson, D. *Eur. J. Solid State lnorg. Chem.* **1992**, *29*, 155.
(36) Bochmann, M.; Coleman, A. P.; Powell, A. K. *Polyhedron* **1992**, *11*, 507.
(37) Dabbousi, B. O.; Bonasia, P. J.; Arnold, J. *J. Am. Chem. Soc.* **1991**, *113*, 3186.
(38) Bonasi, P. J.; Arnold, J. *Znorg. Chem.* **1992**, *31*, 2508.
(39) Arnold, J.; Walker, J. M.; Yu, K. M.; Bonasia, P. J.; Seligson, A. L.; Bourret, E. D. *J. Cryst. Growth* **1992**, *124*, 647.
(40) Bonasia, P. J.; Gindelberger, D. E.; Dabbousi, B. O.; Arnold, J. *J. Am. Chem. Soc.* **1992**, *114*, 5209.
(41) Bonasia, P. J.; Mitchell, G. P.; Hollander, F. J.; Arnold, J. *Inorg. Chem.* **1994**, *33*, 1797.
(42) Arnold, J. Bonasia, P. J. U.S. Patent 5157136, Oct 20, 1992.
(43) Takahashi, Y.; Yuki, R.; Sugiura, M.; Motojima, S.; Sugiyama, K. *J. Cryst. Growth* **1980**, *50*, 491.
(44) Evans, M. A. H.; Williams, J. D. *Thin Solid Films* **1982**, *87*, L1.
(45) Byrom, C.; Malik, M. A.; O'Brien, P.; White, A. J. P. *Polyhedron* **2000**, *19*, 211.
(46) Haiduc, I.; Bryan-Sowerby, D.; Shao-Fang, L. *Polyhedron* **1995**, *4*, 3389.
(47) Lawton, S. L.; Kokotailo, G. T. *Inorg. Chem.* **1969**, *8*, 2410.
(48) Adeogun, A.; Nguyen, C. Q.; Afzaal, M.; Malik, M. A.; O'Brien, P. *Chem. Commun.* **2006**, 2179.
(49) Nguyen, C. Q.; Adeogun, A.; Afzaal, M.; Malik, M. A.; O'Brien, P. *Chem. Commun.* **2006**, 2182.
(50) Park, J.-H.; O'Brien, P.; White, A. J. P.; Williams, D. J. *Inorg. Chem.* **2001**, *40*, 3629.
(51) Garcia-Montalvo, V.; Cea-Olivares, R.; Williams, D. J.; Espinosa-Perez, G. *Inorg. Chem.* **1996**, *35*, 3948. Zaitseva, E. G.; Baidina, I. A.; Stabnikov, P. A.; Borisov, S. V.; Igumenov, I. K. *Zh. Strukt. Khim.* **1990**, *31*, 184.
(52) Dymock, K.; Palenok, G. J.; Slezak, J.; Raston, C. L.; White, A. H. *J. Chem. Soc., Dalton. Trans.* **1976**, 28. Bhattacharya, S.; Seth, N.; Srivastava, D. K.; Gupta, V. D.; Noth, H.; Thomann-Albach, M. *J. Chem. Soc., Dalton. Trans.* **1996**, 2815.
(53) Park, J.-H.; O'Brien, P.; White, A. J. P.; Williams, D. J. *Inorg. Chem.* **2001**, *40*, 3629.
(54) Klug, H. P. *Acta Crystallogr.* **1966**, *21*, 536.
(55) Bonamico, M.; Mazzone, G.; Vaciago, A.; Zambonelli, L. *Acta Crystallogr.* **1965**, *19*, 898.
(56) Miyame, H.; Ito, M.; Iwasaki, H. *Acta Crystallogr.* **1979**, *B35*, 1480.
(57) Domenicano, A.; Torelli, L.; Vaciago, A.; Zambonelli, L. *J. Chem. Soc. A* **1968**, 1351.
(58) Bonamico, M.; Dessy, G. *J. Chem. Soc. A* **1971**, 264.
(59) Hursthouse, M. B.; Malik, M. A.; Motevalli, M.; O'Brien, P. *Polyhedron* **1992**, *11*, 45.
(60) Motevalli, M.; O'Brien, P.; Walsh, J. R.; Watson, I. M. *Polyhedron* **1996**, *15*, 2801.
(61) Saunders, A.; Vecht, A.; Tyrell, G. *Chem. Abstr.* **1988**, *108*, 66226h.
(62) Druz, B. L.; Evtukhov, Y. N.; Rakhlin, M. Y. *Metallorg. Khim.* **1988**, *1*, 645.
(63) Druz, B. L.; Dyadenko, A. I.; Evtukhov, Y. N.; Rakhlin, M. Y.; Rodionov, V. E. *Izv. Akad. Nauk. SSSR, Neorg. Mater.* **1990**, *26*, 34.

(64) Frigo, D. M.; Khan, O. F. Z.; O'Brien, P. *J. Cryst. Growth* **1989**, *96*, 989.
(65) Nomura, R.; Murai, T.; Toyosaki, T.; Matsuda, H. *Thin Solid Films* **1995**, *271*, 4.
(66) Fainer, N. I.; Rumyantsev, Y. M.; Kosinova, M. L.; Kuznetsov, F. A. In *Proceedings of the XIV International CVD Conference and EUROCVD11*; Allendorf, M. D., Bernard, C., Eds.; Electrochemical Society: Pennington, NJ, 1997; Vol. 97-25, p 1437.
(67) Fainer, N. I.; Kosinova, M. L.; Rumyantsev, Y. M.; Salman, E. G.; Kuznetsov, F. A. *Thin Solid Films* **1996**, *280*, 16.
(68) Chunggaze, M.; McAleese, J.; O'Brien, P.; Otway, D. J. *J. Chem. Soc., Chem. Commun.* **1998**, 833.
(69) O'Brien, P.; Otway, D. J.; Walsh, J. R. *Adv. Mater. CVD* **1997**, *3*, 227.
(70) Chunggaz, M.; Malik, M. A.; O'Brien, P. *J. Mater. Chem.* **1999**, *9*, 2433.
(71) O'Brien, P.; Walsh, J. R.; Watson, I. M.; Hart, L.; Silva, S. R. P. *J. Cryst. Growth* **1996**, *167*, 133.
(72) Ludolph, B.; Malik, M. A.; O'Brien, P.; Revaprasadu, N. *Chem. Commun.* **1998**, 1849.
(73) Pike, R. D.; Cui, H.; Kershaw, R.; Dwight, K.; Wold, A.; Blanton, T. N.; Wernberg, A. A.; Gysling, H. J. *Thin Solid Films* **1993**, *224*, 221.
(74) Malik, M. A.; O'Brien, P. *Adv. Mater. Opt. Electron.* **1994**, *3*, 171.
(75) Hursthouse, M. B.; Malik, M. A.; Motevalli, M.; O'Brien, P. *J. Mater. Chem.* **1992**, *9*, 949.
(76) Malik, M. A.; Saeed, T.; O'Brien, P. *Polyhedron* **1993**, *12*, 1533.
(77) Malik, M. A.; Motevalli, M.; Saeed, T.; OBrien, P. *Adv. Mater.* **1993**, *5*, 653.
(78) Agre, V. M.; Shugam, E. A.; Rukhadze, E. G. *Tr. IREA* **1967**, *30*, 369.
(79) Memon, A. A. M.; Afzaal, M.; Malik, M. A.; Nguyen, C.; O'Brien, P.; Raftery, J. *Dalton Trans.* **2006**, 4499.
(80) Van Poppel, L. H.; Groy, T. H.; Caudle, M. T. *Inorg. Chem.* **2004**, *43*, 3180.
(81) Noltes, J. G. *Recl. Tran. Chim. Pays-Bas* **1965**, *84*, 126.
(82) Hursthouse, M. B.; Malik, M. A.; Motevalli, M.; O'Brien, P. *Organometallics* **1991**, *10*, 730.
(83) Nyman, M.; Hampden-Smith, M. J.; Duesler, E. *Chem. Vap. Deposition* **1996**, *2*, 171.
(84) Nyman, M.; Jenkins, K.; Hampden-Smith, M. J.; Kodas, T. T.; Duesler, E. N.; Rheingold, A. L.; Liable-Sands, M. L. *Chem. Mater.* **1998**, *10*, 914.
(85) (a) Schmidpeter, A.; Bohm, R.; Groeger, H. *Angew. Chem., Int. Ed. Engl.* **1964**, *3*, 704. (b) Schmidpeter, A.; Stoll, K. *Angew. Chem., Int. Ed. Engl.* **1967**, *6*, 252. (c) Schmidpeter, A.; Stoll, K. *Angew. Chem., Int. Ed. Engl.* **1968**, *7*, 549.
(86) Malik, M. A.; O'Brien, P. *Chem. Mater.* **1991**, *3*, 999.
(87) Malik, M. A.; Motevalli, M.; O'Brien, P.; Walsh, J. R. *Organometallics* **1992**, *11*, 3436.
(88) Abrahams, I.; Malik, M. A.; Motevalli, M.; O'Brien, P. *J. Organomet. Chem.* **1994**, *465*, 73. (a) Malik, M. A.; Motevalli, M.; O'Brien, P. *Acta Crystallogr.* **1996**, *C52*, 1931. (b) Malik, M. A.; O'Brien, P. *Adv. Mater. Opt. Electron.* **1994**, *3*, 171.
(89) Cheon, J.; Talaga, D. S.; Zink, J. I. *Chem. Mater.* **1997**, *9*, 1208.
(90) Musetha, P. L.; Revaprasadu, N.; Malik, M. A.; O'Brien, P. *Mater. Res. Soc. Sym. Proc.* **2005**, *879E*, Z7.4.1.
(91) Trávníček, Z.; Pastorek, R.; Šindelář, Z.; Klička, R. *Polyhedron* **1995**, *4*, 3627.
(92) Rao, S. R. *Xanthate and related compounds*; Dekker: New York, 1971.
(93) Sceney, C. G.; Hill, J. O.; Magee, R. J. *Thermochim. Acta* **1973**, *6*, 111.
(94) Barreca, D.; Gasparotto, A.; Maragno, C.; Tondello, E. *J. Electrochem. Soc.* **2004**, *151* (6), G428–G435.
(95) Barrecal, D.; Gasparotto, A.; Maragno, C.; Seraglia1, R.; Tondello, E.; Venzo1, A.; Krishnan, V.; Bertagnolli, H. *Appl. Organometal. Chem.* **2005**, *19*, 59.
(96) Tiekink, E. R. T. *Acta Crystallogr.* **2000**, *C56*, 1176.
(97) Abrahams, B. F.; Hoskins, B. F.; Tiekink, E. R. T.; Winter, G. *Aust. J. Chem.* **1988**, *41*, 1117. (a) Cox, M. J.; Tiekink, E. R. T. *Rev. Inorg. Chem.* **1997**, *17*, 1.
(98) Iimura, Y.; Ito, T.; Hagihara, H. *Acta Crystallogr.* **1972**, *B28*, 2271. Johnson, C. K. *ORTEPII Report ORNL-5138*; Oak Ridge National Laboratory: Oak Ridge, TN, 1976.
(99) Rietveld, H. M.; Maslen, E. N. *Acta Crystallogr.* **1965**, *18*, 429.
(100) Tomlin, D. W.; Cooper, T. M.; Zelmon, D. E.; Gebeyehu, Z.; Hughes, J. M. *Acta Crystallogr.* **1999**, *C55*, 717.
(101) Chunggaze, M.; Malik, M. A.; O'Brien, P.; White, A. J. P.; Williams, D. J. *J. Chem. Soc., Dalton Trans.* **1998**, 3839.
(102) Chunggaze, M.; Malik, M. A.; O'Brien, P. *Adv. Mater. Opt. Electron.* **1998**, *7*, 311.
(103) Bhattacharyya, P.; Slawin, A. M. Z.; Williams, D. J.; Woollins, J. D. *J. Chem. Soc., Dalton Trans.* **1995**, 2489.
(104) For a review, see: Silvestru, C.; Drake, J. E. *Coord. Chem. Rev.* **2001**, *223*, 117.
(105) For a review, see: Ly, T. Q.; Woollins, J. D. *Polyhedron* **1998**, *176*, 451.
(106) Afzaal, M.; Crouch, D.; Malik, M. A.; Motevalli, M.; O'Brien, P.; Park, J.-H.; Woollins, J. D. *Eur. J. Inorg. Chem.* **2004**, 171.
(107) Crouch, D. J.; O'Brien, P.; Malik, M. A.; Skabara, P. J.; Wright, S. P. *Chem. Commun.* **2003**, 1454.
(108) Afzaal, M.; Crouch, D. J.; O'Brien, P.; Raftery, J.; Skabara, P. J.; White, A. J. P.; Williams, D. J. *J. Mater. Chem.* **2004**, *14*, 233.
(109) Cupertino, D.; Birdsall, D. J.; Slawin, A. M. Z.; Woollins, J. D. *Inorg. Chim. Acta* **1999**, *290*, 1.
(110) Afzaal, M.; Aucott, S. M.; Crouch, D.; O'Brien, P.; Woollins, J. D.; Park, J. H. *Chem. Vap. Deposition* **2002**, *8*, 187.
(111) Afzaal, M.; Crouch, D.; O'Brien, P.; Park, J. H. *Mater. Res. Soc. Symp. Proc.* **2002**, 692.
(112) Osakada, K.; Yamamoto, T. *J. Chem. Soc., Chem. Commun.* **1987**, 1117.
(113) Brennan, J. G.; Siegrist, T.; Carroll, P. J.; Stuczynski, S. M.; Reynders, P.; Brus, L. E.; Steigerwald, M. L. *Chem. Mater.* **1990**, *2*, 403.
(114) Afzaal, M.; Crouch, D.; Malik, M. A.; Motevalli, M.; O'Brien, P.; Park, J.-H.; Woollins, J. D. *Eur. J. Inorg. Chem.* **2004**, 171.
(115) Afzaal, M.; Crouch, D.; Malik, M. A.; Motevalli, M.; O'Brien, P.; Park, J.-H. *J. Mater. Chem.* **2003**, *13*, 639.
(116) Garje, S. S.; Ritch, J. S.; Eisler, D. J.; Afzaal, M.; O'Brien, P.; Chivers, T. *J. Mater. Chem.* **2006**, *16*, 966.
(117) Briand, G. G.; Chivers, T.; Parvez, M. *Angew. Chem., Int. Ed.* **2002**, *41*, 3468.
(118) Chivers, T.; Eisler, D. J.; Ritch, J. S. *Dalton Trans.* **2005**, 2675.
(119) Bochmann, M. *Chem. Vap. Dep.* **1996**, *2*, 85.
(120) Okamot, Y. O.; Yano, T. *J. Organomet. Chem.* **1971**, *29*, 99.
(121) Chivers, T.; Eisler, D. J.; Ritch, J. S.; Tuononen, H. M. *Angew. Chem., Int. Ed.* **2005**, *44*, 4953.
(122) Ramasamy, K.; Malik, M. A.; O'Brien, P.; Raftery, J. *Dalton Trans.* **2009**, 2196.
(123) Ramasamy, K.; Malik, M. A.; O'Brien, P.; Raftery, J. *Dalton Trans* **2010**, *39*, 1460.
(124) Oliver, J. E.; Chang, S. C.; Brown, R. T.; Borkovec, A. B. *J. Med. Chem.* **1971**, *14*, 773.
(125) Kurzer, F. *Chem. Rev.* **1956**, *56*, 95.
(126) Armstrong, K. E.; Crane, J. D.; Whittingham, M. *Inorg. Chem. Commun.* **2004**, *7*, 784.
(127) Ramasamy, K.; Malik, M. A.; O'Brien, P.; *Chem. Mater.*, submitted for publication.
(128) Nair, P. S.; Radhakrishnan, T.; Revaprasadu, N.; Kolawole, G. A.; O'Brien, P. *J. Chem. Soc., Chem. Commun.* **2002**, 564.
(129) Mlondo, S. N.; Revaprasadu, N.; Christian, P.; O'Brien, P. *Mater. Res. Soc. Symp. Proc.* **2005**, *879E*, Z7.6.1.
(130) Nair, S. P.; Scholes, G. D. *J. Mater. Chem.* **2006**, *16*, 467.
(131) Dance, I. G.; Garbutt, R. G.; Craig, D. C.; Scudder, M. L. *Inorg. Chem.* **1987**, *26*, 4057.
(132) Murray, C. B.; Norris, D. J.; Bawendi, M. G. *J. Am. Chem. Soc.* **1993**, *115*, 8706.
(133) Manna, L.; Scher, E. C.; Li, L. S.; Alivisatos, A. P. *J. Am. Chem. Soc.* **2002**, *124* (24), 7136. Manna, L.; Scher, E. C.; Alivisatos, A. P. *J. Am. Chem. Soc.* **2000**, *122* (51), 12700.
(134) Dabbousi, B. O.; Rodriguez-Viejo, J.; Mikulec, F. V.; Heine, J. R.; Mattoussi, H.; Ober, R.; Jensen, K. F.; Bawendi, M. G. *J. Phys. Chem.* **1997**, *B101* (46), 9463.
(135) Peng, X.; Schlamp, M. C.; Kadavanich, A. V.; Alivisatos, A. P. *J. Am. Chem. Soc.* **1997**, *119* (30), 7019.
(136) Coucouvanis, D. *Prog. Inorg. Chem.* **1979**, *26*, 301.
(137) McCleverty, J. A.; Spencer, N.; Bailey, N. A.; Sharleton, S. L. *J. Chem. Soc., Dalton Trans.* **1980**, 939.
(138) Magee, R. J.; Hill, J. D. *Rev. Anal. Chem.* **1985**, *8*, 5.
(139) Glyde, R. *Chem. Br.* **1997**, *33*, 39.
(140) Trindade, T.; O'Brien, P. *J. Mater. Chem.* **1996**, *6*, 343.
(141) Katari, B. J. E.; Colvin, V. L.; Alivisatos, A. P. *J. Phys. Chem.* **1994**, *98*, 4109.
(142) Dabbousi, B. O.; Bawendi, M. G.; Onisuka, O.; Rubner, M. F. *Appl. Phys. Chem.* **1995**, *66*, 1317.
(143) Murray, C. B.; Kagan, C. R.; Bawendi, M. G. *Science* **1995**, *270*, 1335.
(144) Trindade, T.; O'Brien, P. *Adv. Mater.* **1996**, *8*, 161.
(145) Matijevic, E. *Langmuir* **1986**, *2*, 2.
(146) Hamada, S.; Kudo, Y.; Okada, J.; Kano, H. *J. Colloid Interface Sci.* **1987**, *118*, 356.
(147) Trindade, T.; deJesus, J. D.; O'Brien, P. *J. Mater. Chem.* **1994**, *4*, 1611.
(148) Mann, S.; Webb, J.; Williams, R. J. P. *Biomineralization*; VCH: Weinheim, 1989. O'Brien, P. *Adv. Mater.* **1996**, *8*, 161.

(149) Revaprasadu, N.; Malik, M. A.; O' Brien, P.; Zulu, M. M.; Wakefield, G. *J. Mater. Chem.* **1998**, *8* (8), 1885.
(150) Malik, M. A.; Motevalli, M.; O' Brien, P. *Acta Crystallogr.* **1996**, *C25*, 1931.
(151) Leppert, V. L.; Risbud, S. H.; Fendorf, M. J. *Philos. Mag. Lett.* **1997**, *75*, 29.
(152) Chestnoy, N.; Hull, R.; Brus, L. E. *J. Chem. Phys.* **1986**, *85*, 2237.
(153) Li, G.; Nogami, M. *J. Appl. Phys.* **1994**, *75*, 4276.
(154) Lazell, M.; Norager, S. J.; O'Brien, P.; Revaprasadu, N. *Mater. Sci. Eng.* **2001**, *C16*, 129.
(155) Lazell, M.; O'Brien, P. *Chem Commun.* **1999**, 2041.
(156) Malik, M. A.; O'Brien, P. *Ad. Mater. Opt. Electron.* **1994**, *3*, 171.
(157) Hursthouse, M. B.; Malik, M. A.; Motevalli, M.; O'Brien, P. *J. Mater. Chem.* **1992**, *9*, 949.
(158) Revaprasadu, N.; Malik, M. A.; O'Brien, P.; Wakefield, G. *J. Chem. Soc., Chem. Commun.* **1999**, 1573.
(159) Malik, M. A.; Revaprasadu, N.; O'Brien, P. *Chem. Mater.* **2001**, *13*, 913.
(160) Lazell, M. R.; O'Brien, P. *J. Mater. Chem.* **1999**, *9*, 1381.
(161) Peng, Z. A.; Peng, X. G *J. Am. Chem. Soc.* **2001**, *123*, 183.
(162) Dance, I. G.; Choy, A.; Scudder, M. L. *J. Am. Chem. Soc.* **1984**, *106*, 6285.
(163) Lee, G. S. H.; Fisher, K. J.; Craig, D. C.; Scudder, M.; Dance, I. G. *J. Am. Chem. Soc.* **1990**, *112*, 6435.
(164) Cumberland, S. L.; Hanif, K. M.; Javier, A.; Khitrov, G. A.; Strouse, G. F.; Woessner, S. M.; Yun, C. S. *Chem. Mater.* **2002**, *14*, 1576.
(165) Sarigiannis, D.; Peck, J. D.; Kioseoglou, G.; Petrou, A.; Mountziaris, T. J. *Appl. Phys. Lett.* **2002**, *80* (21), 4024.
(166) Moloto, M. J.; Malik, M. A.; O'Brien, P.; Motevalli, M.; Kolawoli, G. A. *Polyhedron* **2003**, *22*, 595.
(167) Sarigiannis, D.; Mountziaris, T. J.; Peck, J. D.; Kioseoglou, G.; Petrou, A. *Proceedings of the IEEE 27th International symposium on compound semiconductors*; IEEE: Piscataway, NJ, 2000; p 321.
(168) Kagan, C. R.; Murray, C. B.; Nirmal, M.; Bawendi, M. G. *Phys. Rev. Lett.* **1996**, *76*, 1517.
(169) Achermann, M.; Petruska, M. A.; Crooker, S. A.; Klimov, V. I. *J. Phys. Chem. B* **2003**, *107*, 13782.
(170) Pradhan, N.; Goorskey, D.; Thessing, J.; Peng, X. *J. Am. Chem. Soc.* **2005**, *127*, 17586–17587.
(171) Empedocles, S. A.; Norris, D. J.; Bawendi, M. G. *Phys. Rev. Lett.* **1996**, *77*, 3873.
(172) Li, J. J.; Wang, Y. A.; Guo, W.; Keay, J. C.; Mishima, T. D.; Johnson, M. B.; Peng, X. *J. Am. Chem. Soc.* **2003**, *125*, 12567.
(173) Colvin, V. L.; Schlamp, M. C.; Allvisatos, A. P. *Nature* **1994**, *370*, 354.
(174) Klimov, V. I.; Mikhailovsky, A. A.; Xu, S.; Malko, A.; Hollingsworth, J. A.; Leatherdale, C. A.; Eisler, H.; Bawendi, M. G. *Science* **2000**, *290*, 314.
(175) Lee, J.; Sundar, V. C.; Heine, J. R.; Bawendi, M. G. *Adv. Mater.* **2000**, *12*, 1102–1105.
(176) Han, M.; Gao, X.; Su, J. Z.; Nie, S. *Nat. Biotechnol.* **2001**, *19*, 631–635.
(177) Revaprasadu, R.; Malik, M. A.; O'Brien, P. *J. Mater. Res.* **1999**, *14*, 3237. Revaprasadu, R.; Malik, M. A.; O'Brien, P. *Mater. Res. Soc. Symp. Proc.* **1999**, *536*, 353.
(178) Bhargava, R. N.; Gallagher, D.; Nurmikko, A. *Phys. Rev. Lett.* **1994**, *72*, 416.
(179) Gallagher, D.; Heady, W. E.; Racz, J. M.; Bhargava, R. N. *J. Cryst. Growth* **1994**, *138*, 970.
(180) Soo, Y. L.; Ming, Z. H.; Huang, S. W.; Kao, Y. H.; Bhargava, R. N.; Gallagher, D. *Phys. Rev.* **1994**, *B50*, 7602.
(181) Sooklal, K.; Cullum, B. S.; Angel, S. M.; Murphy, C. J. *J. Phys. Chem.* **1994**, *100*, 4551.
(182) Wang, Y.; Herron, N.; Moller, K.; Bein, T. *Solid State Commun.* **1991**, *77*, 33. Levy, L.; Feltin, N.; Ingert, D.; Pileni, M. P. *J. Phys. Chem.* **1997**, *B 101*, 9153.
(183) Counio, G.; Gacoin, T.; Boilot, J. P. *J. Phys. Chem.* **1998**, *B 102*, 5237.
(184) Mikulec, F. V.; Kanu, M.; Bennati, M.; Hall, D. A.; Griffin, R. G.; Bawandi, M. G. *J. Am. Chem. Soc.* **2000**, *122*, 2532.
(185) Pradhan, N.; Peng, X. *J. Am. Chem. Soc.* **2007**, *129*, 3339.
(186) Abdel-Hady, A.; Afzaal, M.; Malik, M. A.; O'Brien, P. Unpublished work,
(187) (a) Jones, A. C. *Chem. Soc. Rev.* **1997**, 101. (b) Kuech, T. F.; Veuhoff, E. *J. Cryst. Growth* **1984**, *68*, 148.
(188) Thrush, E. J.; Cureton, C. G.; Trigg, J. M.; Stagg, J. P.; Butler, B. R. *Chemtronics* **1987**, *2*, 62.
(189) Stringfellow, G. B. *J. Cryst. Growth* **1990**, *105*, 260.
(190) Lee, P. W.; Omstead, T. R.; McKennd, D. R.; Jensen, K. F. *J. Cryst. Growth* **1988**, *93*, 134.
(191) Larsen, C. A.; Buchan, N. I.; Li, S. H.; Stringfellow, G. B. *J. Cryst. Growth* **1988**, *93*, 15.
(192) Maury, F. *Adv. Mater.* **1991**, *3*, 542.
(193) Cowley, A. H.; Jones, R. A. *Polyhedron* **1994**, *13*, 1149.
(194) O'Brien, P.; Haggata, S. *Adv. Mater. Opt. Electron.* **1995**, *5*, 117.
(195) Benz, K. W.; Renz, H.; Weidlein, J.; Pilkuhn, M. H. *J. Electron. Mater.* **1981**, *10*, 185.
(196) Moss, R. H.; Evans, J. S. *J. Cryst. Growth* **1981**, *55*, 129.
(197) Zaouk, A.; Salvetat, E.; Sakaya, J.; Maury, F.; Constant, G. *J. Cryst. Growth* **1981**, *55*, 135.
(198) Maury, F.; Combes, M.; Constant, G.; Carles, R.; Renucci, J. B. *J. Phys. (Paris)* **1982**, *1*, 347.
(199) Maury, F.; Combes, M.; Constant, G. *Proceedings of the EU-ROCVD4*; Bloem, J., Verspui, G., Wolff, L. R., Eds.; Philips Centre for Manufacturing Technology: Eindhoven, The Netherlands, 1983; p 257.
(200) Maury, F.; Constant, G. *Polyhedron* **1984**, *3*, 581.
(201) Zaouk, A.; Constant, G. *J. Phys. (Paris)* **1982**, *C5*, 43.
(202) Maury, F.; Hammadi, A. E.; Constant, G. *J. Cryst. Growth* **1984**, *68*, 88.
(203) Hammadi, A. E.; Maury, F.; Muller, G.; Bensoam, J.; Constant, G. *Acad. Sci. Paris, Ser. II* **1984**, *299*, 1255.
(204) Maury, F.; Hammadi, A. E. *J. Cryst. Growth* **1988**, *91*, 97.
(205) Maury, F.; Hammadi, A. E. *J. Cryst. Growth* **1988**, *91*, 105.
(206) Maury, F. In *Transformation of Organometallics into Common and Exotic Materials: Design and Activation*; Laine, R. M., Ed.; NATO ASI Series E; Martinus Nijhoff: The Netherlands 1988, *141*, 195.
(207) Cowley, A. H.; Benac, B. L.; Ekerdt, J. G.; Jones, R. A.; Kidd, K. B.; Lee, J. Y.; Miller, J. E. *J. Am. Chem. Soc.* **1988**, *110*, 6248.
(208) Yoshida, S.; Misawa, S.; Fujii, Y.; Takada, S.; Hayakawa, H.; Gonda, S.; Itoch, A. *J. Vac. Sci. Technol.* **1979**, *16*, 990.
(209) Ho, K. L.; Jensen, K. F.; Hwang, J. W.; Gladfether, W. L.; Evans, J. F. *J. Cryst. Growth* **1991**, *107*, 376.
(210) Interrante, L. V.; Lee, W.; McConnell, M.; Lewis, N.; Hall, E. *J. Electrochem. Soc.* **1989**, *136*, 472.
(211) Bradely, D. C.; Frigo, D. M.; White, E. A. D. *Eur. Pat. Appl.* **1989**; 0 331 448*Ep*.
(212) Fischer, R. A.; Miehr, A.; Ambacher, O.; Metzger, T.; Born, E. *J. Cryst. Growth* **1997**, *170*, 139.
(213) Slack, G. A.; Tanzilli, R. A.; Pohl, R. O.; Vandersande, J. W. *J. Phys. Chem. Solids* **1987**, *48*, 641.
(214) Callahan, D. L.; Thomas, G. *J. Am. Chem. Soc.* **1990**, *73*, 2167.
(215) Jones, A. C.; Rushworth, S. A.; Houlton, D. J.; Roberts, J. S.; Roberts, V.; Whitehouse, C. R.; Critchlow, G. W. *Chem. Vap. Deposition* **1996**, *2*, 5.
(216) Interrante, L. V.; Carpenter, L. E.; Whitmarsh, C.; Lee, W. *Mater. Res. Soc. Symp.* **1986**, *73*, 359.
(217) Kim, Y.; Kim, J.-H.; Park, J. E.; Bae, J. B.; Kim, B.; Park, J.-T.; Yu, K.-S.; Kim, Y. *Thin Solid Films* **1999**, *339*, 200.
(218) Joo, O.-S.; Jung, K.-D.; Cho, S.-H.; Kyoung, J.-H.; Ahn, C.-K.; Choi, C.-S.; Dong, Y.; Yun, H.; Han, S.-H. *Chem. Vap. Deposition* **2002**, *8*, 273.
(219) Hoffman, D. M.; Rangarajan, S. P.; Athavale, S. D.; Economou, D. J.; Liu, J.-R.; Zheng, Z.; Chu, W.-K. *J. Vac. Sci. Technol. A* **1996**, *14*, 306.
(220) Lakhotia, V.; Neumayer, D. A.; Cowley, A. H.; Jones, R. A.; Ekerdt, J. G. *Chem. Mater.* **1995**, *7*, 546.
(221) Kouvetakis, J.; Beach, D. *Chem. Mater.* **1989**, *1*, 476.
(222) Neumayer, D. A.; Cowley, A. H.; Decken, A.; Jones, R. A.; Lakhotia, V.; Ekerdt, J. G. *J. Am. Chem. Soc.* **1995**, *117*, 5893.
(223) Fischer, R. A.; Miehr, A.; Herdtweck, E.; Mattner, M. R.; Ambacher, O.; Metzger, T.; Born, E.; Weinkauf, S.; Pulham, C. R.; Parsons, S. *Chem.—Eur. J.* **1996**, *8*, 1353.
(224) McMurran, J.; Kouvetakis, J.; Nesting, D. C.; Smith, D. J.; Nubbard, J. L. *J. Am. Chem. Soc.* **1998**, *120*, 5233.
(225) McMurran, J.; Kouvetakis, J.; Smith, D. J. *Appl. Phys. Lett.* **1999**, *74*, 883.
(226) Frank, A. C.; Stowasser, F.; Stark, O.; Kwak, H.-T.; Sussek, H.; Rupp, A.; Pritzkow, H.; Ambacher, O.; Giersig, M.; Fischer, R. A. *Adv. Mater. Opt. Electron.* **1998**, *8*, 135.
(227) Devi, A.; Rogge, W.; Wohlfart, A.; Hipler, F.; Becker, H. W.; Fischer, R. A. *Chem. Vap. Deposition* **2000**, *6*, 245.
(228) Schäfer, J.; Wolfrum, J.; Fischer, R. A.; Sussek, H. *Chem. Phys. Lett.* **1999**, *300*, 152.
(229) Sung, M. M.; Kim, C.; Yoo, S. H.; Kim, C. G.; Kim, Y. *Chem. Vap. Deposition* **2002**, *8*, 50.
(230) Lee, J. H.; Yoo, S. H.; Lee, Y. K.; Kim, C. G.; Yang, Y. S.; Kim, Y.; Jeon, H. *J. Korean Phys. Soc.* **2001**, *39*, S242.
(231) Song, S.; Lee, S. S.; Yu, S. H.; Chung, T.-M.; Kim, C. G.; Lee, S.-B.; Kim, Y. *Bull. Korean Chem. Soc.* **2003**, *24*, 953.
(232) Guo, Q.; Kato, O.; Yoshida, A. *J. Appl. Phys.* **1993**, *1*, 7969.
(233) Schaefer, J.; Wolfrum, J.; Fischer, R. A.; Sussek, H. *Chem. Vap. Deposition* **1999**, *5*, 205.
(234) Bae, B.-J.; Park, J. E.; Kim, B.; Park, J. T. *J. Orgamet. Chem.* **2000**, *616*, 128.
(235) Saitosh, H.; Yarbrough, W. A. *Diamond Relat. Mater.* **1992**, *1*, 137.

(236) Boo, J. H.; Rohr, C.; Ho, W. *Phys. Status Solidi* **1999**, *176*, 705.
(237) Boo, J. H.; Lee, S.-B.; Yu, K.-S.; Kim, Y.; Kim, Y.-S.; Park, J. T. *J. Korean Phys. Soc.* **1999**, *34*, 532.
(238) Lorrette, C.; Weisbecker, P.; Jacques, S.; Pailler, R.; Goyhénèche, J. M. *J. Eur. Ceram. Soc.* **2007**, *27*, 2737.
(239) Beachley, O. T.; Coates, G. E. *J. Chem. Soc.* **1965**, 3241.
(240) Beachley, O. T.; Kopasz, J. P.; Zhang, H.; Hunter, W. E.; Atwood, J. L. *J. Organomet. Chem.* **1987**, *325*, 69.
(241) Cowley, A. H.; Jones, R. A. *Angew. Chem., Int. Ed. Engl.* **1989**, *28*, 1208.
(242) Arif, A. M.; Benac, B. L.; Cowley, A. H.; Greets, R.; Jones, R. A.; Kidd, K. B.; Power, J. M.; Schwab, S. T. *J. Chem. Soc., Chem. Commun.* **1986**, 1543.
(243) Arif, A. M.; Benac, B. L.; Cowley, A. H.; Jones, R. A.; Kidd, K. B.; Nunn, C. M. *New J. Chem.* **1988**, *12*, 553.
(244) Maury, F.; Combes, M.; Constant, G.; Carles, R.; Renucci, J. B. *J. Phys. (Paris)* **1982**, *45*, C1–347.
(245) Maury, F.; Constant, G. *Polyhedron* **1984**, *3*, 581.
(246) Pitt, C. G.; Higa, K. T.; McPhail, A. T.; Wells, R. L. *Inorg. Chem.* **1986**, *25*, 2483.
(247) Wells, R. L.; Purdy, A. P.; Higa, K. T.; McPhail, A. T.; Pitt, C. G. *J. Organomet. Chem.* **1987**, *325*, C7.
(248) Purdy, A. P.; Wells, R. L.; McPhail, A. T.; Pitt, C. G. *Organometallics* **1987**, *6*, 2099.
(249) Malik, M. A.; O'Brien, P.; Norigar, S.; Smith, J. *J. Mater. Chem.* **2003**, *13*, 2591.
(250) Miller, J. E.; Kidd, K. B.; Cowley, A. H.; Jones, R. A.; Ekerdt, J. G.; Gysling, H. J.; Wernberg, A. A.; Blanton, T. N. *Chem. Mater.* **1990**, *2*, 589.
(251) Miller, J. E.; Ekerdt, J. G. *Chem. Mater.* **1992**, *4*, 7.
(252) Ekerdt, J. G.; Sun, Y. M.; Jackson, M. S.; Lakhotia, V.; Pacheco, K. A.; Koschmieder, S. U.; Cowley, A. H.; Jones, R. A. *J. Cryst. Growth* **1992**, *124*, 158.
(253) O'Conner, D.; Phillips, D. *Time-Correlated Single Photon Counting*; Academic: London, 1984.
(254) Malik, M. A.; Afzaal, M.; O'Brien, P.; Bangert, U.; Hamilton, B. *Mater. Sci. Technol.* **2004**, *20*, 959.
(255) Malik, M. A.; O'Brien, P.; Halliwell, M. *J. Mater. Chem.* **2005**, *15*, 2.
(256) Miller, J. E.; Mardones, M. A.; Nail, J. W.; Cowley, A. H.; Jones, R. A.; Ekerdt, J. G. *Chem. Mater.* **1992**, *4*, 447.
(257) Cowley, A. H.; Jones, R. A.; Mardones, M. A.; Nunn, C. M. *Organometallics* **1991**, *10*, 1635.
(258) Lu, J.-P.; Raj, R.; Wernberg, A. *Thin Solid Films* **1991**, *205*, 236.
(259) Wernberg, A. A.; Lawrence, D. J.; Gysling, H. J.; Filo, A. J.; Blanton, T. N. *J. Cryst. Growth* **1993**, *131*, 176.
(260) Andrews, D. A.; Davies, G. J.; Bradley, D. C.; Faktor, M. M.; Frigo, D. M.; White, E. A. D. *Semicond. Sci. Technol.* **1988**, *3*, 1053.
(261) Cowley, A. H.; Jones, R. A.; Nunn, C. M.; Westmorland, D. L. *Chem. Mater.* **1990**, *2*, 221.
(262) Park, H. S.; Schulz, S.; Wessel, H.; Roesky, H. W. *Chem. Vap. Deposition* **1999**, *5*, 179.
(263) Kuczkowski, A.; Schulz, S.; Nieger, M.; Saarenketo, P. *Organometallics* **2001**, *20*, 2000.
(264) Kuczkowski, A.; Fahrenholz, S.; Schulz, S.; Nieger, M. *Organometallics* **2004**, *23*, 3615.
(265) Schuchmann, D.; Kuczkowski, A.; Fahrenholz, S.; Schulz, S.; Florke, U. *Eur. J. Inorg. Chem.* **2007**, *7*, 931.
(266) Schulz, S.; Fahrenholz, S.; Kuczkowski, A.; Assenmacher, W.; Seemayer, A.; Hommes, A.; Wandelt, K. *Chem. Mater.* **2005**, *17*, 1982.
(267) Mićić, O. I.; Ahrenkiel, S. P.; Bertram, D.; Nozik, A. J. *Appl. Phys. Lett.* **1999**, *75*, 478.
(268) Coffer, J. L.; Johnson, M. A.; Zhang, L.; Wells, R. L.; Janik, J. F. *Chem. Mater.* **1997**, *9*, 2671.
(269) Manz, A.; Birkner, A.; Kolbe, M.; Fischer, R. A. *Adv. Mater.* **2000**, *12*, 569.
(270) Pan, G.; Kordesch, M. E.; Patten, P. G. V. *Chem. Mater.* **2006**, *18*, 3915.
(271) Sardar, K.; dan, M.; Schwenzer, B.; Rap, C. N. R. *J. Mater. Chem.* **2005**, *15*, 2175.
(272) Schofield, P. S.; Zhou, W.; Wood, P.; Samuel, I. D. W.; Cole-Hamilton, D. J. *J. Mater. Chem.* **2004**, *14*, 3124.
(273) Choi, J.; Gillan, E. G. *J. Mater. Chem.* **2006**, *16*, 3774.
(274) Schwenzer, B.; Meier, C.; Masala, O.; Seshadri, R.; DenBaars, S. P.; Mishra, U. K. *J. Mater. Chem* **2005**, *15*, 1891.
(275) Green, M.; O'Brien, P. *Chem. Commun.* **1998**, 2459.
(276) Green, M.; O'Brien, P. *J. Mater. Chem.* **2004**, *14*, 629.
(277) Well, R. L.; Self, M. F.; McPhail, A. T.; Aubuchon, S. R.; Woudenberg, R. C.; Jasinski, J. P. *Organommetallics* **1993**, *12*, 2832.
(278) Janik, J. F.; Wells, R. L.; Young, V. G.; Rheingold, A. L.; Guzei, L. A. *J. Am. Chem. Soc.* **1998**, *120*, 532.
(279) Malik, M. A.; O'Brien, P.; Helliwell, M. *J. Mater. Chem.* **2005**, *15*, 1463.
(280) Malik, M. A.; Afzaal, M.; Brien, P.; Bangert, U.; Hamilton, B. *Mater. Sci. Technol.* **2004**, *20*, 959.
(281) Maschke, K.; Levy, F. Physics of Non-tetrahedrally Bonded Binary Compounds. In *Landolt-Bornstein New Series*; Madelung, O., von der Ostem, W., Rossler, U. , Eds.; Springer: Verlag, Berlin, 1983; Vol. 17f, Chapter 9.7. MacKinnon. A. Physics of Non-tetrahedrally Bonded Ternary Compounds. In *Landolt-Bornstein New Series*; Madelung, O., von der Ostem, W., Rossler, U., Eds.; Springer Verlag: Berlin, 1985; Vol. 17h, Chapter 10.1; pp 12−23.
(282) Nomura, R.; Inazawa, S. J.; Kanaya, K.; Matsuda, H. *Polyhedron* **1989**, *8*, 763.
(283) Nomura, R.; Fujii, S.; Kanaya, K.; Matsuda, H. *Polyhedron* **1990**, *9*, 361.
(284) Tuck, D. G. In *Comprehensive Organometallic Chemistry*; Wilkinson, G., Stone, F. G. A.; Abel, E. W., Eds.; Pergamon: Oxford, 1995.
(285) Nomura, R.; Inazawa, S. J.; Kanaya, K.; Matsuda, H. *Appl. Organomet. Chem.* **1989**, *3*, 195.
(286) Nomura, R.; Konishi, K.; Matsuda, H. *Thin Solid Films* **1991**, *198*, 339.
(287) Nomura, R.; Konishi, K.; Matsuda, H. *J. Electrochem. Soc.* **1991**, *138*, 631.
(288) MacInnes, A. N.; Power, M. B.; Barron, A. R. *Adu. Mater. Opt. Electron.* **1992**, *1*, 229.
(289) MacInnes, A. N.; Power, M. B.; Hepp, A. F.; Barron, A. R. *J. Organomet. Chem.* **1993**, *449*, 95.
(290) Gysling, H. J.; Wernberg, A. A.; Blanton, T. N. *Chem. Mater.* **1992**, *4*, 900.
(291) Haggata, S. W.; Malik, M. A.; Motevalli, M.; O'Brien, P.; Knowles, J. C. *Chem. Mater.* **1995**, *7*, 716.
(292) O'Brien, P.; Otway, D. J.; Walsh, J. R. *Chem. Vap. Deposition* **1997**, *3*, 227.
(293) O'Brien, P.; Otway, D. J.; Walsh, J. R. *Thin Solid Films* **1998**, *315*, 57.
(294) Afzaal, M.; Malik, M. A.; O'Brien, P. *Chem. Commun.* **2004**, 334.
(295) Bessergenev, V. G.; Ivanova, E. N.; Kovalevskaya, Y. A.; Gromilov, S. A.; Kirichenko, V. N.; Larionov, S. V. *Inorg. Mater.* **1996**, *32*, 592.
(296) McAleese, J.; O'Brien, P.; Otway, D. J. *Chem. Vap. Deposition* **1998**, *4*, 94.
(297) Horley, G. A.; Chunggaze, M.; O'Brien, P.; White, A. J. P.; Williams, D. J. *J. Chem. Soc., Dalton Trans.* **1998**, 4205.
(298) Horley, G. A.; O'Brien, P.; Park, J.-H.; White, A. J. P.; Williams, D. J. *J. Mater. Chem.* **1999**, *9*, 1289.
(299) Kunze, K.; Bihry, L.; Atanasova, P.; Hampden-Smith, M. J.; Duesler, E. N. *Chem. Vap. Deposition* **1996**, *2*, 105.
(300) Shang, G.; Hampden-Smith, M. J.; Duesler, E. N. *Chem. Commun.* **1996**, 1733.
(301) (a) Shang, G.; Kunze, K.; Hampden-Smith, M. J.; Duesler, E. *Chem. Vap. Deposition* **1996**, *2*, 242. (b) Shang, G.; Hampden-Smith, M. J.; Duesler, E. N. *Chem. Commun* **1996**, 1733.
(302) Garje, S. S.; Copsey, M. C.; Afzaal, M.; O'Brien, P.; Chiversb, T. *J. Mater. Chem.* **2006**, *16*, 4542.
(303) Copsey, M. C.; Chivers, T. *Chem. Commun.* **2005**, 4938.
(304) Dimitrijevic, N. M.; Kamat, P. V. *Langmuir* **1987**, *3*, 1004.
(305) Kamat, P. V.; Dimitrijevic, N. M.; Fessenden, R. W. *J. Phys. Chem.* **1988**, *92*, 2324.
(306) Stoll, S. L.; Gillan, E. G.; Barron, A. G. *Chem. Vap. Deposition* **1996**, *2*, 182.
(307) Revaprasadu, N.; Malik, M. A.; Carstens, J.; O'Brien, P. *J. Mater. Chem.* **1999**, *9*, 2885.
(308) Chikan, V.; Kelly, D. F. *Nano Lett.* **2002**, *2*, 141.
(309) levy, F. *Crystallography and Crystal Chemistry of Materials with Layered Structures*; Reidel: Holland, 1976.
(310) Stoll, S. L.; Gillan, E. G.; Barron, A. *Chem. Vap. Deposition* **1996**, *2*, 182. Gillan, E. G.; Barron, A. R. *Chem. Mater.* **1997**, *9*, 3037. Gillan, E. G.; Bott, S. G.; Barron, A. *Chem. Mater.* **1997**, *9*, 796.
(311) Dutta, D. P.; Sharma, G.; Ghoshal, S.; Prasad, N.; Jain, V. K. *J. Nanosci. Nanotechnol.* **2006**, *6*, 1.
(312) Ghoshal, S.; Kushwah, N. P.; Dutta, D. P.; Jain, V. K. *Appl. Organomet. Chem.* **2005**, *19*, 257.
(313) Dutta, D. P.; Sharma, G.; Tyagi, A. K.; Kulshreshtha, S. K. *Mat. Sci. Eng.* **2007**, *B138*, 60.
(314) Fainer, N. I.; Kosinova, M. L.; Rumyantsev, Y. M.; Salman, E. G.; Kuznetsnov, F. A. *Thin Solid Films* **1996**, *280*, 16.
(315) Trindade, T.; O'Brien, P. *Chem. Vap. Deposition* **1997**, *3*, 75.
(316) Afzaal, M.; Ellwood, K.; Pickett, N. L.; O'Brien, P.; Raftery, J.; Waters, J. *J. Mater. Chem.* **2004**, *14*, 1310.
(317) Ritch, J. S.; Ahmad, K.; Afzaal, M.; Chivers, T.; O'Brien, P. *Inorg. Chem.* **2010**, *49*, 1158.
(318) Akhtar, J.; Bruce, J. C.; Malik, M. A.; Klaus, R. K.; Afzaal, M.; O'Brien, P. *Mater. Res. Soc. Symp. Proc.* **2009**, 1148-PP12-08.

(319) Chuprakov, I. S.; Dahmen, K.-H.; Schneider, J. J.; Hagen, J. *Chem. Mater.* **1998**, *10*, 3467.
(320) Chuprakov, I. S.; Dahmen, K.-H. *J. Phys. IV* **1999**, *9*, 313.
(321) Schneider, J. J.; Hagen, J.; Heinemann, O.; Bruckmann, J.; Krüger, C. *Thin Solid Films* **1997**, *304*, 144.
(322) Suh, S.; Hoffman, D. M.; Atagi, L. M.; Smith, D. C.; Liu, J.-R.; Chu, W.-K. *Chem. Mater.* **1997**, *9*, 730.
(323) Houlton, D. J.; Jones, A. C.; Hycock, P. W.; Williams, E. W.; Bull, J.; Critchlow, G. W. *Chem. Vap. Deposition* **1995**, *1*, 26.
(324) Brown, J. R.; Cheney, M. T.; Hycock, P.; Houlton, D. J.; Jones, A. C.; Williams, E. W. *J. Electrochem. Soc.* **1997**, *144*, 295.
(325) Boyle, T. J.; Alam, T. M.; Rodriguez, M. A.; Zechmann, C. A. *Inorg. Chem.* **2002**, *41*, 25742.
(326) Boyle, T. J.; Ward, T. L.; De'Angeli, S. M.; Xu, H.; Hammetter, W. F. *Chem. Mater.* **2003**, *15*, 765.
(327) Mathur, S.; Sivakov, V.; Shen, H.; Barth, S.; Cavelius, C.; Nilsson, A.; Kuhn, P. *Thin Solid Films* **2006**, *502*, 88.
(328) kai, G.; Baik, N. S.; Miura, N.; Yamazoe, N. *Sens. Actuators B: Chem.* **2001**, *77*, 116.
(329) Talaty, N. N.; Beck, K.; Citeau, H.; Kirschbaum, K.; Giolando, D. M. Z. *Anorg. Allg. Chem* **2009**, *635*, 53.
(330) Mahon, M. F.; Molloy, K. C.; Stanley, J. E.; Rankin, D. W. H.; Robertson, H. E.; Johnston, B. F. *Appl. Organomet. Chem.* **2005**, *19*, 658.
(331) Hibbert, T. G.; Mahon, M. F.; Molloy, K. C.; Price, L. S.; Parkin, I. P. *J. Mater. Chem.* **2001**, *11*, 469.
(332) Barone, G.; Hibbert, T. G.; Mahon, M. F.; Molloy, K. C.; Price, L. S.; Parkin, I. P.; Hardy, A. M. E.; Field, M. N. *J. Mater. Chem.* **2001**, *11*, 464.
(333) Parkin, I. P.; Price, L. S.; Hibbert, T. G.; Molloy, K. C. *J. Mater. Chem.* **2001**, *11*, 1486.
(334) Kana, A. T.; Hibbert, T. G.; Mahon, M. F.; Molloy, K. C.; Parkin, I. P.; Price, L. S. *Polyhedron* **2001**, *20*, 2989.
(335) Bade, B. P.; Garje, S. S.; Niwate, Y. S.; Afzaal, M.; O'Brien, P. *Chem. Vap. Deposition* **2008**, *14*, 292.
(336) Reid, S. D.; Hector, A. L.; Levason, W.; Reid, G.; Waller, B. J.; Webster, M. *Dalton Trans.* **2007**, 4769.
(337) Chen, T.; Hunks, W.; Chen., P. S.; Stauf, G. T.; Cameron, T. M.; Xu, C.; DiPasuale, A. G.; Rheingold, A. L. *Eur. J. Inorg. Chem.* **2009**, 2047.
(338) Trindade, T.; O'Brien, P.; Zhang, X.-M.; Motevalli, M. *J. Mater. Chem.* **1997**, *7*, 1011.
(339) Trindade, T.; Monteiro, O. C.; O'Brien, P.; Motevalli, M. *Polyhedron* **1999**, *18*, 1171.
(340) Lee, S.-M.; Jun, Y.-W.; Cho, S.-N.; Cheon, J. *J. Am. Chem. Soc.* **2002**, *124*, 11244.
(341) Duan, T.; Lou, W.; Wang, X.; Xue, Q. *Colloid Surf. A: Physicochem. Eng. Asp.* **2007**, *310*, 86.
(342) Lee, S. M.; Cho, S. N.; Cheon, J. *Adv. Mater.* **2003**, *15*, 441.
(343) Zhihua, Z.; Lee, S. H.; Vittal, J. J.; Chin, W. S. *J. Phys. Chem. B* **2006**, *110*, 6649.
(344) Pradhan, N.; Katz, B.; Efrima, S. *J. Phys. Chem. B* **2003**, *107*, 13843.
(345) Acharya, S.; Gautam, U. J.; Sasaki, T.; Bando, Y.; Golan, Y.; Ariga, K. *J. Am. Chem. Soc.* **2008**, *10*, 4594.
(346) Machol, J. L.; Wise, F. W.; Patel, R. C.; Tanner, D. B. *Phys. Rev. B* **1993**, *48*, 2819.
(347) Krauss, T. D.; Wise, F. W. *Phys. Rev. B* **1997**, *55*, 9860.
(348) Krauss, T. D.; Wise, F. W.; Tanner, D. B. *Phys. Rev. Lett.* **1996**, *76*, 1376.
(349) Luther, J. M.; Zheng, H.; Sadtler, B.; Alivisatos, A. P. *J. Am. Chem. Soc.* **2009**, *131*, 16851.
(350) Berhanu, D.; Govender, K.; Smyth-Boyle, D.; Archbold, M.; Halliday, D. P.; O'Brien, P. *Chem. Commun.* **2006**, 4709.
(351) Sun, J.; Buhro, W. E. *Angew. Chem., Int. Ed.* **2008**, *47*, 3215.
(352) Koktysh, D. S.; McBride, J. R.; Rosenthal, S. J. *Nanoscale Res. Lett.* **2007**, *2*, 144.
(353) Haycock, P. W.; Horley, G. A.; Molloy, K. C.; Myers, C. P.; Rushworth, S. A.; Smith, L. M. *J. Phys. IV* **2001**, *11*, Pr-3–1045.
(354) Haycock, P. W.; Horley, G. A.; Molloy, K. C.; Myers, C. P.; Rushworth, S. A.; Smith, L. M. *Chem. Vap. Deposition* **2001**, *7*, 191.
(355) Horley, G. A.; Mahon, M. F.; Molloy, K. C.; Haycock, P. W.; Myers, C. P. *Inorg. Chem.* **2002**, *41*, 5052.
(356) Myers, C. P.; Haycock, P. W.; Pichot, M.; Horley, G. A.; Molloy, K. C.; Rushworth, S. A.; Smith, L. M. *Chem. Vap. Deposition* **2004**, *10*, 35.
(357) Rodriguez-Castro, J.; Mahon, M. F.; Molloy, K. C. *Chem. Vap. Deposition* **2006**, *12*, 601.
(358) Rodriguez-Castro, J.; Dale, P.; Mahon, M. F.; Molloy, K. C.; Peter, L. M. *Chem. Mater.* **2007**, *19*, 3219.
(359) Rodriguez-Castro, J.; Molloy, K. C.; Liu, Y.; Lai, C. S.; Dong, Z.; White, T. J.; Tiekink, E. R. T. *J. Mater. Chem.* **2008**, *18*, 5399.
(360) Garje, S. S.; Eisler, D. J.; Ritch, J. S.; Afzaal, M.; O'Brien, P.; Chivers, T. *J. Am. Chem. Soc.* **2006**, *128*, 3120.
(361) Kang, S. W.; Rhee, S. W. *Thin Solid Films* **2004**, *468*, 79.
(362) Bedoya, C.; Condorelli, G. G.; Finocchiaro, S. T.; Di Mauro, A.; Fragalà, I. L.; Cattaneo, L.; Carella, S. *Chem. Vap. Deposition* **2005**, *11*, 261.
(363) Monteiro, O. C.; Trindade, T.; Park, J.-H.; O'Brien, P. *Chem. Vap. Deposition* **2000**, *6*, 230.
(364) Koh, Y. W.; Lai, C. S.; Du, A. Y.; Tiekink, E. R. T.; Loh, K. P. *Chem. Mater.* **2003**, *15*, 4544.
(365) Waters, J.; Crouch, D.; Raftery, J.; O'Brien, P. *Chem. Mater.* **2004**, *16*, 3289.
(366) Cupertino, D.; Birdsall, D. J.; Slawin, A. M. Z.; Woollins, J. D. *Inorg. Chem. Acta* **1999**, *290*, 1.
(367) Lin, Y.-F.; Chang, H.-W.; Lu, S.-Y.; Liu, C. W. *J. Phys. Chem. C* **2007**, *111*, 18538.
(368) Arivuoli, D.; Gnanam, F. D.; Ramasamy, P. *J. Mater. Sci. Lett.* **1988**, *7*, 711.
(369) Xie, G.; Qiao, Z.-P.; Zeng, M.-H.; Chen, X.-M.; Gao, S.-L. *Cryst. Growth Des.* **2004**, *4*, 513.
(370) Han, Q.; Chen, J.; Yang, X.; Lu, L.; Wang, X. *J. Phys. Chem. C* **2007**, *111*, 14072.
(371) Lou, W.; Chen, M.; Wang, X.; Liu, W. *Chem. Mater.* **2007**, *19*, 872.
(372) Tian, L.; Tan, H. Y.; Vittal, J. J. *Cryst. Growth Des* **2008**, *8*, 734.
(373) Li, R. F.; Lee, J.; Yang, B. C.; Horspool, D. N.; Aindow, M.; Papadimitrakopoulos, F. *J. Am. Chem. Soc.* **2005**, *127*, 2524.
(374) Spalla, O.; Nabavi, M.; Minter, J.; Cabane, B. *Colloid Polym. Sci.* **1996**, *274*, 555.
(375) Chang, H.-W.; Sarkar, B.; Liu, C. W. *Cryst. Growth. Des.* **2007**, *7*, 2691.
(376) Ko, T. Y.; Yang, C. H.; Sun, K. W.; Chang, H. W.; Sarker, B.; Liu, C. W. *Cent. Eur. J. Chem.* **2009**, *7*, 197.

CR900406F